Translation T-10

Contributions to the Question of a Velocity Formula and Roughness Data for Streams, Channels and Closed Pipelines

by

Dr. A. Strickler

Bern, Switzerland, 1923

Translation by Thomas Roesgen and William R. Brownlie

at

W. M. Keck Laboratory of Hydraulics and Water Resources
Division of Engineering and Applied Science
CALIFORNIA INSTITUTE OF TECHNOLOGY
Pasadena, California

Translation T-10 January 1981

Swiss Department of the Interior

Report of the Bureau of Water Affairs

edited under the charge of Dr. Carl Mutzner

No. 16

Contributions to the Question of a Velocity Formula and Roughness Data for Streams, Channels and Closed Pipelines

by

Dr. A. Strickler

Chief of the Section for Low Pressure Systems and Navigation

Bern, Switzerland, 1923

Translation by Thomas Roesgen and William R. Brownlie

at

W. M. Keck Laboratory of Hydraulics and Water Resources

Division of Engineering and Applied Science

California Institute of Technology

Pasadena, California

Translation T-10 January 1981

ABOUT THIS TRANSLATION

This widely referenced, but seldom seen report is of both historic and engineering interest. While much of the work presented has since been eclipsed by more recent work, the velocity equation for open channels (Eq. 37) is still in use. It is interesting to learn how this equation came into being, particularly in light of the fact that it predates the well known von Karman-Prandtl logarithmic velocity distribution equation. Also of interest, is the plethora of velocity equations for open channels and pipes, which existed over sixty years ago (particularly when one considers that the search for a satisfactory equation continues to this day). A final benefit of this translation is that the extensive tabulations of data have been preserved for a new constituency.

Every attempt has been made to translate as literally as possible, to preserve the flavor of the original report. Therefore, certain phrases may seem somewhat awkward. A few archaic German idioms required a somewhat looser translation. The data in Tables 1 through 14 have been reproduced directly from the original report, with the substitution of captions in English. Therefore, the data entries contain commas which should be replaced by decimal points to convert to the North American convention.

The preparation of this translation was supported by the National Science Foundation, under Grant CME 79-20311. Special thanks to Joan Mathews and Melinda Hendrix-Werts for their excellent typing and to Theresa Fall, for preparation of the tables and figures.

W.R. Brownlie, January 1981

PREFACE

The number of formulas for the computation of the water velocity in streams, artificial channels and closed pipelines has increased substantially during the last decades. The purpose of the present work consisted originally only of an investigation of the range of validity of the older and newer formulas, namely those of a pure power (law) type, which recently have attracted more attention by the technicians. An increase in the number of formulas was not intended.

In the further pursuit of this goal, however, the necessity and possibility occurred to establish a new, generally valid formula, of which the pure power law $V_m = KR^{\mu}j^{\nu}$ represents only an approximation, with a certain range of validity, in so far as one understands the exponents μ and ν as constants.

Bern, February 1929

The Director of the Swiss Bureau of Water Affairs:

Dr. C. Mutzner

INDEX

I. Text

II. Figures

List of Symbols

		units in kg-m-sec system
J	= relative slope (slope of the water level	dimensionless
R	= hydraulic radius = cross-sectional area/ wetted perimeter[1]	m
v_m	= water velocity as a mean over the whole profile	m/sec
v	= water velocity at an arbitrary point of the cross-section	m/sec
v_o	= water velocity at an arbitrary point of the water surface in open channels	m/sec
V_o	= maximum velocity in the cross-section	m/sec
$\bar{v}$	= mean water velocity in a vertical	m/sec
v_s	= water velocity at the bed	m/sec

[1] According to the collection in Forchheimer's "Hydraulics" (6).

T	= mean water depth in a cross-section	m
t	= depth of an arbitrary point of the cross-section, below the water level	m
t_a	= depth from the surface to the bed in a vertical	m
T_a	= maximum depth in the cross-section width of the water level	m
B_o	= width of the water level	m
ε	= roughness coefficient of basin	
n	= roughness coefficient of Ganguillet and Kutter	
c	= velocity coefficient according to $v_m = c\sqrt{RJ}$	
k, k_1, k_2	= coefficients, variable with the roughness	
D	= pipe diameter	m
D_1	= diameter of the cylinder inscribed to the unevenness	m
h_w	= loss of head	m
Δp	= pressure loss = $h_w \cdot \gamma$	kg/m^2
r_a	= pipe radius	m
r	= radius of a ring layer in the circular pipe	m
λ	= drag coefficient according to $J = \lambda \frac{v_m^2}{4R \cdot 2g}$	
$a, b, a_1, b_1, f, m, s, M, N, P, \beta,$	= coefficients	
η	= coefficient of internal fluid friction or viscosity	kg sec/m^2
γ	= specific weight of the fluid	kg/m^3
γ/g	= specific mass of the fluid	kg sec^2/m^4
τ	= temperature of the fluid	° Celsius
ρ	= equivalent diameter of the wall irregularities	m
g	= gravitational acceleration	m/sec^2

L	= length of a river section (for stagnation [backwater] computations) or of a pipe line	m
U	= wetted perimeter of the cross-section	m
O	= U.L = wetted surface (pipe lines)	m^2

A. Short Survey of the More Important (Velocity) Formulas

a) Formulas for open channels, rivers and streams. The quantity c in Chezy's formula:

$$v_m = c\sqrt{RJ} \tag{1}$$

is commonly represented as a function of the other quantities R and J, as well as of the roughness ρ of the walls, or of a selected number of those quantities. For those cases, where c is represented by a power law, Eq. 1 can then be written as a power law, too:

$$v_m = F(\rho)R^{\mu}J^{\nu} \tag{2}$$

Some of the authors, who stated the magnitude of the exponents μ and ν, as well as the function $F(\rho)$, are mentioned in the following[1]:

Lahmeyer	$v_m = 183.5\ R^{2/3}J^{2/3}$ for straight river sections	(3)
de Saint-Venant	$v_m = 60\ R^{11/21}J^{11/21}$	(4)
Humphreys & Abbot	$v_m = (5.0 \text{ to } 5.7)R^{1/2}J^{1/4}$ (shorted)	(5)
Gauckler	$v_m = k_1R^{4/3}J$ for $J < 0.0007$	(6)
	$v_m = k_2R^{2/3}J^{1/2}$ for $J > 0.0007$	
Hagen for streams	$v_m = 3.34\ R^{1/2}J^{1/5}$	(7)
small channels	$v_m = 4.9\ RJ^{1/5}$	
for large, regular channels	$v_m = 43.7\ R^{2/3}J^{1/2}$	
Manning (for channels)	$v_m = \frac{1}{n} R^{2/3}J^{1/2}$ [2]	(8)

[1]According to the collection in Forchheimer's "Hydraulics" (6).
[2]The coefficient, n, is identical with the Ganguillet-Kutter coefficient.

Hermanek $v_m = 30.7\ TJ^{1/2}$ for $T < 1.50$ m (9)

for streams and rivers $v_m = 34\ T^{3/4}\ J^{1/2}$ for $1.5 < T < 6$ m

$v_m = 44.5\ T^{0.6}\ J^{1/2}$ for $T > 6$ m

Forchheimer $v_m = k_3 R^{0.7}\ J^{0.5}$ [1]) (10)

Beyerhaus $v_m = k_3\ R^{0.7}\ J^{0.46}$ (10a)

Christen $v_m = \sqrt{2k_4^3}\ T^{1/2}\ J^{1/2}\ \sqrt[8]{B_o}$ (11)

Not of a power law shape and thus somewhat more complicated in their structure, are the formulas of

Kutter (short formula) $$v_m = \frac{100\sqrt{R}}{m+\sqrt{R}}\ R^{1/2}\ J^{1/2} \tag{12}$$

Bazin (new formula) $$v_m = \frac{87}{1+\frac{\varepsilon}{\sqrt{R}}}\ R^{1/2}\ J^{1/2} \tag{13}$$

$$= \frac{87\sqrt{R}}{\varepsilon+\sqrt{R}}\ R^{1/2}\ J^{1/2}$$

Ganguillet & Kutter $$v_m = \frac{23+\frac{1}{n}+\frac{0.00155}{J}}{1+(23+\frac{0.00155}{J})\ \frac{n}{\sqrt{R}}}\ R^{1/2}\ J^{1/2} \tag{14}$$

Hessle $$v_m = (25+12.5\sqrt{R})R^{1/2}\ J^{1/2} \tag{15}$$

Matakiewicz $$v_m = \frac{116\ J^{0.493+10J}}{2.2+T^{2/3+0.15/T^2}}\ T \tag{16}$$

Manning (for streams) $$v_m = 34(1+0.25\ R - \frac{0.03}{\sqrt{R}})\ R^{1/2}\ J^{1/2} \tag{8a}$$

The formulas without variable roughness coefficients, even the newer ones, Eqs. 9 and 16, obviously cannot hold in general, since it appears evident that the therein assumed relation between roughness, head and average water depth is not valid for all gravel carrying water courses;

[1]Forchheimer found for water depths of several millimeters in a smooth wood channel: $v_m = 100\ T^{0.7}\ J^{0.5}$.

also for a given cross-section it is not satisfied for all water levels; apart from that these formulas cannot be applied to rigid walls. The hydraulic engineer has thus preferred, in most cases, the Ganguillet-Kutter formula despite its somewhat complicated structure, because it has relatively broad limits of validity. In more recent times it has been criticized because of a fundamentally incorrect structure (14).

b) Formulas for closed pipelines:

General Formula $$v_m = \sqrt{\frac{2g}{\lambda}}\, D^{0.5}J^{0.5} \text{ or } J = \lambda \frac{v_m^2}{D \cdot 2g} \quad (17)$$

Eytelwein $$v_m = 25.1\ D^{0.5}J^{0.5} \text{ or } J = 0.00159 \frac{v_m^2}{D} \quad (17a)$$

Woltmann $$v_m = 45.8\ D^{4/7}J^{4/7} \text{ or } J = 0.00124 \frac{v_m^{1.75}}{D} \quad (18)$$

de Saint-Venant $$v_m = 51\ D^{7/12}J^{7/12} \text{ or } J = 0.001182 \frac{v_m^{12/7}}{D} \quad (19)$$

Lampe $$J = 0.0007555 \frac{v_m^{1.802}}{D^{1.25}} \quad (20)$$

Fanning $$v_m = k_5 D^{0.5} J^{0.5} \text{ or } J = \frac{1}{k_5^2} \frac{v_m^2}{D} \quad (21)$$

Christen $$v_m = k_6 D^{0.625} J^{0.5} \text{ or } J = \frac{1}{k_6^2} \frac{v_m^2}{D^{1.25}} \quad (22)$$

Reynolds a) for wide pipe

$$\left.\begin{array}{l} v_m = k_7 D^{0.765} J^{0.59} \\ \text{to} \quad k_8 D^{0.50} J^{0.50} \end{array}\right\} \begin{array}{l} J = \lambda_1 \dfrac{v_m^{1.7 \text{ to } 2.0}}{D^{1.3 \text{ to } 1.0}} \\ \lambda_1 = 0.000385 \text{ to } 0.00232 \end{array} \quad (23)$$

b) for capillaries

$$J = \lambda_2 \frac{v_m}{D^2}$$

Flamant, Saph & Schoder, Blasius

$$v_m = k_9 D^{0.71} J^{0.57} \text{ or } J = \lambda_3 \frac{v_m^{1.75}}{D^{1.25}} \tag{24}$$

According to Blasius, for water at 15°C, and smooth pipes:

$$\lambda_3 = 0.000528$$

Tutton

New, cast iron and tarred pipes

$$v_m = 34.8\ D^{0.66} J^{0.51} = 88\ R^{0.66} J^{0.51} \quad ^{1)}$$

Pipes in usage (encrusted)

$$v_m = 27.8\ D^{0.66} J^{0.51} = 70\ R^{0.66} J^{0.51} \tag{25}$$

Stove pipes $\quad v_m = 33.4\ D^{0.66} J^{0.51} = 84\ R^{0.66} J^{0.51}$

Riveted pipes $\quad v_m = 30.8\ D^{0.66} J^{0.51} = 77.5\ R^{0.66} J^{0.51}$

Asphalt coated wrought iron pipes

$$v_m = 45.8\ D^{0.62} J^{0.55} \sim 115\ R^{0.62} J^{0.55}$$

Large tile structures

$$v_m = (24.4 \div 34.5) D^{0.65} J^{0.52}$$
$$= (61.5 \div 87) R^{0.65} J^{0.52}$$

The variations in the magnitude of the exponents of D and J, or of v_m and D cited in these formulas, are at least as big as in those for open channels.

Not of a pure power law structure are the formulas of

de Prony $\quad J = a_2 \frac{v_m^2}{D} + b_2 \frac{v_m}{D}$ (26)

Weisbach $\quad J = a_3 \frac{v_m^2}{D} + b_3 \frac{v_m^{1.5}}{D}$ (27)

Darcy $\quad J = a_4 \frac{v_m^2}{D} + b_4 \frac{v_m^2}{D^2}$ (28)

Gauckler $$J = a_6 \frac{(\sqrt{v_m} + 0.25\, D\sqrt[4]{v_m}\,)^4}{D^{4/3}} \qquad (28a)$$

Kutter, for new pipes $$J = \left(\frac{0.15+\sqrt{R}}{100\sqrt{R}}\right)^2 v_m^{\,2} \qquad (28b)$$

Lang (1887) $$J = \left(a_5 \frac{v_m^{\,2}}{D} + b_5 \frac{v_m^{\,1.5}}{D^{1.5}}\right)\left(\frac{D}{D_1}\right)^5 \qquad (29)$$

Biel $$1000\ J = \left(\frac{a}{R} + \frac{f}{R^{1.5}}\right) v_m^{\,2} + \frac{b(\eta)}{\gamma R^{1.5}}\, v_m \qquad (30)$$

$$= \frac{a_1}{R}\, v_m^{\,2} + \frac{b_1}{R}\, v_m$$ [1]

Lang (1911) (according to Forchheimer's Hydraulics)

$$J = \lambda_1 = \frac{v_m(v_m - v_k)}{gD} + 0.88\, \frac{\eta^{1/2} v_m (v_m - v_k)^{1/2}}{g^{1/2}\gamma^{1/2} D^{1.5}}$$

$$+\ 32\, \frac{\eta v_m}{\gamma D^2} + 0.000025\ v_m v_k \qquad (31)$$

$$\lambda_1 = 0.0045 \text{ to } 0.01$$

The following should be noticed, concerning the formulas of section b:

Their validity is (as by the way for all formulas mentioned so far) restricted to water velocities which are larger than the "critical velocity" v_k. Below the latter the pure laminar or stratified flow prevails, for which in circular pipe,

$$v_m = \frac{\gamma}{2\eta}\, J \left(\frac{r_a}{2}\right)^2 = \frac{\gamma}{2\eta}\, JR^2 \qquad (32)$$ [2]

or $$J = \frac{2\eta}{\gamma R^2}\, v_m \qquad (32a)$$

According to Poiseuille, for water $\eta = \dfrac{0.0001817}{1+0.0336\tau+0.000221\tau^2}$

[1] Table of the a,f and b.(see p. 49).

[2] The common derivation of this equation will be developed in section D.

Above the critical velocity, "turbulent flow" is considered[1] which is generally described by the equation

$$J = \frac{\lambda}{4R}\,\frac{v_m^{\,2}}{2g} \tag{17}$$

However, λ is not constant.

The magnitude of the critical velocity was given by Reynolds as

$$v_k = \frac{2000\eta g}{D\gamma} \quad {}^{2)} \tag{33}$$

Although the pressure loss of pure laminar flow is proportional to the velocity (acc. to Eq. 32a), the one for pure turbulent flow (acc. to Eq. 17) is proportional to the square of the velocity, the equations of de Prony (Eq. 26) and Biel (Eq. 30) could be understood in the way that the total pressure loss is composed of a part each of laminar and turbulent flow. The exponents of D or R in the second terms of Eqs. 26 and 30, however, do not correspond to that of Eq. 32a. In Eq. 28 of Darcy's, D^2 would occur in the second term, however, the exponent of v_m does not correspond to laminar flow.

Equations 26 to 30, thus, do not show a strictly logical structure.

Biel restricts the validity of his equation (Eq. 30) even somewhat more in that it shall not hold directly above the critical velocity, but first above the "upper limiting velocity" v_{g2}. The meaning of the latter is evident from the plot in Fig. 21; Biel drew the finely dotted line through the measured points and thus marked off a "transition region" between the laminar flow for $v_m < v_k$ and the turbulent flow for $v_m > v_{g2}$.

---

[1]On the fundamental differences between laminar and turbulent flow, see Prásil (9) or Forchheimer (6).

[2]Thus the critical velocity for water at 20°C is, e.g.
for a pipe of D=0.01 m: v_k=0.20 m/sec
for a pipe of D=0.50 m: v_k=0.004 m/sec.

Finally the formal equation of pure power law shape, set up by Eisner should be mentioned, which holds for open channels and closed pipelines, and which he set up based on the conditions of a similarity rule (16).

$$v_m = k_o^{\varphi}\,\rho^{\psi}\,R^{1.5\varphi-\psi-1}\,J^{0.5\varphi} \tag{34}$$

Eisner calls k_o the "form factor" of the cross-section and ρ the measure of roughness.

The exponents, φ and ψ, are numbers, which according to Eisner cannot be derived from the similarity rule, but must be determined by experiment.

Having given a short survey of the 34 formulas mentioned in this chapter (they could be increased by at least the same number!), a fact that particularly attracts attention is that sometimes even the same author has given different formulas for open channels and closed pipes. However, the postulate that the general law of energy loss holds for both types doesn't require further discussion at the present time.

B. Set Up of a Simple Approximation Formula for Mean Velocity, and Criticism of Some Existing Formulas

In this report, an attempt is made to establish a pure power law formula, based on a larger number of measurements, mainly performed in open water courses, but also in pipelines of sufficient diameter ($D > 0.15$ m). It will be attempted to show the validity of an already existing formula, respectively.

In selecting those measurements, which have been performed by the "Eidgenoessisches Amt für Wasservirtschaft" (The Swiss Bureau of Water Affairs) the number of data sets was not as important as the range of the individual variables; these ranges extended

for J from 0.00004 to 0.025
for R from 0.037 to 7.14 m
for the roughness: smoothed cement to head-sized stones.

Furthermore, only such measurement stations were chosen, at which the flow can truly be considered to be uniform.

The determination of the exponents and the coefficient in the equation

$$v_m = kR^{\mu}J^{\nu}$$

was expedited in the following manner:

1. First some measurement sets were selected with a constant slope but variable hydraulic radius. The mean velocities v_m were plotted as a function of the hydraulic radius in a logarithmic coordinate system (Fig. 4). Since the equation

$$\log v_m = \log(kJ^{\nu}) + \mu \log R$$

represents a straight line, the value of μ can easily be read from the slope of this straight line. According to Figure 4, the exponent μ reaches the value 2/3 for the artificial sluices, adits and rivers displayed there.

2. Then, some measurement series with constant (or nearly constant) hydraulic radius but variable slope were plotted in a similar way (Fig. 5), and the value $\nu = 1/2$ was found as the exponent of J; for the case of the E.T.H. pipeline, the exponent is somewhat larger (0.52).

However, these measurement series do not yet allow a final conclusion on the <u>general</u> validity of the law

$$v_m = kR^{2/3}J^{1/2} \quad ,$$

whose existence was derived for these 17 data series.

Since R and J vary simultaneously in the majority of measurements on open water courses, it was tried to represent the mean velocity v_m as a function of the product $R^{2/3}J^{1/2}$. This was done for some boulder carrying water courses in Figs. 6 to 13. For the case that we really deal with one and the same roughness, the individual points of a series apparently have to lie in one straight line if the above power law shall have a true general validity. The slope of the straight line versus the abscissa then represents the coefficient k. A continuous proportionality of the v_m-values with respect to the $R^{2/3}J^{1/2}$ values does not exist for the measurements shown in Figs. 6 to 13, but in most cases, a transition can be observed from a "lower state" (smaller v_m, larger k) to an "upper state" (larger v_m, smaller k); in one case, even two of such transitions occur (Danube).

Below this transition, the trend of the v_m-line is linear, as far as can be seen from Figs. 6 to 13, or in other words, the k value is constant in that range, and the law $v_m = kR^{2/3}J^{1/2}$ is in fact fulfilled here.

It will be shown later that this transition occurs at the flow velocity at which the river bottom falls into general movement and exceeds the critical drag force; by this means the roughness of the bed is increased. This fact, which is by the way long known, expresses itself of course also in the coefficient of every other formula; Fig. 14 shows for the Rhine at Basle the sudden increase of Kutter's roughness coefficient n and the coefficient ε of Bazin in exceeding a velocity v_m of about 2.4 m/sec.

The upper transition in Vienna comes from the fact that in exceeding the related R-value the lowland is flooded, where apparently different roughness conditions exist.

A steadily curved v_m-line, as is sketched in Figs. 6, 7, 8 and 10 by finely dotted lines, i.e., corresponding to a continuous decrease of the k-value or to a continuous increase of roughness would in most of the cases fit the measurement points less well.

The examples under consideration offer too few safe criteria for a judgment of the further course of the v_m-line or of k above the transition (e.g. in Basle and Mastrils for $v_m > 3.0$ m/sec, in Arau and Nol for $v_m > 2.0$ m/sec). This topic does, however, no longer relate directly to our objective, the examination of the validity of the formula $v_m = kR^{2/3}J^{1/2}$.

Within the limits of roughness, which exist for the measurements contained in tables 1 to 10 (finest material: smoothed cement, most coarse material: head-sized stones) and for not too small dimensions in diameter (R > 0.037 m) the equation

$$v_m = kR^{2/3}J^{1/2} = kR^{1/6}R^{1/2}J^{1/2} \qquad (35)$$

or

$$c = k\sqrt[6]{R} \quad ^{1)} \qquad (35a)$$

can be considered as generally valid and this not only for slopes $J > 0.0007$, as was assumed by Gauckler (see. Eq. 6) but also for $J < 0.0007$ (cp. to Rhine/Nol, Rhine/Waldshut, Rhine/Basel, Sitter adit etc.). It is valid for open water courses as well as for pipelines. [2)]

---

[1]The dimension of k is $m^{1/3}\ sec^{-1}$.

[2]Of course, there also exists a limit of validity for the relation between R and the roughness, e.g. for large stones about R = 1.0 m.

In order to represent the various values of roughness in a clear way, or of the coefficient k respectively, the "reduced velocities" v' and v" were computed:

$$v' = \frac{v_m}{R^{2/3}} = \text{velocity which would occur in the}$$

respective case, maintaining slope and the roughness, but reducing the profile radius to 1.0 m;

$$v'' = \frac{v_m}{J^{1/2}}\,0.001^{1/2} = \text{velocity that would show up in}$$

keeping the cross-section, but reducing the slope to 0.001. In Figs. 15 and 16, the thus reduced velocities are combined in logarithmic diagrams.

In Fig. 15 the v'-points are collected along curves of constant k values [1] which appear as a straight line with slope 0.50 in the logarithmic diagram; thus the exponent of J again yields $\nu = 0.50$. The k values, divided by 100, can be read from the ordinate at $J = 0.1\ ^{\circ}/_{\circ\circ} = 0.0001$ since

$$v' = \frac{kR^{2/3}J^{1/2}}{R^{2/3}} = k \cdot 0.01$$

The line which results for T=R=1.0 after Matakiewicz (Eq. 10), is plotted as comparison. It can be seen that this curve crosses the set of v'-lines for rivers, in a way which corresponds on the whole to the different conditions; the deviations are yet significant (cp. our remark on page 2). The same comparison with the formula of Matakiewicz is also carried out in Figs. 6-13.

In a similar manner, the velocities reduced to constant slope

[1] For a movable river bed only the values for resting gravel were considered.

$J = 0.001$ are shown in Fig. 16 and they are compared with the corresponding values after Matakiewicz and Hermanek. For the latter formula the same remarks hold as for that of Matakiewicz.

In the following, an attempt is made to find the dependence of the coefficient k on the actual measure of wall roughness. For boulder carrying (gravel) rivers the latter can be expressed by the mean diameter ρ of the gravel particles. In this it is to be considered that river gravel is, in most cases, of a flat nature. The ratio of the three principal axes certainly is a variable within broad limits; however, quite often the approximate ratio 1:2:3 can be found, e.g. in the Rhine at Basle [1]. Some difficulties lie in the definition of the mean size of the pebbles, since in the same river cross-section, particle sizes can be found, in most cases, that range from the smallest to those of considerable size. The same definition of the roughness measure ρ can also be applied to fixed walls by interpreting ρ here as the diameter of small spheres with which the walls would have to be furnished to reach the equivalent hydraulic roughness effect as with a similar wall, furnished with a natural roughness.

For the series of measurement stations, which are contained in Tables 1 to 5, the mean diameters of the gravel grains were estimated. In each case an upper and a lower limit of ρ are assumed and shown in Fig. 17. These limits should not correspond to the uneven principal dimensions of <u>one</u> mean pebble, but they represent the mixture of different sized pieces, wherein single grains of extremely small or large dimensions can of course not be taken into consideration. For the Danube at Vienna the corresponding data could be taken from the

---

[1] cp. Lit. No. 7, p. 11: No. 1: stone of coarse-grained granite 20 x 15 x 6 cm.

publication of Schaffernak.[1] It follows from Fig. 5 on page 10 that the mean diameter lies within the limits of 10 and 30 mm. For cast iron pipes, not too rough boards, smoothed concrete and fine mud the mean size of the unevennesses can be estimated as 0.1 to 0.5 mm, for good ashlar masonry as 1 to 3 mm, for rough ashlar or fine gravel with a lot of sand as 3 to 10 mm.

In Fig. 17 the k values determined from the measurements are plotted for these degrees of roughness. It can be recognized in the logarithmic diagram that

$$k = \text{proportional } \rho^{-1/6} = \frac{\text{prop.}}{\sqrt[6]{\rho}} \tag{36}$$

By introducing this expression in Eq. 35 and replacing the proportionality factor of Eq. 36 by the expression $\alpha\sqrt{2g}$, it follows that

$$v_m = \frac{\alpha\sqrt{2g}}{\sqrt[6]{\rho}} R^{2/3} J^{1/2} = \alpha\sqrt{2g} \sqrt[6]{\frac{R}{\rho}} \sqrt{RJ} \tag{37}$$

or

$$J = \frac{1}{\alpha^2} \sqrt[3]{\frac{\rho}{R}} \cdot \frac{v_m^{\,2}}{R \cdot 2g} \tag{37a}$$

α is a dimensionless, absolute constant of magnitude 4.75; $\frac{1}{\alpha^2} = 0.0445$; $\alpha\sqrt{2g} = 21.1$ it may also be emphasized in here that the range of validity of Eqs. 37 is given by the limits which were mentioned for Eq. 35.

The flow or drag formula respectively reduces thus to a remarkably simple form for this relatively wide range of validity. In Chezy's equation

---

[1]Lit. No. 10.

$$v_m = c\sqrt{RJ}$$

$$c = 21.1\sqrt[6]{\frac{R}{\rho}} \tag{38}$$

is established, or in the general drag formula

$$J = \lambda' \frac{v_m^2}{R \cdot 2g} = \lambda \frac{v_m^2}{4R \cdot 2g}$$

the drag coefficient is

$$\lambda' = 0.0445\sqrt[3]{\frac{\rho}{R}} \qquad \text{or} \qquad \lambda = 0.178\sqrt[3]{\frac{\rho}{R}} \tag{39}$$

If ρ is understood as the measure of absolute wall roughness, one can characterize the quotient ρ/R as the measure of the proportional or relative roughness and the value $\sqrt[3]{\rho/R}$ as the "relative roughness factor".

Based on the preceding it is now obvious why in gravel beds the k value diminishes when the critical drag force, or velocity, respectively, is exceeded: whereas for resting gravel the stones generally lie flat and act with a smaller ρ upon the flowing water, the pebbles now roll over and act also with the larger dimension upon the water. In addition, those pebbles which temporarily lift totally off the ground also increase the wall roughness (4, p. 20 and 120). Finally, the water velocity has to decrease for a moving bottom also because part of the energy of the flowing water is used up by the movement of the bottom.

It shall also be noticed that the described transition, i.e., the increase in roughness, is not connected to the transition from tranquil flow to shooting flow. According to the publication of

Boess (2) a tranquil flow occurs in a rectangular cross-section, if the water depth is $T > \frac{v_m^2}{g}$, whereas the shooting flow is characterized by $T < \frac{v_m^2}{g}$. For Basel ($Q = 5500\ m^3/sec$) and Waldshut ($Q = 2346\ m^3/sec$ the corresponding values are, e.g.:

$$\text{Basel } \frac{v_m^2}{g} = \frac{3.57^2}{9.81} = 1.3 \text{ m} \qquad (T = \text{about } 7 \text{ m})$$

$$\text{Waldshut } \frac{v_m^2}{g} = \frac{2.78^2}{9.81} = 0.79 \text{ m} \qquad (T = \text{about } 4.2 \text{ m})$$

Even for the largest discharges measured, the flow is still tranquil for these two profiles.

For the rest, there is, in all experiments considered, no recognizable deviation from the law $v_m = kR^{2/3}J^{1/2}$, and also no change in the k-value, which could be attributed to the two different flow states (tranquil and shooting). In the Muehleberg adit the 6 measurement points are distributed among both states (18). The experiment series of Darcy and Bazin No. 7, 8 and 39 (Table 9 and Fig. 4) represent complete series for showing flowoff.

It shall be emphasized that as a base for hydraulic calculations the k values determined directly from measurements deserve preference to the relative roughness factor computed only from the gravel size, since the actual mean of the sediment grain size is in fact difficult to estimate. However, where there are no water quantity or velocity measurements available for a water course, an approximate guess for the roughness factor can be gained by comparison of the gravel size with other river courses.

For the measurement stations Mastrils, St. Margrethen, Nol, Waldshut, Basel and Aarau the limit velocities (or "critical velocities")[1)]

[1]Not identical with the critical velocity v_k of laminar flow.

were determined from Figs. 6 to 11. The velocities v_s' close to the bottom (about 5 cm above) could be taken for the corresponding water amounts from the original measurement; they were plotted in Figure 18 as a function of the gravel size, "ρ" = $\left(\frac{21.1}{k}\right)^6$, and were compared with the results of the laboratory experiments of Schaffernak (10). The limit or critical velocities found for the 6 mentioned Swiss hydrometric stations fit well into the critical zone determined by Schaffernak; thus the proof is given that the transitions in the diagrams of Figs. 6 to 13 indeed can be attributed to the onset of the sediment movement.

From these explanations it should be evident that in general the true roughness does not increase continuously with rising water level, but that in principle only two different roughnesses exist, which are separated by a transition zone. If the "roughness coefficient," n, after Ganguillet-Kutter and, ε, after Bazin increase somewhat in a certain profile for rising water level, and completely within the range of resting sediment, then this results from an incorrect construction of these formulas. Figure 19 makes a comparison in this respect possible: whereas the c-line after Ganguillet-Kutter fits the line $c = k\sqrt[6]{R}$ well in a quite extended domain (e.g. for k = 34.5 from R = 0.7 to R = 4.0 m or for k = 89.5 from R = 0.1 to R = 1.0), the c-lines computed according to Bazin and the short formula of Kutter diverge more.

With respect to the formula of Manning (Eq. 8)

$$v_m = \frac{1}{n} R^{2/3} J^{1/2}$$

which shows the correct setup in the exponents, it may be remarked that the values of $1/n$ do not have the same magnitude as the k-values. The deviations can be learned from tables 1 to 8; they are considerable especially for extreme slopes.

Finally some roughness coefficients, f, and fundamental factors, a, shall be given which result from the formula of Biel (Eq. 30) using the measurements contained in tables 1 to 10. This latter formula shall be valid for open sluices and closed pipelines, for all fluids and gases. Some typical results are:

Rhine at Basle	a = 0.25	f = 0.59
Seine at Raconnay	0.175	0.425
O.W. Channel, Rheinfelden	0.12	0.27
Sitter Addit	0.05	0.08
Test Channel of Bazin (cement)	0.026	0.07

In contrast to Biel's conception, who gave the fundamental factor, a, as a constant = 0.12, we thus find variable values for a, within the domains of examination covered. A clear comparison is made possible by Fig. 20, where the values $a_1 = a + f/\sqrt{R}$, after Biel, are contrasted with the corresponding values $\frac{1000}{c^2} = \frac{1000}{k^2 \sqrt[3]{R}}$ of the second formula (Eq. 6) of Gauckler. It clearly can be seen therefore that the lowest degree of roughness the deviations mainly appear for $R > 0.4$ m, i.e., in a range, for which Biel had no, or only a few, measurements available. The deviations are only very small for $k = 50$, i.e., for that degree of roughness, for which $a = 0.12$, which results from the experiments. This is just the value Biel stated himself.

The older formula of Lang for cast-iron pipes is also represented in Fig. 20; as can be seen, it yields much too high pressure losses for pipe diameters over 0.4 m ($R > 0.1$ m).

C. Derivation of Generally Valid Velocity and Drag Formulas

The approximation formula derived in section B must not a priori be assumed to be sufficiently precise for very small cross-sections and very smooth walls, because for its creation only measurements were used with $R > 0.037$ m and walls with $\rho > 0.1$ to 0.5 mm. In the present section it shall now be attempted to set up a generally valid formula for the mean velocity or the pressure loss in turbulent flow, respectively, based on measurement results for dimensions and roughness below these limits.

In Biel's formula, of which - being one of the newest - one would actually expect a general validity, an inconsistency was emphasised previously at the end of section B, that the "fundamental factor", a, is in fact not constant. Furthermore, it seems remarkable that the "viscosity factor", b, is dependent on the roughness according to the table on page 49. If b shall be a property of water, it is difficult to imagine that the wall exerts an influence on this physical property of water. It would thus appear more logical if b were a real constant. Likewise, the set up of the term linear in v_m has already been criticised, in that R occurs in the denominator raised to the power 1.5, whereas for the pure fluid viscosity, whose influence actually shall be expressed in the linear term, it has been shown theoretically and experimentally that the pressure loss is inversely proportional to the square of the diameter, or the hydraulic radius respectively.

However, a theoretically satisfying formula can be set up, based on the same data which Biel used, together with those newly published in the present paper.

For this purpose, the $\frac{J}{v_m}$ vs. v_m diagrams which Biel added to his work in the appendix, shall be interpreted in a somewhat different manner. In Figs. 21 to 27, a short selection of these diagrams is reprinted, and in Fig. 28, a measurement series of the present writer is added. Biel extracted the a_1 and b_1 values[1] from those diagrams in the way that he drew a straight line like the finely dotted one through the points above the upper limit velocity v_{g2} (e.g. Fig. 21); from the ordinate segment he computed b_1, and from the slope of the straight line the value a_1. In departure from this conception the position shall the taken that all points above the critical velocity v_k, that is not only above v_{g2}, belong to a uniform state and that they lie on a hyperbola, whose asymptote is the dashed-dotted line (Fig. 21).

The equation of this hyperbola has the form

$$\frac{J}{v_m} = \frac{1}{R}(M \cdot v_m + N - \frac{P}{v_m}) \tag{40}$$

Its physical meaning can be shown based on the following derivation:

The resistance, W, in kg, to be overcome by the flow over a pipe distance L can be considered to be proportional to the wetted surface, O, in m^2, the specific weight, γ, in kg/m^3, and to a function ϕ of the mean velocity v_m.[2] This resistance balances the force, k = pressure loss, h_w, in m, times specific weight, γ, in kg/w^3, times tube diameter, F, in m^2.

---

[1] $1000J = \frac{a_1}{R} v_m{}^2 + \frac{b_2}{R} v_m$

[2] The further examination shows then that ϕ (v_m) is also dependent on the profile radius.

$$W = O \cdot \gamma \cdot \phi(v_m) = \Delta p \cdot F = h_w \cdot \gamma \cdot F \tag{41}$$

Since O = circumference x length = U·L

it is $U \cdot L \cdot \gamma \cdot \phi(v_m) = h_w \cdot \gamma \cdot F$

or $\frac{U}{F}\,\phi(v_m) = \frac{h_w}{L} = J$

$J = \frac{1}{R}\,\phi(v_m)$

or $\frac{\Delta p}{L} = \frac{\gamma}{R}\,\phi(v_m)$ [1]

Whereas Biel set $\phi(v_m) = \frac{a_1}{1000}\,v_m^{\,2} + \frac{b_1}{1000}\,v_m$, it seems that, according to the aforementioned, the form $\phi(v_m) = Mv_m^{\,2} + Nv_m - P$ corresponds better with the results of the experimental investigations.

Thus, for the pressure head loss per meter tube length the equation follows

$$J = \frac{1}{R}\,(Mv_m^{\,2} + Nv_m - P) \tag{41a}$$

or for the pressure loss per meter tube length

$$\frac{\Delta p}{L} = \frac{\gamma}{R}\,(Mv_m^{\,2} + Nv_m - P) \tag{41b}$$

Dividing by v_m, it follows

$$\frac{J}{v_m} = \frac{M}{R}\,v_m + \frac{N}{R} - \frac{P}{Rv_m}$$

i.e., one obtains Eq. 40. For the determination of M and N it was proceeded in the way described previously; in the diagrams of Figs. 21 to 28, the sections of the dashed-dotted asymptote on the ordinate axes represent the values $\frac{N}{R}$, the slopes of the asymptotes versus the abscissa axes the values $\frac{M}{R}$; the $\frac{P}{R}$ value

[1]The further examination shows then that $\phi\,(v_m)$ is also dependent on the profile radius.

appears as ordinate section in between the fully drawn $\frac{J}{v_m}$ curve and the dashed-dotted asymptote for $v_m = \underline{1}$ m/sec. By multiplication of these values with R, one obtains M, N and P.[1)]

In Fig. 29, the 1000M and 1000N values were plotted as functions of the hydraulics radius for different roughnesses, in logarithmic coordinates. It follows from these plots:

1. $N = 2\pi \frac{\eta}{\gamma} R^{-1}$, if as an average water temperature of all measurement stations 12° (Celsius, transl.) is assumed, thus $\eta = 0.000134$. For R = 1.0 it usually follows from the diagram 1000N = 0.00084

$$N_{R=1} = 6.3 \frac{0.000134}{1000} = 6.3 \frac{\eta}{\gamma} = 2\pi \frac{\eta}{\gamma}$$

The inconsistency reproved in Biel's formula that the viscosity factor b is variable with the roughness, now disappears totally in that "b" is replaced by the absolute constant 2π. The further deficiency that the term linear in v_m contains $R^{1.5}$ in the denominator disappears, too, and one obtains for linear term

$$J_2 = \frac{1}{R} Nv_m = 2\pi \frac{\eta}{\gamma} \frac{v_m}{R^2}$$

This term shows the theoretically correct form and is π times as large as the pressure loss (gradient) of the pure laminar flow, which is, according to Eq. 32a

$$J = 2 \frac{\eta}{\gamma} \frac{v_m}{R^2}$$

---

[1]In order to obtain more reasonable numbers, M and N were replaced in Figs. 21 to 28 by their 1000-fold values, $a_1 = 1000M$, and $b_1 = 1000N$. These numbers a_1 and b_1 differ somewhat in magnitude from those which have been determined by Biel.

This latter point is also obvious from Figs. 21 to 27: the ordinate section of the asymptote is 3.14 times as large as the value J/v_m of the laminar flow.

Furthermore, from Fig. 29:

2. For very small dimensions

$$M = \frac{1}{s^2}$$

where s is a constant, independent of R;

for a somewhat larger hydraulic radius, however,

$$M = \frac{1}{k^2} R^{-1/3}$$

The "critical radius", i.e. that one which corresponds to the onset of the deviation from $M = \frac{1}{s^2}$, is larger for smoother walls. For drawn brass tubes it lies at about 0.0075 (D=3 cm), for wrought iron gas pipes it lies presumably below 0.003 (D=1.2 cm). Thus, the pressure loss term, quadratic in v_m, (the "pure turbulence term") above the "critical hydraulic radius", is

$$J_1 = \frac{1}{R} \cdot M \cdot v_m^2 = \frac{v_m^2}{k^2 R^{4/3}}$$

Below the critical hydraulic radius, it is

$$J_1 = \frac{v_m^2}{s^2 R}$$

3. Finally, the line of P-values contained in Fig. 29 shows that within the group of lead, brass and copper pipes below the critical hydraulic radius

$$P = \text{proportional } R^{-2}$$

P can also be determined by mere computation from the condition that for the critical velocity v_k the pressure loss of the laminar flow has to be the same as for turbulent flow, i.e.

$$2\,\frac{\eta}{\gamma}\,\frac{v_k}{R^2} = \frac{M}{R}\,v_k^{\,2} + \frac{N}{R}\,v_k - \frac{P}{R}$$

If $M = \frac{1}{s^2}$ and $N = 2\pi\,\frac{\eta}{\gamma}\,\frac{1}{R}$, as was found before, so it becomes

$$P = \frac{v_k^{\,2}}{s^2} + 2(\pi-1)\,\frac{\eta}{\gamma}\,\frac{1}{R}\,v_k$$

$$P = \left(\frac{2000\eta g}{s4R\gamma}\right)^2 + 2(\pi-1)\,\frac{\eta}{\gamma}\,\frac{1}{R}\,\frac{2000\eta g}{4R\gamma}$$

$$P = \left(\frac{\eta g}{\gamma R}\right)^2\left[\left(\frac{2000}{4s}\right)^2 + 218\right]$$

As can be seen, P, under otherwise identical circumstances, is in fact inversely proportional to the square of the hydraulic radius. A sample calculation, e.g. for R = 0.002 and y = 0.000148 (at $\tau = 7°C$) yields:

$$P = \left(\frac{0.000148\cdot 9.81}{1000\cdot 0.002}\right)^2\ \left[\left(\frac{2000}{4\cdot 70}\right)^2 + 218\right]$$

$$P = (0.000725)^2\cdot 261$$

$$1000P = 0.138$$

In Fig. 29 a value of 1000P = 0.15 can be read off for R = 0.002m, which is in sufficient agreement with the result of 0.138.

Since now the M-, N- and P values are known, they can be substituted into Eq. 41.[1] Thus, for smooth pipes (lead, copper, brass) with radii smaller than 3 cm (or profile radii below about 7 mm), the resulting pressure loss of turbulent flow is:

$$J = \frac{v_m^{\,2}}{s^2R} + \frac{2\pi\eta}{\gamma R^2}\,v_m - \left(\frac{\eta g}{\gamma}\right)^2\,\frac{\left[\left(\frac{2000}{4s}\right)^2+218\right]}{R^3} \qquad (42)$$

$$\frac{\Delta p}{L} = \frac{\gamma}{s^2R}\,v_m + \frac{2\pi\eta}{R^2}\,v_m - \frac{(\eta g)^2}{\gamma}\,\frac{\left[\left(\frac{2000}{4s}\right)^2 + 218\right]}{R^3} \qquad (42a)$$

for drawn brass pipes s = 70

for drawn lead pipes s = 79

[1]In Fig. 26a, Eq. 41 is shown graphically.

It shall be remarked, that for higher velocities the 3rd term (coming from P) is of minor importance compared with the others, and the significance decreases as pipe radius increases (c.p. Figs. 21 and 22 or 26 and 27).[1)]

For walls with irregularities and for profile radii above about 7 mm

$$J = \frac{v_m^2}{k^2 R^{4/3}} + \frac{2\pi\eta}{\gamma R^2} v_m - \left(\frac{2000\eta g}{4k}\right)^2 \frac{1}{R^{3.33}} \tag{43}$$

As far as higher velocities and profile radii are concerned, the 3rd term can be neglected, so that

$$J = \frac{v_m^2}{k^2 R^{1.33}} + \frac{2\pi\eta}{\gamma R^2} v_m \tag{43a}$$

or

$$\frac{\Delta p}{L} = \frac{\gamma}{k^2 R^{1.33}} v_m^2 + \frac{2\pi\eta}{R^2} v_m \tag{43b}$$

Solving equation (43a) for the velocity, it becomes

$$v_m = \sqrt{k^2 R^{4/3} \cdot J + \left(\frac{\pi\eta}{\gamma} \frac{k^2}{R^{2/3}}\right)} - \frac{\pi\eta k^2}{\gamma R^{2/3}} \tag{43c}$$

The equations (43), (43a) and (43b) are not only valid for water, but generally for fluids and gases. This follows from the points Nos. 73, 75, 86, 92 and 93 entered in Fig. 29 (numeration according to "Biel", 1). These measurements deal with atmospheric air, pressurized air, natural gas and steam. The a_1 and 1000M-values respectively are dependent on R in the same way and lie on the same lines in Fig. 29, as the results for water for corresponding wall material.

---

[1] For very large η-values, e.g. for oil, this term must not be neglected.

The following table shows the physical properties of these gases in comparison to those of water:

No. acc. to Biel & type	D m	R m	1000M	$k=\sqrt{\frac{1}{MR}}$	1000M	γ kg/m	$\frac{\eta}{\gamma}=\frac{NR}{2\pi}$	$10^6\cdot\eta$
				Cast Iron Pipes				
75 nat. gas	0.05	0.0125	0.63	83	0.625	0.5	$1.24\cdot10^{-6}$	0.62
79 sat. vapor 5 atm.	0.075	0.0188	0.375	100	0.94	2.6	$2.83\cdot10^{-6}$	7.35
86 sat. vapor	0.14	0.035	0.375	90	-	-	-	-
93 atm. air	0.325	0.081	0.325	85	0.241	1.24	$3.11\cdot10^{-6}$	3.86
M.L. water	0.15	0.0375	0.394	87	0.0277	1000	$0.166\cdot10^{-6}$	166
				Wrought Iron Pipes				
73 comp. air	0.047	0.01175	0.229	138	-	-	-	-
73 sat. vapor	0.047	0.01175	0.235	137	-	-	-	-
82 sat. vapor 3.5 atm.	0.10	0.025	0.262	114	0.92	1.9	$3.68\cdot10^{-6}$	7.0
92 comp. air 7.2 atm.	0.30	0.075	0.133	134	0.036	8.6	$0.43\cdot10^{-6}$	3.7
28 water	0.0395	0.00988	0.286	128	0.074	1000	$0.116\cdot10^{-6}$	116

Although the η and the $\frac{\eta}{\gamma}$ values vary within broad limits, the k values agree with those found earlier for water. This fact proves that k, and thus also $(\frac{\Delta p}{L})_1 = \frac{\gamma v_m^2}{k^2 R^{4/3}}$, i.e., the turbulence term of the pressure loss, is totally independent of the viscosity, η.

Equations 42 and 43 represent the generally valid expressions for the pressure loss or the gradient in flows above the critical velocity, that is for turbulent flow. In the following, they shall be applied to some specific areas of validity.

1. Smooth Brass Pipes, $s = 70$

range: $D = 0.01$ to 0.04 m

or $R = 0.0025$ to 0.01 m

$v = 1$ to 4 m/s

The calculation of some values using Eq. 42 and their plotting in a logarithmic coordinate system (not attached to this paper) show that within the above-mentioned range, the general equation (Eq. 42) can be replaced with sufficient precision by

$$J = 0.00009 \frac{v_m^{1.75}}{R^{1.25}} \tag{44}$$

This equation has the form as it was set up by Saph and Schoder based on their experiments in smooth brass pipes, and also as was given by Blasius as the equation of pressure loss in turbulent flow.

Solving Eq. 44 for the mean velocity v_m gives

$$v_m = k' \, R^{0.71} \, J^{0.57} \tag{44a}$$

If one applies Eisner's Eq. 34

$$v_m = K_0^{\varphi} \, \rho^{\psi} \, R^{1.5\varphi-\psi-1} \, J^{0.5\varphi}$$

to this range of validity, the φ and ψ-values result from the conditions

$$\left.\begin{aligned} 0.5\varphi &= 0.57 \\ 1.5\varphi - \psi - 1 &= 0.71 \end{aligned}\right\} \quad \begin{aligned} \varphi &= 1.14 \\ \psi &= 0 \end{aligned}$$

Thus is becomes

$$v_m = K^{1.14} \, \rho^0 \, R^{0.71} \, J^{0.57}$$

The roughness factor ρ contains the exponent 0; with $\rho^0 = 1$ the roughness loses its influence. This conclusion is apparently related to the fact that the pipes can be described as "smooth", i.e. not affected by roughness, although in the mathematical sense $\rho \neq 0$.

2. Wrought Iron Pipes of Moderate Diameter

$k = 30$; range: $D = 0.10$ to 0.40 m

$R = 0.025$ to 0.10 m

$v = 0.5$ to 4.0 m/s

The same calculation according to Eq. 43a and plotting as under 1 yields

$$J = \lambda'' \frac{v_m^{1.90}}{R^{1.40}} \tag{45}$$

or $$v_m = k'' R^{0.735} J^{0.525} \tag{45a}$$

The φ- and ψ-values of Eisner's formula are for this range:

$$\left.\begin{aligned} 0.5\varphi &= 0.525 \\ 1.5\varphi-\psi-1 &= 0.735 \end{aligned}\right\} \qquad \begin{aligned} \varphi &= 1.05 \\ \psi &= -0.16 \end{aligned}$$

$$v_m = K_0^{1.05} \rho^{-0.16} R^{0.735} J^{0.57}$$

3. Cast Iron Pipes with $D > 0.10$ m and $v_m > 1$ m/s

$k = 89$. Under these conditons, the linear term in v_m becomes so small that it can be neglected in comparison to the quadratic one; thus only the latter remains, which sall be denoted the "mere turbulence term."

$$J = \frac{v_m^{2}}{k^2 R^{1.33}} \tag{46}$$

or $$v_m = k\, R^{0.66} J^{0.50} \tag{46a}$$

This is Eq. 35, which we had already set up in section B based on the measurements used there and which is also nearly identical with the formulas of Tutton. Thus it proves, according to the investigations of section C, to be a sufficiently exact approximation formula for the roughnesses III and higher (following Biel's classification), as well as for profiles with $R > 0.025$ m.

Disregarding the influences of fluid viscosity, and considering only the "mere turbulence," one has to substitute in Eq. 41 for $\Phi(v_m) = \frac{v_m^2}{k^2R^{1/3}}$, i.e. the drag becomes

$$W = \frac{\sigma \cdot \gamma \cdot v_m^2}{k^2R^{1/3}} = \sqrt[3]{\frac{\rho}{R}}\,\frac{\sigma \cdot \gamma \cdot v_m^2}{\alpha^2 2g} \tag{46b}$$

We had found the expression $\sqrt[3]{\frac{\rho}{R}}$ already in Eq. 39 and denoted it as the "relative roughness factor." <u>The resistance to be overcome by the flow over a certain distance thus is proportional to the relative roughness factor $\sqrt[3]{\frac{\rho}{R}}$, proportional to the wetted surface σ, proportional to the specific weight of the fluid γ and proportional to the velocity head $\frac{v_m^2}{2g}$</u>.

Eisner's numbers φ and ψ are for this range of validity:

$$\left.\begin{aligned} 0.5\varphi &= 0.5 \\ 1.5\varphi-\psi-1 &= 0.666 \end{aligned}\right\} \qquad \begin{aligned} \varphi &= 1.5 \\ \psi &= -0.166 = -\frac{1}{6} \end{aligned}$$

$$v_m = K_0\ \rho^{-1.6}\ R^{0.666}\ J^{0.50}$$

$$= K_0 \sqrt[6]{\frac{R}{\rho}} \cdot \sqrt{RJ}$$

This form is identical with Eq. 37, derived in section B.

The formula of Forchheimer, $v_m = k_3R^{0.7}J^{0.5}$, which Eisner especially emphasises in his publication, would yield the following φ- and ψ- values:

$$\left.\begin{aligned} 0.5\varphi &= 0.5 \\ 1.5\varphi-\psi-1 &= 0.7 \end{aligned}\right\} \qquad \begin{aligned} \varphi &= 1.5 \\ \psi &= -0.20 = -\frac{1}{5} \end{aligned}$$

$$v_m = K_0\ \rho^{-1/5}\ R^{0.7}\ J^{0.5}$$

$$= K_0 \sqrt[5]{\frac{R}{\rho}}\ \sqrt{RJ}$$

4. Finally, an attempt is made to apply Eisner's formula to laminar flow.

$$v_m = \frac{\gamma}{2\eta} R^2 J$$

$$\left.\begin{array}{r} 0.5\varphi = 1 \\ 1.5\varphi - \psi - 1 = 2 \end{array}\right\} \qquad \begin{array}{l} \varphi = 2 \\ \psi = 0 \end{array}$$

$$v_m = K_0^2 \rho^0 R^2 J$$

Also in this case, the wall roughness has no effect, since $\rho^0 = 1$; this corresponds to the theoretical point of view.

Eisner's formula thus represents a generally valid equation of power law from, but with variable exponents.

At this point, the meaning of the so called Reynolds number $\frac{v_m D\gamma}{\eta g} \equiv \frac{v_m D}{\delta}$ shall be discussed briefly. The drag coefficient λ in $J = \lambda \frac{v_m^2}{D \cdot 2g}$, which, as is well known, is not constant, not even for given wall material, often is shown as a function of Reynolds number (see e.g. Blasius, 21). For smooth pipes and within certain limits for diameter and velocity, a positive dependence of λ on the Reynolds number alone could in fact be found. This can be seen from the dashed area shown in Fig. 30 for the experiments of Saph-Schoder with brass pipes. From the determined relation $\lambda = 0.3164 \left[\frac{v_m D}{\delta}\right]^{-1/4}$, which holds above the critical value $\left[\frac{v_m D}{\delta}\right] = 2000$ (below which, the flow is laminar) Blasius found the equation

$$J = \lambda \frac{v_m^2}{D \cdot 2g} = 0.316 \left[\frac{v_m D}{\delta}\right]^{-1/4} \cdot \frac{v_m^2}{D \cdot 2g}$$
$$= \frac{0.158\ \eta^{1/4}\ v_m^{1.75}}{g^{3/4}\ \gamma^{1/4}\ D^{1.25}}$$

However, the copper pipe investigated by Lang deviates from this power law for higher velocities; three other pipes with the same natural wall roughness diverge even more. For further increasing Reynolds number (over 200,000) the drag coefficient λ becomes independent of Reynolds number. According to Blasius λ then is dependent on the ratio $\frac{\rho}{D}$ or $\frac{\rho}{R}$. This dependecy is obviously given by our relation stated on page 14, $\lambda = 0.78\sqrt[3]{\frac{\rho}{R}}$.

As a final result of section C, it can be recalled that beside the result of the generally valid formulas (Eqs. 42 and 43, page 23), the pure power law v_m $F(\rho)$ R^{μ} J^{ν} can be applied, but that the exponents μ and ν are variable. For the area of application, which especially interests the hydraulic engineer, i.e. for streams and rivers, channels, adits, conduits and pipes with diameters of over about 0.10 m, for practical computation the very convenient power law

$$v_m = k\ R^{2/3}\ J^{1/2}$$

or

$$v_m = k\ \sqrt[6]{R}\ \sqrt{RJ}$$

yields sufficiently exact results.

D. The Velocity distribution in the Cross-section

Whereas in the preceding paragraphs only the mean velocity in the cross-section was treated, here also the change of the velocity at various points of a given cross-section shall be looked into.

The development of new equations, which are based on the results of section C, might be preceded by a short survey of some existing formulas for very broad, open water cases (6).

1. Eytelwein $v = (1-0.0127t)\ v_0$

   at the bed $v_s = (1-0.0127t_a)\ v_0$

2. Bazin $v = v\ -\ 20\ (\frac{t}{t_a})^2\ \sqrt{RJ}$

(parabola with the origin of the horizontal axis at the water surface, see Fig. 31, bottom graph)

at the bed $\quad v_s = v_o - 20\sqrt{RJ}$

from that $\quad v_m = v_o - \frac{20}{3}\sqrt{RJ}$

on the other hand, also according to Bazin

$$v_m = \frac{87\sqrt{R}}{\varepsilon + \sqrt{R}}\sqrt{RJ}$$

$$v_o = \left(\frac{87\sqrt{R}}{\varepsilon + \sqrt{R}} + \frac{20}{3}\right)\sqrt{RJ}$$

3. Hagen $\quad v = v_o\ (1 - 0.0582\sqrt{t}\ )$

(parabola with vertical axis in a distance v_s away from the ordinate axis, see Fig. 31)

at the bed $\quad v_x = v_o\ (1 - 0.0582\sqrt{t_a}\ )$

4. Christen

$$v = v_o\sqrt[8]{1 - \frac{t}{t_a}} = \frac{\sqrt{2\sqrt[4]{k^5}}}{0.4354}\sqrt{TJ}\sqrt[8]{B_o(1 - \frac{t}{t_a})}$$

(parabola of 8th order with vertical axis coinciding with the ordinate axis)

at the bed $\quad v_s = 0.$

In general it can be said that the equation for v should have the same structure as the one which had been quoted for v_m in section A at the corresponding place. It seems obvious that v_m is only a special value of v. This is the case just as well for the velocity v_o at the surface; in other words, the quotients $\frac{v}{v_o}$ and $\frac{v_o}{v_m}$ must be mere numbers. These conditions however are not fulfilled totally by any of the aforementioned 4 formulas; since after Eytelwein it is $\frac{v}{v_o} = 1 - 0.0127t$

after Hagen $\frac{v}{v_o} = 1 - 0.0582\sqrt{t}$

after Bazin $\frac{v}{v_o} = \frac{v_o - 20\left(\frac{t}{t_a}\right)^2 \sqrt{RJ}}{\left(\frac{87\sqrt{R}}{\varepsilon + \sqrt{R}} + \frac{20}{3}\right)\sqrt{RJ}}$

In these three cases the quotient $\frac{v}{v_o}$ appears wrongly not as mere numbers or ratio values.

The formula of Christen $v = v_o \sqrt[8]{1 - \frac{t}{t_a}}$ would be correct in the structure, but in

$$v = \frac{\sqrt{2}\,\sqrt[4]{k^5}}{0.4354}\sqrt{TJ}\,\sqrt[8]{B_o\left(1 - \frac{t}{t_a}\right)}$$

the exponent of k is different from that in the equation for v_m (Eq. 11). Furthermore, it is to be remarked that formulas which give a value $v_s > 0$, a priori violate the obviously correct opinion, that due to the adhesion of the fluid to the wall, the velocity has to be zero directly at the bed, assuming it is smooth.[1] Also in this respect, Christen's formula is still the best; however, what cannot appear correct in it is the fact that it yields for $B_o = \infty$ also in infinitely high velocity. This opposes the practical understanding since even for infinitely large width the hydraulic radius has a finite magnitude, namely $= t_a$; thus also the velocity has to be of finite magnitude.

---

[1]The carrying of gravel at the bed, which only can happen for a velocity different from zero is no proof against the corrections of the above opinion; for as a rough movable bed we no longer deal with a mathematically uniform flow state in the whole profile, due to wall irregularities, and the carrying of movable parts is a consequence of vortex creation behind the irregularities.

a) Laminar Flow

Before a new formula is set up for the velocity distribution of turbulent flow, the known derivation of the equation for laminar flow shall be reproduced. According to Newton (9, p.7, and 1, p.3) the frictional force, which acts through the movement of neighboring fluid layers on a moderately thin layer, is

proportional to the coefficient, η, of inner friction,

proportional to the contact area, F,

proportional to the difference, ∂v, of the velocities on opposite sides of the layer, and

inversely proportional to the thickness ∂z of the layer;

$$K = \eta F \frac{\partial v}{\partial z}$$

1. For a circular pipe, if one set z = r, the results are

$$dv = \frac{1}{\eta} \frac{K}{F} dr$$

(with increasing r, v decreases, thus minus sign)

$$\frac{K}{F} = \frac{h_w \gamma \pi r^2}{L 2\pi r} = \frac{1}{2} J \gamma r$$

$$dv = - \frac{\gamma}{2\eta} J \cdot r \cdot dr$$

$$v = - \frac{\gamma}{\eta} \left(\frac{r}{2}\right)^2 J + C$$

Since for $r = r_a$, due to the adhesion of the fluid to the wall v becomes = 0, it is

$$0 = - \frac{\gamma}{\eta} \left(\frac{r_a}{2}\right)^2 J + C$$

thus

$$v = \frac{\gamma}{\eta} J \left[\left(\frac{r_a}{2}\right)^2 - \left(\frac{r}{2}\right)^2 \right] \tag{47}$$

The mean v_m can be computed from the condition

$$\pi r_a^2 \cdot v_m = \int_o^{r_a} 2\pi r \, dr \, v$$

$$\pi r_a^2 \cdot v_m = \frac{2\pi\gamma}{\eta} J \int_o^{r_a} \left[\left(\frac{r_a}{2}\right)^2 - \left(\frac{r}{2}\right)^2 \right] \cdot r \cdot dr$$

$$= \frac{2\pi\gamma}{\eta} J \left[\left(\frac{r_a}{2}\right)^2 \cdot \left(\frac{r^2}{2}\right) - \frac{r^4}{16} \right]_o^{r_a}$$

$$\underline{\underline{v_m}} = \frac{\gamma}{2\eta} J \left(\frac{r_a}{2}\right)^2 = \underline{\underline{\frac{\gamma}{2\eta} J R^2}} \tag{48}$$

In the pipe center, for $r = 0$, it becomes

$$v = V_o = \frac{\gamma}{\eta} J \left(\frac{r_a}{2}\right)^2 = 2 v_m \tag{49}$$

$$V_o = 2 v_m$$

$$v = 2 v_m \left[1 - \left(\frac{r}{r_a}\right)^2 \right] = V_o \left[1 - \left(\frac{r}{r_a}\right)^2 \right] \tag{49a}$$

The condition stated on page 31, that $\frac{v}{V_o}$ or also $\frac{v}{v_m}$ have to be mere numbers, thus is fulfilled in this case.

The profile of the velocity, plotted versus the radius, has the known parabola shape (see 9, p.147; 1, p.3; or the present work, Fig. 31).

2. <u>For a very broad, square profile of depth t_a, open on top</u> the corresponding integration of the equation yields

$$K = \eta F \frac{\partial v}{\partial z}$$

$$v = \frac{1}{2} \frac{\gamma}{\eta} J \, (t_a^2 - t^2)$$

$$v_m = \frac{1}{3} \frac{\gamma}{\eta} J \, t_a^2$$

$$V_o = \frac{3}{2} v_m$$

$$v = \frac{3}{2} v_m \left[1 - \left(\frac{t}{t_a}\right)^2 \right] = V_o \left[1 - \left(\frac{t}{t_a}\right)^2 \right]$$

Equations 47 to 49a have been derived based on a simple theoretical understanding of the nature of laminar flow. If there existed a theory just as simple for turbulent flow, the corresponding formulas for the latter obviously could be derived easily. Because of the lack of such a theory it shall now be tried to set up a formula for v (velocity at an arbitrary point of the cross-section), based only on the empirically found formula $v_m = k\sqrt[6]{R}\sqrt{RJ}$ and the condition of an identical structure.

b) Turbulent Flow

1. Square profile of infinite width; $R = t_a$

On trial, the statement is made

$$v = \frac{7}{6} k \sqrt[6]{t_a - t} \sqrt{RJ} \tag{50}$$

The structure is here the same as for v_m; the value $\sqrt[6]{R}$ is replaced by the value $\sqrt[6]{t_a - t}$.

A further criterion for the correctness of Eq. 50 lies in the condition of the mean value:

$$B_o \cdot t_a \cdot v_m = \int_o^{t_a} B_o \cdot dt \cdot v$$

$$t_a \cdot v_m = \frac{7}{6} k\sqrt{RJ} \int_o^{t_a} (t_a - t)^{1/6}\, dt$$

$$= \frac{7}{6} k\sqrt{RJ} \left[\frac{(t_a - t)^{7/6}}{-\frac{7}{6}}\right]_o^{t_a} = \frac{7}{6}\,\frac{6}{7}\, k\sqrt{RJ}\;\; t_a^{7/6}$$

$$v_m = k\, t_a^{1/6}\sqrt{RJ} = k\, R^{1/6}\sqrt{RJ}$$

By averaging we thus come back again to the equation for v_m; the statement $v = \frac{7}{6} k \sqrt[6]{t_a - t}\,\sqrt{RJ}$ is apparently correct.

The combination of Eq. 50 with the one for v_m yields

$$v = \frac{7}{6} v_m \sqrt[6]{1 - \frac{t}{t_a}} \tag{51}$$

$$v_o = \frac{7}{6} v_m \tag{51a}$$

$$v = v_o \sqrt[6]{1 - \frac{t}{t_a}} \tag{51b}$$

Finally, it remains to check whether for $t = t_a$, v_s becomes zero (adhesion condition).

For Eq. 50, substituting $t = t_a$, gives $v = 0$.

In Fig. 31, the velocities in the vertical, measured with a wing, are plotted for the measurement profiles on the St. Margarethen, O.W. channel Rheinfelden and the channel, San Giovanni Lupatoto (channel center)[1]; comparison with the curve given by Eq. 51 results in quite good agreement.

The practical rules, long known to the water measurement specialist, that in broad profiles for each vertical the surface velocity is about $\frac{7}{6}$ times the mean, and that the mean velocity is present at about $\frac{6}{10}$ of the depth, or $\frac{4}{10}$ above the bed, are now confirmed by our Eq. 51a and by the diagrams in Fig. 31.

As an important conclusion, the theorem can be obtained from Eq. 51 and the measurements displayed in Fig. 31, that the shape of the velocity profile is independent of the roughness. The observation that in flat profiles with large stones, the velocity decreases faster towards the bed, does not mean a contradiction hereto, since for a water depth of e.g. only 0.30 m and stones of 0.15 m diameter the equation

[1]The plotted data are ratio=averages from a larger number of verticals.

$$v_m = \alpha \sqrt{2g}\sqrt[6]{\frac{R}{\rho}}\sqrt{RJ}$$

apparently no longer holds, since we no longer deal with an "ordered flow" in this case.

2. Full circular profile with large diameter

The trial form for the velocity in an arbitrary point of the cross-section is

$$v = \frac{13}{12} k \sqrt[12]{(\frac{r_a}{2})^2 - (\frac{r}{2})^2} \sqrt{RJ} \tag{52}$$

The expression under the 12th root is equivalent to the value $\sqrt[6]{R}$ in $v_m = k \sqrt[6]{R} \sqrt{RJ}$, the condition of identical structure for v and v_m is fulfilled.

The mean value condition is

$$\pi r_a^2 v_m = \int_o^{r_a} 2\pi r \cdot dr \cdot v$$

substituting $(\frac{r}{2})^2 \equiv \sigma$

then $(\frac{r_a}{2})^2 \equiv \sigma_a$

and $\frac{r}{2} dr = d\sigma$

Thus it becomes

$$r_a^2 v_m = \frac{13}{12} 4k \sqrt{RJ} \int_o^{\sigma_a} (\sigma_a - \sigma)^{1/12} d\sigma$$

$$(\frac{r_a}{2})^2 v_m = \frac{13}{12} k \sqrt{RJ} \left[\frac{(\sigma_a-\sigma)^{13/12}}{-\frac{13}{12}}\right]_o^{\sigma_a} = \frac{13}{12}\frac{12}{13} k \sqrt{RJ}\, \sigma_a^{13/12}$$

$$(\frac{r_a}{2})^{24/12} v_m = k \sqrt{RJ} (\frac{r_a}{2})^{26/12}$$

$$v_m = k \sqrt{RJ} (\frac{r_a}{2})^{1/6} = k \sqrt[6]{R} \sqrt{RJ}$$

Equation 52 thus, in fact, gives the required mean value for v.

Equation 52 can be transformed into

$$v = \frac{13}{12} v_m \sqrt[12]{1 - (\frac{r}{r_a})^2} \tag{52}$$

Furthermore, the velocity in the pipe center is

$$V_o = \frac{13}{12} v_m \tag{52a}$$

$$v = V_o \sqrt[12]{1 - (\frac{r}{r_a})^2} \tag{52b}$$

(Compare with Eq. 49a, for laminar flow)

In Fig. 32, two measurement series in a pipe with large diameter are displayed. The curve computed from Eq. 52 agrees well with the experimentally determined one; the somewhat eccentric position of the main flow (probably because of a throttle valve) makes a dip appear in the middle, which however is not related to the nature of turbulent flow. As a comparison, a v-curve is also plotted in this supplement, as it results from the equation set up by Prof. Prášil (9, p. 146)

$$v = \frac{5}{4} c \sqrt{RJ} \sqrt[4]{(\frac{r_a}{2})^2 - (\frac{r}{2})^2}$$

$$v = \frac{5}{4} v_m \sqrt[4]{1 - (\frac{r}{r_a})^2}$$

This formula has been derived based on the assumption of a constant, R-independent c-value in Chézy's equation $v_m = c \sqrt{RJ}$

The velocity distribution in the Sitter-adit is shown in Fig. 33. Although the profile is not exactly circular, and not even running full, the deviation of the calculated v-line from the experimentally determined velocity distribution is nevertheless not significant.

3. Smaller circular profiles

For Eq. 45a: $v_m = k'' R^{0.735} J^{0.525} \sim k'' R^{1/4} R^{0.5} J^{0.525}$

the distribution of v can be set up in a similar manner as

$$v = \frac{9}{8} v_m \sqrt[8]{1 - (\frac{r}{r_a})^2} \tag{53}$$

$$v_m = \frac{8}{9} V_o = 0.89\ V_o$$

The velocity distribution, therefore, represents a combination of pure turbulence and pure friction (laminar flow). Such a case is displayed in Fig. 34. The measurement points agree comparatively well with the computed curve. Regarding the somewhat larger deviation at the point where v = 4.4 m/sec, it should be noted that it is partially an inaccuracy in the measurement, because with this value a smaller mean value v_m would result than was given by Darcy (about 4.35 m/sec instead of 4.5 m/sec). According to Forcheimer (6, p. 117 to 120), where the experiments of Hele-Shaw are quoted, the motion close to the wall moreover seems to be only laminar and not turbulent, even for larger pipe diameters. The velocities close to the wall then become somewhat smaller than according to the above equation, which was derived under the assumption of a uniform state in the whole cross-section. (This also can be recognized at Niagara and the Sitter adit.) Under these circumstances, the velocity in the pipe center is then somewhat greater, so that the relation $v_m = 0.82\ V_o$ to $0.857\ V_o$, experimentally determined by Williams, Hubbel and Frenckell, can probably be considered to be correct, whereas we have found $v_m = \frac{12}{13} V_o = 0.923\ V_o$ for the pure turbulent motion.

4. <u>Rectangle of finite width</u>

A strictly mathematical treatment of this profile shape is not possible in a single way. Thus, an attempt is made to obtain an approximate formula in an independent way by a combination of the results found so far.

For an infinitely wide rectangular profile the mean velocity is the same for all verticals, namely

$$\bar{v} = k\ t_a^{2/3}\ J^{1/2}$$

The variation of $\bar{v}$ over the <u>finite</u> width can approximately be

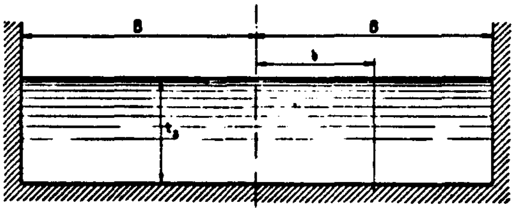

assumed to be equal to the variation of the velocity over the diameter of a circular profile; it can be substituted

$$J = \vartheta\ k\ t_a^{2/3}\ J^{1/2}\ \sqrt[12]{1 - (\tfrac{b}{B})^2} \qquad (54)$$

The factor ϑ is a function of the ratio $\frac{2B}{t_a}$. For large widths, the velocity will approach that magnitude which would exist in an infinitely wide profile of same depth; thus converges for increasing ratio $\frac{2B}{t_a}$ to the value 1. From measurements in the Sitter adit, where for smaller fillings the profile can be considered nearly as a rectangle, as well as from those in the headwater channel Rheinfelden, the results are:

for $\frac{2B}{t_a}$	=	1.5	2.0	2.9	5.8	11.0	∞
ϑ	=	0.61	0.66	0.75	0.88	0.98	1.0
$v_m : v_{max}$	=	0.867	0.875	0.874	0.848		0.857

In Figs. 35 to 37, three examples are considered. The computation of the $\bar{v}$ was performed in the way that the individually somewhat variable t_a-values were inserted in Eq. 54. The agreement with the measured results is satisfactory.

5. Triangular profile

For this profile the variation of $\bar{v}$ can also be assumed to follow Eq. 54; in this case, t_a is variable. If the ratio $\frac{2B}{R} = \frac{4B}{T_a}$ becomes ∞ for finite T_a, the triangle turns into a rectangle of infinite width. For this case, the factor ϑ has to become = 1.

From measurements in the approximately triangular, although not symmetric, profiles of Basle, Nol and Aarau it follows:

for	$\frac{2B}{R}$ =	25	50	65	∞
	ϑ =	0.85	0.91	0.92	1.0

Figures 38 and 39 show the checking of one measurement each for Basle and Nol.

6. The ratio of the maximum surface velocity, V_o, and the mean velocity, v_m, in natural river profiles

The measurement results contained in Tables 1 to 5 for natural river profiles show that the ratio $\frac{\bar{v}}{v_o}$ does not retain the value $\frac{6}{7}$, but that it is smaller for triangular cross-sections and that it is larger for rectangular profiles, increasing with decreasing channel width, as compared to the depth. Based on this result, as well as on the earlier findings, it will be attempted in the following, to set up a relation between the mean velocity v_m and the maximum surface velocity V_o for relatively broad profiles. Such a formula is of importance for practical hydrometrics, in that it would become, by this means, extraordinarily easy to compute the mean velocity and thus the flow rate (where often an accuracy of 5 to 8% sufficies), depending on the surface velocity measured on the line of most rapid flow and the already determined cross-section.

From the three equations

$$\overline{V} = \vartheta\, k\, T_a^{2/3}\, J^{1/2} \qquad 1)$$

$$v_m = k\, R^{2/3}\, J^{1/2}$$

$$\frac{\overline{V}}{V_o} = \frac{\overline{v}}{v_o} \qquad 2)$$

it follows that

$$\frac{v_m}{V_o} = \frac{\overline{v}}{v_o} \cdot \frac{1}{\vartheta} \left(\frac{R}{T_a}\right)^{2/3} \qquad (55)$$

The applicability of the approximate formula (Eq. 55) for natural channels, which are neither too irregular nor too great in depth (as compared to width), is illustrated by the following table:

	R m	T_a m	$\frac{\overline{v}}{v_o}$	$\frac{2B}{R}$	ϑ	v_m m/sec	v_o m/sec	$v_m : v_o$ after measurement	$v_m : v_o$ acc. to Eq. 55
Nol (triangular profile)									
22.II.05	2.94	5.0	0.825	24.0	0.85	0.536	0.797	0.673	0.68
13. V .16	3.60	6.35	0.823	24.2	0.85	1.37	2.17	0.631	0.66
Waldshut (triang. profile)									
27. I .05	2.336	4.25	0.853	64	0.92	1.054	1.685	0.626	0.624
31. I .20	3.14	6.19	0.84	54	0.91	1.771	2.837	0.624	0.593
Basel (triang. profile)									
31. I .89	2.157	3.80	0.856	70	0.92	0.99	1.52	0.652	0.638
parabola shaped XI.67	2.10	2.50	0.823	95	0.97 *)	1.945	2.63	0.74	0.755
Kaiserstuhl (nearly rectang. profile)									
24. I . 04	1.846	2.33	0.876	47.6	0.99	1.145	1.595	0.718	0.748
27. I . 03	1.993	2.566	0.875	46	0.99	1.261	1.74	0.725	0.745
O.W. Channel Rheinfelden (nearly rectang. profile)	3.772	4.673	0.885	14.8	0.99	1.993	2.540	0.785	0.77

*) For these parabola shaped profiles, ϑ will be considered as the average between the ϑ-values for triangles and rectangles.

---

[1] $\overline{V}$ = mean velocity in the vertical of largest depth T_a.

[2] The ratio $\overline{v}/v_o$ shall be assumed equal for all verticals of a certain cross-section.

7. The influence of the profile shape on the mean velocity, v_m

For an infinitely wide rectangular profile, as well as for a full circular cross-section, the mean velocity, by integration, is

$$v_m = k\, R^{1/6} \sqrt{RJ}$$

based on the concepts of a velocity distribution in pure turbulent flow, as explained in this work.

The validity of this equation is thereby not proved at all for other profile shapes. In fact, already Bazin found that the sharp corners in a rectangular profile diminish the mean velocity compared to a semicircular cross-section. Just as every hydraulics specialist knows, during the onset of flooding, for rivers with broad over-banks, the discharge and thus v_m, is not likely to decrease, although the hydraulic radius will suddenly decrease.

The term hydraulic radius in the sense used thus far, i.e. as uniquely determining the magnitude of the mean velocity, thus can be valid only for cross-sectional shapes of a certain continuity and regularity of configuration (no sharp corners or sudden changes in width); strictly speaking, it could only be accepted for a few shapes, e.g. for the infinitely wide rectangle and the full circle.

E. Application on Stagnation (Backwater, transl.) Computations

For uniform water motion (neither accelerated nor decelerated) the total slope J or the level difference Δh = JL of a stage is used to overcome the energy loss of turbulent flow; for decelerated, but steady-state flow over obstructions, however, the total head loss JL of a section is commonly divided into friction loss and the change of the velocity head uniform: $$LJ = \Delta h = \frac{v_m^2 L}{c^2 R} \tag{56}$$

during deceleration: $$LJ = \Delta h = \frac{v_m^2 L}{c^2 R} + \frac{v_1^2 - v_2^2}{2g} \tag{57}$$

or $$\Delta h = \frac{Q^2 UL}{c^2 F^3} + \beta \frac{v_1^2 - v_2^2}{2g} \tag{57a}$$

$$\equiv A_1 + \beta A_2$$

For a regular pattern of the cross-sections, the mean velocity v_1 in the lower profile of a section is in most cases smaller than v_2 in the upper profile, so that consequently A_2 becomes negative. The difference of water levels from the upper to the lower end of a stage decreases for decelerated flow by the modulus of the gain in velocity head compared to uniform flow. Now, the conversion of flow energy into pressure head energy does not occur free of losses, so that the value $\frac{v_1^2 - v_2^2}{2g}$ has to be multiplied by an efficiency factor β. This can be assumed to be about $\frac{2}{3}$ according to experiments of Andres (17), for open water courses, if there is no formation of roles. In contrast to this, one can consider the continuous conversion of pressure head to velocity as nearly loss-free, so that $\beta = 1$ if $A_2 > 0$.

Some experiences in low head systems with stagnation computations for the projects and the subsequent observation of the measured decelerations, showed that the latter often did not extend so far upstream as could have been assumed according to computations. The reasons might lie partially in the completely unjustified use of inappropriate stagnation formulas, but mostly in the incorrect choice of the roughness coefficients.

Based on an example (bars at Laufenburg on the Rhine) it thus will be investigated in this final section whether, by the use of the formulas gained in section B and the viewpoints on the roughness of gravel beds, a stagnation computation could be performed, which is confirmed as reliable by the measurement of an actual backwater curve.

The computations are contained in Tables 12 to 14, and plotted in Fig. 40 in the form of a longitudinal section.

The bar field at Laufenburg consists mainly of two parts: a lower section with rocky bed from 17.140 km to 15.739 km and an upper section with a gravel bed, above 15.739 km. For the rocky lower part, the mean k-value was determined as 14.9, for the gravel bed with stationary sediment as k = 35 (computed from the unobstructed low water), for moving sediment as k = 30.5 (from the unobstructed high water). The transition from the higher value k = 35 to the lower one, k = 30.5, was assumed between v_m = 2.2 and 2.4 m/sec in two steps, first from 35 to 32.5, then from 32.5 to 30.5. It shall be explicity emphasized, that also for the high water level Q = 2280 m^3/sec, the higher roughness of the moving sediment was inserted only in the uppermost section of the bar field, where v_m > 2.2 m/sec. The use of the higher roughness also in the lower part of the bar field, which often can be seen in the prevailing practice, had to lead to incorrect results, in that the stagnation extended less far for this water passage than was computed.

The practical realization of the computations in Tables 12 to 14, with $c = k \sqrt[6]{R}$ is much simpler than according to Ganguillet-Kutter, because c is independent of the head. The question at hand, whether in Kutter's c-formula the head of the choked level should be inserted or the friction head, is thus totally eliminated. The computation was performed in the usual way upstream of the bar field in that a certain level height was assumed on trial at the upper end of an individual section, and F, R, v_1, v_2 and c were computed from that. The values obtained in that way, substituted into Eq. 57a, had to yield again the assumed value Δh. If this was not the case, the process was repeated until agreement was reached.

Figure 40 shows a sufficient approximation of the stagnation curves computed in this way, to the real, measured backwater lines.

F. Final Summary

The main results of the present study can be summarized in the following way:

1. For cross-sections with profile radii over 6-7 mm the pressure loss per m pipe length of an arbitrary liquid, in the domain of turbulent flow, is

$$\frac{\Delta p}{L} = \frac{\gamma}{k^2 R^{1.33}} v_m^2 + \frac{2\pi\eta}{R^2} v_m$$

or the gradient (slope of the water level)

$$J = \frac{1}{k^2 R^{1.33}} v_m^2 + \frac{2\pi\eta}{\gamma R^2} v_m$$

2. If the hydraulic radius exceeds the value of about 3 to 4 cm, the latter equation can be reduced, for water, without creation of an essential error to the formula

$$J = \frac{v_m^2}{k^2 R^{1.33}}$$

which is identical to Gauckler's second velocity formula

$$v_m = k\, R^{2/3}\, J^{1/2}$$

Within the ranges of dimensions, roughnesses and velocities that occur in hydraulic engineering, the second Gauckler formula can thus be considered a generally valid equation for the mean velocity of uniform motion in rivers, channels and closed pipes (see table of k-values, p. 47).

3. The velocity coefficient k is inversely proportional to the 6th root of the roughness measure ρ (diameter of the sediment grain or of the uneveness) and it is namely

$$k = \frac{21.1}{\sqrt[6]{\rho}}$$

For flat river pebbles in their state of rest, usually the smallest dimension is considered; for moving gravel a larger one, approximately corresponding to the middle principal axis is used.

4. For turbulent flow, the velocity in the vertical of a wide sluice, open on top, is distributed according to the equation

$$v = \frac{7}{6} v_m \sqrt[6]{1 - \frac{t}{t_a}}$$

in a circular, full running pipe of sufficient diameter according to

$$v = \frac{12}{13} v_m \sqrt[12]{1 - (\frac{r}{r_a})^2}$$

Table of Coefficients

	k New Formula	n Gang-Kutter	$\frac{1}{n}$ Mann-ing	ε Bazin	$\sqrt{2k_4^3}$ Christen	f Biel
Rock, coarse	15 ÷ 20					
Rock, medium	20 ÷ 28					
Head-sized stones	25 ÷ 30				11.3÷15.6	0.90
Gravel, coarse, ap. 50/100/150	35	0.030	33.3	1.75	18.2	0.75
Gravel, medium, ap. 20/40/60	40	0.025	40	1.30	29.8	0.50
Gravel, fine, ap. 10/20/30	45	0.022	45.5		42.1	
Fine gravel with lots of sand, coarse ashlar masonry	50	0.020	50	0.85	34.5	0.29
Good ashlar masonry	60	0.017	58.8	0.46	39.3	0.18
Well planked concrete, unplastered						
Homestone ashlars, well fitted bricks	80	0.013	76.9	0.16	56.1	0.072
Riveted sheet metal tube, several times overlapped in the perimeter	65 ÷ 70					
Dto., 1 sheet in the perimeter	85 ÷ 100					
New, castiron pipes, smoothed concrete, wooden panels, staves, fine mud	90	0.012	83.3			0.036÷ 0.054
Pipes with moderate incrustation	70					
Flattened cement, planed wood	100	0.010	100	0.06	71.7	
Glass pipes, galvanized pipes	125 ÷ 135					0.018
Drawn brass and copper pipes	150					0.0064

Literature Used

1. R. Biel,
On the Head Loss in the Transfer of Liquid and Gaseous Fluids.
Berlin, 1907.

2. P. Boess,
Computation of the Water Level Position during the Change of the Flow State.
Diss. Karlsruhe, 1919.

3. T. Christen,
The Law of Translation of Water in Regular Channels, Rivers and Pipes.
Leipzig, 1903.

4. Dr. Leon W. Collet,
The Carrying of Gravel in Certain Water Courses of Switzerland.
Annals of Switzerland, National Hydrography, Vol. II,
Bern, 1916.

5. Dr. J. Eppes,
The Development of Hydrometry in Switzerland.
Edited by the Swiss Hydrometric Bureau,
Bern, 1907

6. Ph. Forchheimer,
Hydraulics.
Berlin, 1914.

7. C. Ghezzi,
The Discharge Conditions of the Rhine at Basle.
Communication No. 8 of the Section for Water Affairs of the Swiss Department of the Interior,
Bern, 1915.

8. W. R. Kutter,
The New Formulas for the Motion of Water in Channels and Regular River Sections.
Vienna, 1871.

9. Prof. Dr. F. Prásil,
Technical Hydrodynamics.
Berlin, 1913.

10. Prof. Dr. F. Schaffernak,
New Foundations for the Computation of the Gravel Carriage in River Courses.
Leipzing and Vienna, 1922.

11. R. Weyrauch,
Hydraulic Computation.
Stuttgart, 1915.

12. Contributions to the Hydrography of Austria: III Issue: The Hydrometric Survey on the Danube Close to Vienna in the Year 1897. Vienna, 1899.

Journals

13. The Water Force, Munich, 1. June 1922, Issue 11, p. 207. Dipl. Mg. F. Eisner: The New Velocity Formula

14. Central Paper of the Construction Administration, Berlin 1921, No. 27, 2 April. Administrative Advisor and Construction Councillor Bayerhaus: The Sophism from the Mississippi - Measurements of Humphreys and Abbott and the Faulty Structure of the Ganguillet-Kutter Formula.

15. Central Paper of the Construction Administration, Berlin 1922, No. 1/2, 4 January. Dr. ing. Krey: The foundations of the General Discharge Formula $v = A\ R^b\ J^c$.

16. Central Paper of the Construction Administration, Berlin 1922, No. 63, 5 August. The Foundations of the General Discharge Formula $v = A\ R^b\ J^c$ (submitted Drs. Krey, Eisner and Beyerhaus).

17. Communications of Research Works of the Association of German Engineers, Issue 76 (see also Forchheimer, Lit. No. 5, p. 230).

18. Switzerland Water Affairs, Zurich, 25 July 1922. A. J. Keller: The Experiments on the Bottom Discharge Adit Muehleberg and Their Processing.

19. Switzerland, Construction Journal, 1908, Vol. 52, p. 206.

20. Switzerland, Construction Journal, 1911, Vol. 58, p. 100.

21. Journal of the Association of German Engineers, 1912. Vol. 56, No. 16, p. 639.

During the printing of this paper, the following was published:

Prof. Dr. Ph. Forchheimer, The Flow of Water Through Pipes and Drains, Especially Through Canals of Large Dimensions. Berlin 1923.

[1] Table of a, f, and b: (see p. 5)

Degree of Roughness	I	II	III	IV	V
Coefficient, a	0.12	0.12	0.12	0.12	0.12
Roughness coefficient, f	0.0064	0.018	0.036	0.054	0.072
Viscosity coefficient, b	0.95	0.71	0.46	0.27	0.27
$\frac{b(n)}{\gamma}$ for water of 12°C	0.0118	0.0088	0.0057	0.0032	0.0032
" for water of 100°C	0.00294	0.0022	0.00142	0.00084	0.00084

TABLE 1

MEASUREMENT Location & Date	Type	Q m^3/sec	V_m m/sec	J	T m	B_o m	R m	$R^{2/3}$ $m^{2/3}$	$R^{1/2}$ $m^{1/2}$	$J^{1/2}$	C from $v_m = C\sqrt{RJ}$	Gang.-Kutter n	$\frac{V}{V_o}$	Bazin ε	Hermanek V_m m/sec	Matakiewicz V_m m/sec	$V_m = k \cdot R^{2/3} \cdot J^{1/2}$: $R^{2/3} \cdot J^{1/2}$	$V' = \frac{V_m}{R^{2/3}}$	V''	k	$\frac{1}{n}$
Hinter-Rhein, Domleschg Rothenbrunnen																					
22. I. 1898	Fl.	12,85	0,891	0,00288	0,475	30,32	0,473	0,608	0,688	0,0537	24,13	0,0344	0,799	1,79	0,78	1,02	0,0327	1,47	0,522	27,3	29,1
17. III. 1913	Fl.	17,83	0,920	0,00508	0,416	46,55	0,411	0,553	0,641	0,0713	20,14	0,0392	0,754	2,13	0,91	1,03	0,0395	1,67	0,408	23,3	25,5
30. III. 1899	Fl.	18,18	0,941	0,00241	0,612	31,50	0,608	0,718	0,780	0,0490	24,58	0,0360	0,785	1,98	0,92	1,16	0,0392	1,31	0,607	24,0	27,8
7. XII. 1915	Fl.	22,13	0,929	0,00525	0,487	48,89	0,481	0,614	0,693	0,0725	18,49	0,0442	0,750	2,56	1,08	1,27	0,0446	1,51	0,405	20,8	22,6
21. VIII. 1915	Schw.	61,16	1,520	0,00578	0,810	49,69	0,791	0,856	0,890	0,0760	22,47	0,0419	—	2,57	1,89	1,85	0,0650	1,78	0,632	23,3	23,8
7. IX. 1902	Schw.	106,46	1,956	0,00534	1,040	52,28	1,020	1,013	1,010	0,0731	26,49	0,0379	—	2,31	2,33	2,20	0,0740	1,92	0,842	26,4	26,4
7. VI. 1900	Schw.	185,80	2,484	0,00496	1,410	53,10	1,377	1,238	1,173	0,0704	30,06	0,0357	—	2,22	3,04	2,65	0,0872	2,01	1,115	28,6	28,0
16. VI. 1901	Schw.	352,26	3,344	0,00462	1,950	53,80	1,885	1,525	1,372	0,0680	35,85	0,0315	—	1,95	3,81	3,27	0,1035	2,19	1,550	32,3	31,8
Rhein Felsberg																					
6. II. 1902	Fl.	24,30	0,928	0,00202	0,722	36,25	0,706	0,792	0,840	0,0448	24,555	0,0374	0,813	2,13	0,990	1,17	0,0355	1,170	0,655	26,1	26,7
5. IV. 1899	Fl.	79,70	1,369	0,00265	1,040	55,90	1,026	1,017	1,013	0,0515	26,255	0,0383	0,808	2,35	1,645	1,715	0,0523	1,348	0,840	26,2	26,1
23. VIII. 1915	Schw.	107,16	1,786	0,00270	1,046	57,45	1,028	1,018	1,015	0,0519	33,900	0,0297	—	1,59	1,660	1,74	0,0527	1,755	1,085	33,9	33,7
1./2. VIII. 1899	Schw.	167,90	1,841	0,00190	1,388	65,70	1,359	1,228	1,165	0,0436	30,657	0,0375	—	1,62	1,855	1,90	0,0535	1,500	1,340	34,4	26,7
9. VI. 1900	Schw.	235,46	1,943	0,00221	1,790	67,70	1,748	1,450	1,322	0,0469	31,247	0,03605	—	2,34	2,470	2,43	0,0680	1,340	1,360	28,6	27,8
7. VI. 1900	Schw.	329,72	2,312	0,00252	2,050	69,40	2,000	1,586	1,414	0,0502	32,590	0,0354	—	2,37	2,920	2,87	0,0797	1,458	1,455	29,0	28,2
17. VI. 1901	Schw.	389,70	2,651	0,00380	2,000	73,40	1,968	1,570	1,403	0,0617	30,655	0,0377	—	2,58	3,520	3,17	0,0970	1,690	1,360	27,3	26,5
Rhein Mastrils																					
7. II. 1898	Fl.	28,64	0,872	0,000856	0,873	37,72	0,855	0,900	0,924	0,0292	32,23	0,0300	0,845	1,571	0,780	1,09	0,0262	0,97	0,942	33,3	33,3
11. II. 1902	Schw.	31,17	0,982	0,001233	0,908	34,89	0,878	0,918	0,937	0,0351	29,84	0,0325	—	1,794	0,975	1,17	0,0322	1,07	0,855	30,5	30,8
8./9. IV. 1899	Fl.	97,60	1,640	0,00155	1,17	50,9	1,153	1,10	1,07	0,0394	38,8	0,02648	0,815	1,334	1,41	1,52	0,0434	1,49	1,315	37,8	37,8
8. IX. 1902	Schw.	218,20	2,396	0,005016	1,16	78,55	1,265	1,17	1,125	0,0708	31,9	0,0322	—	2,13	2,52	2,32	0,0830	2,05	1,070	29,0	31,0
2./3. VIII. 1899	Schw.	253,65	2,526	0,00590	1,28	78,5	1,252	1,163	1,12	0,0768	29,39	0,0358	—	2,21	3,03	2,55	0,0895	2,16	1,040	28,2	27,9
8. V. 1900	Schw.	408,44	3,001	0,00562	1,67	81,55	1,633	1,39	1,28	0,0750	31,33	0,0354	—	2,28	3,73	3,00	0,1040	2,16	1,265	28,8	28,2
16. VI. 1901	Schw.	1095,47	4,086	0,00500	3,09	86,9	2,999	2,08	1,730	0,0707	33,37	0,0373	—	2,24	5,60	4,62	0,1470	1,96	1,825	27,8	26,8
Rhein St. Margrethen																					
9. II. 1921	Fl.	47,65	0,878	0,00087	0,685	79,24	0,685	0,777	0,827	0,0295	35,9	0,0253	—	1,18	0,62	0,83	0,0228	1,13	0,94	38,4	39,5
8. II. 1922	Fl.	54,69	0,900	0,00087	0,769	79,00	0,770	0,842	0,877	0,0295	34,8	0,0271	—	1,31	0,70	0,91	0,0248	1,065	0,96	36,3	36,9
28. II. 1919	Fl.	70,44	1,039	0,00087	0,885	79,86	0,885	0,923	0,940	0,0295	37,5	0,0257	—	1,24	0,80	1,01	0,0272	1,13	1,11	38,2	38,9
26. II. 1920	Fl.	93,78	1,120	0,00087	1,036	80,76	1,040	1,027	1,02	0,0293	37,4	0,0266	—	1,35	0,93	1,12	0,0303	1,09	1,21	37,0	37,6
12. IV. 1922	Fl.	116,96	1,215	0,00086	1,208	79,66	1,208	1,134	1,10	0,0293	37,8	0,0271	—	1,44	1,06	1,24	0,0332	1,07	1,31	36,7	36,9
27. IX. 1921	Fl.	147,73	1,326	0,00086	1,369	81,41	1,370	1,230	1,17	0,0293	38,7	0,0270	—	1,45	1,23	1,38	0,0360	1,08	1,43	37,0	37,0
27. IV. 1920	Fl.	236,51	1,593	0,0009	1,785	83,16	1,785	1,470	1,335	0,030	39,8	0,0276	—	1,58	1,56	1,68	0,0441	1,08	1,67	36,2	36,2
10. IX. 1920	Fl.	244,84	1,597	0,0009	1,860	82,40	1,860	1,510	1,36	0,030	39,2	0,0281	—	1,66	1,59	1,73	0,0453	1,06	1,68	35,2	35,6
20. VI. 1919	Fl.	648,92	2,020	0,0009	2,587	124,17	2,587	1,883	1,61	0,030	41,7	0,0279	—	1,75	2,26	2,20	0,0565	1,07	2,12	35,7	35,8

Measurements of the Swiss Bureau of Water Affairs

Fl. = wing
Schw. = float

NOTE: Commas in data entries should be replaced by decimal points to convert to the North American convention.

TABLE 2

MEASUREMENT: Location & Date	Type	Q m^3/sec	v_m m/sec	J	T m	B_0 m	R m	$R^{2/3}$ $m^{2/3}$	$R^{1/2}$ $m^{1/2}$	$J^{1/2}$	c from $v_m = c\sqrt{RJ}$	Gang.-Kutter n	$\frac{v}{v_0}$	Bazin ε	Hermanek v_m m/sec	Matakiewicz v_m m/sec	$v_m = k \cdot R^{2/3} \cdot J^{1/2}$: $R^{2/3} \cdot J^{1/2}$	$v' = \frac{v_m}{R^{2/3}}$	v''	k	$\frac{1}{n}$
Rhein Nol																					
22. II. 1905	Fl.	113,18	0,536	0,000038	2,99	70,40	2,942	2,055	1,73	0,00617	50,693	0,02676	0,825	1,255	0,476	0,48	0,0127	0,26	2,74	42,2	37,4
12. I. 1904	Fl.	161,66	0,700	0,000055	3,07	75,20	3,011	2,08	1,73	0,0074	54,39	0,0239	0,784	1,02	0,585	0,64	0,0154	0,335	2,99	45,4	41,8
5. II. 1915	Fl.	182,00	0,762	0,000071	3,09	77,60	3,018	2,09	1,74	0,0084	52,16	0,0247	0,812	1,095	0,665	0,75	0,0176	0,365	2,86	43,3	40,5
23./24. I. 1903 .	Fl.	207,65	0,842	0,000091	3,12	79,00	3,065	2,11	1,75	0,00955	50,42	0,0253	0,807	1,275	0,760	0,82	0,0201	0,40	2,78	42,0	39,6
18. u. 20. V.1901	Fl.	356,58	1,209	0,000151	3,41	86,40	3,354	2,24	1,83	0,01253	52,686	0,02369	0,781	1,185	1,065	1,08	0,0281	0,54	3,05	43,0	42,2
13. V. 1916	Fl.	437,90	1,369	0,000235	3,68	87,00	3,600	2,35	1,90	0,0153	47,07	0,0268	0,823	1,605	1,380	1,49	0,0360	0,58	2,825	38,0	37,3
4. VIII. 1905 ..	Schw.	449,13	1,41	0,000249	3,61	88,3	3,54	2,32	1,88	0,0158	47,42	0,0265	0,799	1,57	1,410	1,50	0,0366	0,61	2,82	38,5	37,8
20. VI. 1910....	O. Fl.	987,05	2,139	0,000408	4,90	94,04	4,766	2,84	2,185	0,0202	48,507	0,0266	—	1,750	2,270	2,28	0,0574	0,75	3,36	37,3	37,6
Rhein Kaiserstuhl																					
1. II. 1905	Fl.	161,90	1,038	0,000394	1,790	87,00	1,777	1,465	1,33	0,01985	39,23	0,0286	0,882	1,620	1,04	1,155	0,0291	0,710	1,650	35,7	35,0
24. I. 1904	Fl.	186,72	1,145	0,000360	1,865	87,60	1,846	1,502	1,36	0,01897	44,48	0,02518	0,876	1,305	1,025	1,145	0,0285	0,764	1,900	40,2	39,8
23. I. 1904	Schw.	187,74	1,134	0,000360	1,887	87,70	1,871	1,520	1,367	0,01897	43,75	0,0257	—	1,355	1,035	1,160	0,0288	0,748	1,885	39,3	39,0
28. I. 1903	Schw.	227,64	1,234	0,000386	2,02	91,20	1,993	1,580	1,41	0,01963	44,49	0,0255	—	1,348	1,13	1,25	0,0311	0,783	1,985	39,8	39,2
27. I. 1903	Fl.	232,58	1,261	0,000386	2,02	91,20	1,993	1,580	1,41	0,01963	45,464	0,0249	0,875	1,289	1,13	1,25	0,0311	0,800	2,030	40,7	40,2
7. X. 1904	Schw.	290,82	1,357	0,000397	2,19	97,90	2,125	1,670	1,47	0,0199	46,29	0,0248	—	1,290	1,22	1,34	0,0333	0,813	2,160	40,8	40,3
31. VII. 1904 ..	Schw.	386,85	1,522	0,000405	2,52	100,90	2,48	1,830	1,57	0,0201	48,03	0,0243	—	1,255	1,36	1,435	0,0366	0,833	2,410	41,6	41,2
22. VI. 1910....	O. Fl.	1014,13	2,480	0,000430	5,08	80,50	4,87	2,870	2,21	0,0207	54,31	0,0230	—	1,322	2,37	2,46	0,0593	0,866	3,780	41,9	43,5
Rhein Waldshut																					
13./14. II. 1905	Fl.	283,61	0,901	0,000195	2,20	143,30	2,171	1,675	1,470	0,01396	43,79	0,02672	0,908	1,455	0,86	0,94	0,0234	0,538	2,04	38,4	37,4
23. u. 27. I. 1905	Fl.	368,50	1,054	0,000226	2,36	148,00	2,336	1,760	1,528	0,01500	45,87	0,02564	0,853	1,36	0,97	1,10	0,0263	0,598	2,22	40,0	39,0
27./28. I. 1904 .	Fl.	422,11	1,182	0,000302	2,36	151,40	2,334	1,757	1,528	0,01735	44,52	0,02633	0,857	1,46	1,12	1,24	0,0305	0,673	2,16	38,8	38,0
30./31. I. 1903 .	Fl.	518,05	1,365	0,000425	2,45	154,60	2,428	1,805	1,558	0,02060	42,49	0,02776	0,850	1,61	1,37	1,52	0,0372	0,757	2,09	36,7	36,0
13. X. 1904	Schw.	751,15	1,615	0,000360	2,86	163,00	2,822	1,996	1,68	0,0187	50,669	0,0234	—	1,17	1,395	1,52	0,0373	0,810	2,72	43,3	42,7
31. I. 1920	Fl.	957,64	1,771	(0,00040)	3,18	169,80	3,140	2,143	1,77	0,0200	50,10	0,0234	0,840	1,31	1,620	1,72	0,0428	0,825	2,79	41,2	42,7
28. V. 1921	Fl.	1045,27	1,816	(0,00042)	3,35	171,72	3,290	2,212	1,81	0,0205	49,00	0,0242	0,769	1,41	1,725	1,79	0,0453	0,823	2,80	40,1	41,3
8. VIII. 1905 ..	Schw.	1544,53	2,246	0,000488	3,88	176,60	3,831	2,449	1,96	0,0231	51,54	0,0237	—	1,47	2,170	2,16	0,0566	0,918	3,07	39,9	42,2
7. VIII. 1905 ..	Schw.	1842,03	2,443	0,000590	4,25	177,85	4,158	2,585	2,038	0,0243	49,41	0,02532	—	1,575	2,44	2,55	0,0630	0,945	3,17	38,8	39,5
8. VI. 1907.....	Schw.	1859,32	2,544	0,000831	4,12	177,55	4,046	2,540	2,010	0,0288	43,87	0,0289	—	1,950	2,83	2,90	0,0734	1,000	2,79	34,7	34,6
14. VII. 1909 ..	O. Fl.	2156,89	2,675	0,000995	4,11	196,41	4,055	2,540	2,015	0,03155	39,96	0,0321	—	2,130	3,09	3,11	0,0803	1,055	2,67	33,3	31,2
13. VII. 1909 ..	O. Fl.	2346,80	2,780	0,001105	4,22	200,22	4,166	2,585	2,040	0,0332	43,17	0,0295	—	2,290	3,31	3,31	0,0860	1,075	2,65	32,3	33,9

Measurements of the Swiss Bureau of Water Affairs

O.Fl. = Surface Measurement with wing

TABLE 3

MEASUREMENT Location & Date	Type	Q m^3/sec	v_m m/sec	J	T m	B_o m	R m	$R^{2/3}$ $m^{2/3}$	$R^{1/2}$ $m^{1/2}$	$J^{1/2}$	C $v_m = c\sqrt{RJ}$	Gang.-Kutter n	$\frac{v}{v_o}$	Bazin ε	Hermanek v_m m/sec	Matakiewicz v_m m/sec	$v_m = k \cdot R^{2/3} \cdot J^{1/2}$: $R^{2/3} \cdot J^{1/2}$	$v' = \frac{v_m}{R^{2/3}}$	v''	k	$\frac{1}{n}$
Rhein Basel																					
31. I. 1889	Fl.	325,80	0,991	0,000290	2,18	151,17	2,157	1,67	1,468	0,01703	39,35	0,0297	0,856	1,76	1,04	1,15	0,0284	0,60	1,835	34,9	33,6
9./11. I. 1889 ..	Fl.	385,37	1,082	0,000340	2,21	160,70	2,198	1,69	1,480	0,0184	39,52	0,0296	0,832	1,76	1,13	1,22	0,0311	0,64	1,860	33,6	33,8
4./5. III. 1913 .	Fl.	463,86	1,330	0,000475	2,278	152,70	2,263	1,72	1,503	0,0218	40,69	0,0287	0,845	1,72	1,38	1,48	0,0375	0,77	1,925	35,5	34,8
4./5. III. 1913 .	Fl.	515,87	1,406	0,000535	2,34	156,52	2,325	1,755	1,523	0,0232	39,87	0,0295	—	1,82	1,49	1,57	0,0406	0,80	1,915	34,6	33,9
6. XII. 1912 ...	Fl.	655,44	1,580	0,000635	2,476	167,52	2,461	1,82	1,568	0,0252	39,97	0,0296	0,845	1,86	1,69	1,73	0,0460	0,87	1,975	34,3	33,8
29. XII. 1913 ..	O. Fl.	669,23	1,848	0,000071	2,058	176,00	2,051	1,613	1,430	0,0327	39,43	0,0290	—	1,728	1,905	2,00	0,0528	1,145	1,785	35,0	34,5
22. XII. 1914 ..	O. Fl.	726,77	1,698	0,000669	2,540	168,50	2,522	1,86	1,590	0,0259	41,34	0,0287	—	1,78	1,775	1,89	0,0500	0,91	2,03	34,0	34,8
6.–13. XI. 1867	Fl. u. Schw.	828,84	1,945	0,000232	2,117	201,27	2,100	1,64	1,448	0,03505	38,24	0,0301	0,823	1,848	2,08	2,17	0,0575	1,190	1,775	33,8	33,2
31. III. 1913 ...	O. Fl.	839,48	1,737	0,000722	2,691	179,60	2,672	1,925	1,634	0,02685	39,55	0,0304	—	1,961	1,91	2,03	0,0518	0,900	2,035	33,5	32,9
31. III. 1913 ...	O. Fl.	895,14	1,812	0,000736	2,746	179,92	2,727	1,95	1,650	0,0271	40,45	0,0297	—	1,88	1,96	2,00	0,0530	0,93	2,11	34,2	33,7
12. VI. 1912....	O. Fl.	1492,30	2,300	0,000920	3,551	182,70	3,514	2,31	1,875	0,0304	40,45	0,0310	—	2,18	2,68	2,64	0,0703	1,00	2,38	32,7	32,2
1. VII. 1911 ...	O. Fl.	1678,10	2,454	0,000866	3,727	183,50	3,689	2,39	1,920	0,0294	43,42	0,0288	—	1,928	2,675	2,75	0,0705	1,025	2,63	34,8	34,7
30. VI. 1911....	O. Fl.	1703,90	2,462	0,000894	3,768	183,65	3,729	2,41	1,930	0,0300	42,64	0,0294	—	2,01	2,76	2,75	0,0725	1,02	2,58	33,9	34,0
13. VI. 1896....	O. Fl.	2260,60	2,625	0,001054	4,494	191,66	4,426	2,695	2,100	0,03245	38,43	0,0342	—	2,658	3,40	3,38	0,0870	0,976	2,55	30,2	29,2
12. VII. 1910 ..	Log.	2538,00	2,729	0,001100	5,014	185,50	4,927	2,90	2,220	0,0332	37,3	0,0356	—	2,91	3,79	3,68	0,0962	0,940	2,601	28,4	28,1
12. VII. 1910 ..	O. Fl.	2775,00	2,989	0,001122	4,844	191,65	4,780	2,84	2,190	0,03350	40,81	0,0322	—	2,474	3,72	3,60	0,0952	1,050	2,82	31,3	31,1
13. VI. 1876....	Schw.	5500,00	3,570	0,001100	—	—	7,140	3,71	2,670	0,0332	40,0	0,0342	—	3,10	4,75	4,55	0,1225	0,963	3,390	29,2	29,2
Rhein bei Istein																					
Kalkfels	—	—	2,18	0,0050	—	—	1,28	1,18	1,13	0,0706	27,4	0,0386	—	2,46	2,77	2,48	0,0833	1,85	0,98	26,3	25,9
	—	—	1,83	0,0025	—	—	1,52	1,32	1,23	0,050	29,7	0,0377	—	2,37	2,32	2,25	0,066	1,38	1,15	27,8	26,5
Germersheim (Pfalz)																					
Grebenau 1866 .	Fl.	—	1,54	0,000247	—	—	3,308	2,22	1,817	0,0157	53,70	0,0218	—	1,105	1,305	1,40	0,0348	0,695	3,10	44,2	45,8
Speyer (Pfalz)																					
Strauß	Fl.	—	0,887	0,000112	—	—	2,96	2,01	1,72	0,01058	48,60	0,0260	—	1,34	0,825	0,92	0,0212	0,443	2,65	41,9	38,5
Rhein in Holland																					
Brünings Nr. 1 .	—	—	1,122	0,000220	—	—	2,64	1,91	1,62	0,01482	46,4	0,0267	—	1,40	1,04	1,17	0,0283	0,587	2,38	39,5	37,5
„ „ 2 .	—	—	0,910	0,000115	—	—	3,52	2,30	1,875	0,01073	45,1	0,0286	—	1,74	0,935	0,99	0,0247	0,395	2,67	36,8	35,0
„ „ 3 .	—	—	0,918	0,000111	—		3;79	2,43	1,95	0,01053	44,8	0,0299	—	1,84	0,973	1,03	0,0257	0,377	2,76	35,7	33,4
„ „ 4 .	—	—	1,474	0,000220		—	3,80	2,43	1,95	0,01482	50,8	0,0255	—	1,38	1,37	1,50	0,0361	0,605	3,14	40,9	39,2
„ „ 5 .	—	—	1,310	0,000115	—	—	4,90	2,89	2,213	0,0107	59,0	0,0224	—	1,26	1,20	1,23	0,0310	0,452	3,86	42,2	44,7
„ „ 6 .	—	—	1,210	0,000110			5,11	2,97	2,260	0,0105	50,6	0,0270	—	1,58	1,21	1,28	0,0312	0,410	3,63	38,8	37,0
Krayenhoff Nr. 1	—	—	0,845	0,000116			1,82	1,49	1,347	0,0108	58,0	0,0192	—	0,67	0,58	0,60	0,0161	0,566	2,47	52,4	52,1
„ „ 2	—	—	0,889	0,000117	—		2,31	1,75	1,52	0,0108	53,8	0,0220	—	0,92	0,69	0,75	0,0189	0,508	2,60	47,0	45,4
„ „ 3	—	—	0,965	0,000104	—		3,38	2,25	1,84	0,0102	51,2	0,0250	—	1,28	0,87	0,95	0,0229	0,430	2,98	42,0	40,0
„ „ 4			0,999	0,0000998	—		3,41	2,27	1,845	0,0100	54,0	0,0235	—	1,11	0,85	0,94	0,0227	0,440	3,16	44,0	42,6
„ „ 5		—	1,090	0,0000977	—		5,015	2,93	2,240	0,0099	49,1	0,0283	—	1,75	1,12	1,19	0,0291	0,372	3,47	37,5	35,3

Measurement of the Swiss Bureau of Water Affairs

From W. R. Kutter, Lit. No. 8

TABLE 4

MEASUREMENT Location & Date	Type	Q m^3/sec	V_m m/sec	J	T m	B_o m	R m	$R^{2/3}$ $m^{2/3}$	$R^{1/2}$ $m^{1/2}$	$J^{1/2}$	c from $v_m = c\sqrt{RJ}$	Gang.-Kutter n	$\frac{v}{V_0}$	Bazin ε	Her-manek V_m m/sec	Mata-kiewicz V_m m/sec	$V_m = k \cdot R^{2/3} \cdot J^{1/2}$: $R^{2/3} \cdot J^{1/2}$	$v' = \frac{v_m}{R^{2/3}}$	v''	k	$\frac{1}{n}$
(Discharge of the lower Grindelwald glacier)																					
14. II. 1908	Fl.	0,107	0,279	0,000639	0,202	1,90	0,172	0,309	0,415	0,0252	26,61	0,0244	—	0,935	0,157	0,264	0,0078	0,903	0,35	35,8	41,0
Aare Brienzwiler																					
29. III. 1917 ...	Fl.	3,95	0,606	0,00299	0,491	13,27	0,480	0,613	0,693	0,0547	15,99	0,0504	0,802	3,07	0,82	1,09	0,0335	0,99	0,349	18,0	19,8
13. II. 1913	Fl.	4,98	0,890	0,00394	0,405	13,82	0,392	0,537	0,626	0,0628	22,64	0,0348	0,780	1,78	0,78	1,05	0,0337	1,66	0,447	26,3	28,7
12. III. 1918 ...	Fl.	5,16	0,705	0,00329	0,555	13,20	0,535	0,660	0,732	0,0574	16,813	0,0497	0,762	3,07	0,98	1,19	0,0379	1,07	0.387	18,6	20,1
3. VII. 1913 ...	O. Fl.	49,02	1,956	0,002325	1,474	17,00	1,38	1,240	1,175	0,0482	34,53	0,0309	—	1,79	2,18	2,12	0,0597	1,42	1,28	32,7	32,4
15. V. 1912	Schw.	77,10	2,183	0,00260	1,82	19,48	1,70	1,425	1,302	0,0510	33,00	0,0335	—	2,13	2,72	2,57	0,0726	1,29	1,35	30,1	29,8
25. VI. 1912....	Schw.	99,12	2,414	0,00233	2,02	20,31	1,88	1,522	1,370	0,0483	36,40	0,0308	—	1,89	2,77	2,68	0,0736	1,28	1,58	32,8	32,5
5. VIII. 1912 ..	Schw.	121,88	2,596	0,00222	2,22	21,22	2,04	1,608	1,430	0,0471	38,60	0,0292	—	1,80	2,92	2,83	0,0756	1,27	1,74	34,3	34,3
Lütschine Gsteig																					
6. II. 1908	Fl.	2,36	0,572	0,00220	0,342	12,10	0,329	0,477	0,573	0,0469	21,27	0,0351	0,777	1,77	0,49	0,75	0,0223	1,20	0,385	25,6	28,5
23. II. 1912	Fl.	3,04	0,512	0,00180	0,377	15,75	0,362	0,508	0,602	0,0424	20,06	0,0379	0,762	2,02	0,49	0,73	0,0215	1,01	0,382	23,8	26,4
18. III. 1907 ...	Fl.	3,42	0,658	0,00420	0,415	12,55	0,399	0,542	0,632	0,0648	16,08	0,0476	0,728	2,78	0,82	1,06	0,0352	1,22	0,321	18,8	21,0
28. II. 1912	Schw.	5,75	0,722	0,00317	0,482	16,58	0,460	0,597	0,678	0,0563	18,94	0,0426	—	2,43	0,83	1,09	0,0336	1,21	0,406	21,5	23,5
15. VI. 1912....	Schw.	34,78	1,785	0,00585	1,105	17,63	1,016	1,010	1,007	0,0765	23,15	0,0434	—	2,77	2,58	2,32	0,0773	1,76	0,737	23,1	23,0
15. V. 1912	Schw.	44,66	1,946	0,00565	1,280	17,95	1,165	1,110	1,080	0,0752	23,98	0,0433	—	2,85	2,95	2,56	0,0835	1,76	0,816	23,3	23,1
Simme Wimmis																					
5. II. 1907	Fl.	4,36	0,614	0,001369	0,467	15,20	0,446	0,583	0,668	0,037	24,85	0,0330	0,886	1,67	0,530	0,78	0,0216	1,055	0,525	28,5	30,3
15. I. 1907	Fl.	5,04	0,690	0,001368	0,480	15,20	0,459	0,596	0,678	0,037	27,54	0,0302	0,857	1,47	0,545	0,79	0,0221	1,160	0,588	31,3	33,1
Aare Thalmatten																					
20. III. 1911 ...	Fl.	48,96	1,025	0,00141	0,728	65,75	0,720	0,805	0,850	0,0376	32,17	0,0290	0,854	1,45	0,840	1,01	0,0303	1,28	0,860	33,8	34,5
21./22. III. 1911	Fl.	61,88	1,136	0,00141	0,810	67,40	0,801	0,864	0,895	0,0376	33,80	0,0282	0,857	1,415	0,933	1,10	0,0325	1,31	0,953	35,0	35,5
21. VII. 1911 ..	O. Fl.	192,20	1,655	0,00136	1,420	81,55	1,403	1,253	1,185	0,0369	37,94	0,0281	—	1,540	1,610	1,66	0,0462	1,32	1,420	35,8	35,6
27. VI. 1910....	O. Fl.	346,25	1,950	0,00110	2,075	85,43	2,056	1,620	1,433	0,0320	41,00	0,0278	—	1,490	1,920	1,99	0,0518	1,20	1,925	37,7	36,0
Aare Aarau																					
25. X. 1913	Fl.	111,78	1,125	0,000633	1,170	85,00	1,158	1,10	1,076	0,02515	41,55	0,0247	0,854	1,17	0,900	1,065	0,0276	1,01	1,415	40,8	40,4
3. X. 1913	Fl.	191,82	1,519	0,000905	1,385	91,20	1,371	1,23	1,170	0,03007	43,12	0,0245	0,843	1,20	1,27	1,40	0,0370	1,24	1,598	41,1	40,8
19. VIII. 1921 .	Fl.	265,32	1,687	0,001076	1,686	93,27	1,600	1,37	1,264	0,03280	40,60	0,0266	—	1,43	1,65	1,72	0,0450	1,23	1,625	37,6	37,6
21. VIII. 1913 .	Fl.	295,23	1,716	0,001365	1,845	93,22	1,817	1,49	1,352	0,0369	34,40	0,0323	0,793	2,07	1,95	2,07	0,0550	1,15	1,465	31,2	31,0
14. VIII. 1905 .	Schw.	430,15	1,966	0,001296	2,330	94,20	2,266	1,72	1,504	0,0360	36,28	0,0323	—	2,09	2,025	2,38	0,0620	1,16	1,720	31,8	31,0
12. VIII. 1905 .	Schw.	576,88	2,311	0,001316	2,630	94,88	2,553	1,86	1,597	0,0362	39,87	0,0297	—	1,88	2,55	2,60	0,0673	1,24	2,020	34,3	33,7

TABLE 5

MEASUREMENT Location & Date	Type	Q m^3/sec	v_m m/sec	J	T m	B_o m	R m	$R^{2/3}$ $m^{2/3}$	$R^{1/2}$ $m^{1/2}$	$J^{1/2}$	C from $v_m = c\sqrt{RJ}$	Gang.-Kutter n	$\frac{\bar{v}}{v_o}$	Bazin ε	Hermanek v_m m/sec	Matakiewicz v_m m/sec	$v_m = k \cdot R^{2/3} \cdot J^{1/2}$: $R^{2/3} \cdot J^{1/2}$	$v' = \frac{v_m}{R^{2/3}}$	v''	k	$\frac{1}{n}$	
Reuß Seedorf																						
18. III. 1916 ...	Fl.	15,71	1,132	0,00348	0,523	26,55	0,515	0,643	0,717	0,0590	26,736	0,03200	–	1,62	0,95	1,21	0,0380	1,76	0,604	29,8	31,2	Measurement of the Swiss Bureau of Water Affairs
12. IX. 1912 ...	Fl.	44,25	1,675	0,00296	0,947	27,90	0,926	0,95	0,962	0,0543	31,99	0,03070	–	1,65	1,58	1,71	0,0516	1,76	0,975	32,5	32,6	
2. IX. 1915	Fl.	52,27	1,767	0,00320	1,055	28,05	1,029	1,04	1,014	0,0566	30,80	0,03270	–	1,85	1,83	1,77	0,0589	1,70	0,990	30,1	30,6	
14. VI. 1912....	O. Fl.	93,69	2,177	0,00303	1,445	29,80	1,400	1,25	1,182	0,0550	33,42	0,03205	–	1,89	2,43	2,33	0,0688	1,64	1,250	31,7	31,2	
28. VI. 1916....	Fl.	112,64	2,385	0,00311	1,570	30,15	1,522	1,32	1,233	0,0557	34,68	0,03135	–	1,85	2,65	2,52	0,0737	1,81	1,355	32,4	31,9	
3. VIII. 1912 ..	O. Fl.	121,62	2,438	0,00304	1,640	30,40	1,583	1,36	1,258	0,0552	35,14	0,03116	–	1,85	2,72	2,58	0,0752	1.80	1,400	32,6	32,1	
Drance de Bagne Châble																						
31. X. 1912	Fl.	3,62	0,740	0,00420	0,377	13,00	0,357	0,503	0,597	0,0648	19,11	0,0395	0,798	2,12	0,75	1,01	0,0326	1,47	0,362	22,7	25,3	
27. V. 1913	Schw.	14,08	1,600	0,00620	0,676	13,00	0,615	0,723	0,784	0,0787	25,91	0,0344	–	1,85	1,63	1,67	0,0570	2,22	0.642	28,1	29,1	
23. VII. 1912 ..	Schw.	20,18	1,880	0,00638	0,828	13,00	0,735	0,815	0,857	0,0798	27,45	0,0339	–	1,86	2,02	1,92	0,0650	2,31	0,753	28,9	29,5	
5. VIII. 1913 ..	Schw.	37,08	2,446	0,00557	1,165	13,00	0,990	0,993	0,995	0,0747	32,93	0,0303	–	1,62	2,67	2,34	0,0743	2,47	1,035	32,8	33,0	
Rhone Sion																						
13. II. 1902	Fl.	24,11	0,788	0,000927	0,797	38,35	0,781	0,848	0,883	0,0304	29,29	0,03226	0,792	1,742	0,737	0,95	0,0258	0,93	0,819	30,6	31,0	
1. VIII. 1896 ..	Schw.	208,00	1,795	0,00133	1,925	60,00	1,893	1,53	1,375	0,0364	35,77	0,03171	–	1,960	2,02	2,08	0,0557	1,17	1,560	32,25	31,5	
2./3. VII. 1897 .	Schw.	498,00	2,525	0,00126	3,260	60,45	3,074	2,115	1,750	0,0355	40,57	0,03010	–	2,000	2,93	2,93	0,0747	1,20	2,250	33,8	33,2	
Rhone Porte du Scex																						
27. III. 1901 ...	Fl.	34,94	0,672	0,000352	0,908	57,30	0,900	0,933	0,948	0,0187	37,75	0,0259	0,885	1,22	0,52	0,69	0,0174	0,720	1,13	38,6	38,6	
21. I. 1903	Fl.	42,78	0,836	0,000525	0,880	58,05	0,875	0,916	0,936	0,0229	39,00	0,0250	0,892	1,15	0,62	0,805	0,0210	0,913	1,15	39,8	40,0	
16. III. 1899 ...	Fl.	56,09	0,934	0,000460	1,030	58,167	1,019	1,013	1,007	0,0214	43,13	0,0233	0,881	1,03	0,68	0,825	0,0217	0,914	1,37	43,0	43,0	
29. V. 1887	Fl.	87,70	1,266	0,001002	0,969	71,47	0,960	0,973	0,980	0,0320	40,80	0,0243	0,852	1,14	0,95	1,11	0,0311	1,300	1,25	40,7	41,2	
22. V. 1899	Schw.	285,34	1,927	0,000835	2,220	66,70	2,180	1,680	1,475	0,0289	45,15	0,0253	–	1,365	1,79	1,88	0,0486	1,150	2,11	39,7	39,5	
17. VII. 1900 ..	Schw.	479,00	2,400	0,000909	2,880	69,25	2,820	1,995	1,675	0,0302	47,42	0,0249	–	1,39	2,275	2,34	0,0602	1,200	2,51	40,0	40,2	
17. VII. 1900 ..	Schw.	533,10	2,492	0,000917	3,050	70,05	2,980	2,070	1,725	0,0303	47,66	0,0250	–	1,415	2,38	2,47	0,0628	1,205	2,60	39,8	40,0	
1. VII. 1897 ...	Schw.	789,00	2,730	0,000918	3,500	82,60	3,367	2,250	1,835	0,0303	49,11	0,0246	–	1,420	2,63	2,72	0,0683	1,215	2,84	40,1	40,7	
Mississippi Vicksburg					max.																	
1858 Nr. 1			1,074	0,00002227	19,0	–	9,497	4,48	3,08	0,00472	73,0	0,0264	–	0,555	0,80	–	0,0212	0,241	7,20	51,0	37,9	From W.R. Kutter
1858 „ 2			1,694	0,00003029	25,0	–	15,886	6,325	3,99	0,00551	77,2	0,0254	–	0,530	1,29	–	0,0348	0,268	9,70	48,6	39,4	
1858 „ 3			1,926	0,00004811	27,0	–	17,484	6,75	4,18	0,00693	66,4	0,0280	–	1,295	1,71	–	0,0468	0,285	8,78	41,2	35,7	
1858 „ 4			2,118	0,00006379	31,0	–	19,538	7,27	4,42	0,00798	60,0	0,0308	–	1,995	2,12	–	0,0580	0,291	8,36	36,4	32,5	
1858 „ 5			2,080	0,00004365	31,0	–	19,666	7,29	4,43	0,00661	71,0	0,0265	–	0,997	1,75	–	0,0482	0,287	9,95	43,3	37,7	

TABLE 6

MEASUREMENT Location & Date	Type	Q m^3/sec	V_m m/sec	J	T m	B_o m	R m	$R^{2/3}$ $m^{2/3}$	$R^{1/2}$ $m^{1/2}$	$J^{1/2}$	c from $v_m = c\sqrt{RJ}$	Gang.-Kutter n	n. G.-Kutter V_m bei	Bazin ε	Hermanek V_m m/sec	Matakiewicz V_m m/sec	$V_m = k \cdot R^{2/3} \cdot J^{1/2}$: $R^{2/3} \cdot J^{1/2}$	$v' = \frac{v_m}{R^{2/3}}$	v''	k	$\frac{1}{n}$
Seine Poissy													n = 0,0270								
Nr. 1	—	—	0,704	0,000090	—	—	2,164	1,67	1,468	0,00950	50,4	0,02325	0,621	1,060	0,57	0,62	0,0159	0,435	2,35	44,4	43,1
„ 2	—	—	0,705	0,000087	—	—	2,340	1,76	1,530	0,00933	49,4	0,02420	0,646	1,165	0,60	0,65	0,0164	0,400	2,38	43,0	41,3
„ 3	—	—	0,720	0,000057	—	—	3,426	2,26	1,850	0,00755	51,5	0,02660	0,704	1,265	0,65	0,79	0,0170	0,318	3,02	42,3	37,6
„ 5	—	—	0,723	0,000050	—	—	4,136	2,57	2,030	0,00707	50,3	0,02820	0,762	1,480	0,70	0,88	0,0182	0,280	3,22	40,0	35,5
„ 6	—	—	0,791	0,000054	—	—	4,328	2,65	2,080	0,00735	51,7	0,02760	0,812	1,440	0,75	0,91	0,0195	0,298	3,40	40,6	36,2
„ 9	—	—	1,015	0,000075	—	—	5,445	3,08	2,335	0,00866	50,3	0,02875	1,083	1,710	1,05	1,11	0,0267	0,330	3,70	38,2	34,8
Saône Raconnay													n = 0,0280								
Nr. 5	Fl.	—	0,565	0,00004	—	—	3,314	2,23	1,820	0,00632	49,1	0,0281	0,575	1,390	0,53	0,66	0,0141	0,253	2,81	40,0	35,6
„ 6	Fl.	—	0,582	0,00004	—	—	3,539	2,32	1,880	0,00632	48,9	0,0288	0,604	1,465	0,55	0,69	0,0146	0,252	2,92	39,7	34,7
„ 7	Fl.	—	0,592	0,00004	—	—	3,598	2,35	1,895	0,00632	49,3	0,0288	0,612	1,425	0,56	0,70	0,0148	0,252	2,94	39,9	34,7
„ 8	Fl.	—	0,687	0,00004	—	—	4,044	2,53	2,010	0,00632	54,0	0,02675	0,667	1,600	0,61	0,75	0,0160	0,270	3,42	42,8	37,4
„ 9	Fl.	—	0,722	0,00004	—	—	4,463	2,71	2,110	0,00632	54,1	0,0273	0,716	1,605	0,66	0,80	0,0171	0,266	3,61	42,2	36,6
„ 10	Fl.	—	0,725	0,00004	—	—	4,825	2,85	2,195	0,00632	52,2	0,0290	0,757	1,460	0,70	0,84	0,0180	0,255	3,61	40,2	34,5
Donau Wien													n = 0,0261								
10. XI. 1897 ...	Fl.	977,5	1,59	0,000439	2,46	249,3	2,31	1,75	1,52	0,0209	49,9	0,0229	1,40	1,13	1,39	1,52	0,0367	0,91	2,39	43,3	43,7
3. XI. 1897	Fl.	1099,3	1,67	0,000452	2,64	250,1	2,46	1,83	1,57	0,0212	50,1	0,0232	1,48	1,14	1,50	1,64	0,0387	0,91	2,49	43,2	43,1
19. X. 1897	O. Fl.	1401,2	1,81	0,000477	3,07	252,2	2,84	2,02	1,68	0,0218	49,2	0,0242	1,665	1,28	1,72	1,84	0,0440	0,90	2,62	41,2	41,3
30. IV. 1897....	Fl.	1884,1	2,01	0,000508	3,58	262,1	3,28	2,22	1,82	0,0225	49,2	0,0246	1,90	1,42	1,99	2,14	0,0499	0,90	2,82	40,2	40,7
7. V. 1897	O. Fl.	2115,5	2,14	0,000518	3,76	262,8	3,43	2,28	1,86	0,0228	50,8	0,0240	1,98	1,36	2,08	2,21	0,0520	0,94	2,97	41,3	41,7
16. VI. 1897....	O. Fl.	2928,4	2,44	0,000551	4,52	265,6	4,05	2,54	2,02	0,0235	51,7	0,0240	2,27	1,38	2,47	2,57	0,0598	0,96	3,27	40,9	41,7
30. VI. 1897....	O. Fl.	3188,0	2,51	0,000557	4,76	266,5	4,24	2,62	2,07	0,0236	51,7	0,0242	2,325	1,42	2,58	2,67	0,0618	0,96	3,35	40,6	41,3
4. VI. 1897.....	O. Fl.	3286,9	2,51	0,000561	4,91	267,0	4,37	2,67	2,09	0,0237	50,7	0,0248	2,38	1,51	2,63	2,73	0,0633	0,94	3,34	39,7	40,3
14.–16. IX. 1897	Fl.	3233,9	2,45	0,000563	4,95	267,1	4,40	2,69	2,10	0,0237	49,2	0,0256	2,40	1,61	2,67	2,74	0,0638	0,91	3,27	38,4	39,1
28. V. 1897	O. Fl.	3615,0	2,52	0,000576	5,34	268,5	4,70	2,81	2,17	0,0240	48,4	0,0264	2,53	1,74	2,84	2,88	0,0674	0,90	3,32	37,2	37,9
18. V. 1897	O. Fl.	4060,4	2,65	0,000588	5,68	269,2	4,97	2,91	2,24	0,0242	49,0	0,0262	2,67	1,75	3,02	3,02	0,0704	0,91	3,46	37,7	38,2
7. VIII. 1897 ..	O. Fl.	3919,2	2,46	0,000592	5,91	269,8	5,15	2,98	2,27	0,0243	44,6	0,0296	2,73	2,15	3,13	3,09	0,0725	0,82	3,18	34,0	33,8
6. VIII. 1897 ..	O. Fl.	5400,0	2,79	0,000602	7,11	272,2	6,05	3,32	2,46	0,0245	46,2	0,0289	3,00	2,15	3,50	3,54	0,0813	0,84	3,60	34,3	34,6
5. VIII. 1897 ..	O. Fl.	6368,0	2,89	0,000590	8,08	272,3	6,75	3,57	2,60	0,0243	45,8	0,0298	3,20	2,34	3,74	—	0,0868	0,81	3,76	33,4	33,6
2. VIII. 1897 ..	O. Fl.	6955,5	3,01	0,000582	8,48	273,3	7,03	3,67	2,66	0,0241	47,1	0,0289	3,24	2,26	3,82	—	0,0883	0,82	3,94	34,0	34,6
3. VIII. 1897 ..	O. Fl.	7017,8	2,97	0,000580	8,68	272,3	7,17	3,72	2,67	0,0241	46,1	0,0298	3,27	2,35	3,85	—	0,0895	0,80	3,90	33,2	33,6

From W. R. Kutter, Lit. No. 8

From: Contributions to the Hydrography of Austria. III issue: the Hydrometric survey of the Danube at Vienna in 1897.

TABLE 7

MEASUREMENT Location & Date	Type	Q m^3/sec	v_m m/sec	J	T m	B_o m	R m	$R^{2/3}$ $m^{2/3}$	$R^{1/2}$ $m^{1/2}$	$J^{1/2}$	c	$\frac{1000}{c^2}$	Gang.-Kutter n	$v_m = k \cdot R^{2/3} \cdot J^{1/2}$: $R^{2/3} \cdot J^{1/2}$	v'	v''	k	$\frac{1}{n}$	REFERENCES
INTAKES																			
Headwater channel to the electric power plant Rheinfelden																			
5. II. 1904	Fl.	455,54	1,993	0,000261	4,11	55,73	3,172	2,42	1,940	0,0161	63,518	0,248	0,019019	0,0390	0,823	3,90	50	52,6	
6. X. 1904	Schw.	484,84	2,175	0,000332	3,98	55,59	3,671	2,38	1,915	0,0182	62,300	0,257	0,019300	0,0434	0,913	3,77	50	51,8	
Swiss commercial channel Thun																			Measurements of the Swiss Bureau of Water Affairs
28. VIII. 1906	Fl.	6,002	0,608	0,000145	2,225	4,43	1,002	1,001	1,000	0,0120	50,440	0,337	0,019800	0,0120	0,608	1,60	50	50,5	
Intake in S. Giovanni Lupatoto																			
14. VIII. 1904	Fl.	23,746	1,012	0,000057	2,22	10,55	1,780	1,470	1,332	0,00755	100,470	0,099	0,010900	0,0111	0,688	4,24	91,2	91,8	Dr. Epper: The Development of Hydrography in Switzerland, Table 86b.
Headwater channel of the electric power plant Aarau																			
30. VI. 1895	Fl.	17,33	0,637	0,000111	1,80	15,06	1,601	1,368	1,264	0,0105	47,71	0,440	0,0232	0,0168	0,466	1,92	38,0	43,1	
20. XI 1905	Fl.	38,14	1,014	0,000120	2,37	15,89	2,016	1,595	1,420	0,01094	65,19	0,236	0,0173	0,0175	0,636	2,92	58,0	57,8	Dr. Epper: Ibid., Table 83 & 84
Drain of the Simplon Adit	Fl.	1,122	2,586	0,00683	0,433	1,005	0,232	0,378	0,482	0,0826	64,06	0,244	0,0126	0,0312	6,84	0,99	82,0	79,4	Dr. Epper: Ibid., Table 66 & 67
TORRENT SHELLS																			
Shell of Grunnbach at Thunersee, at Kutter, 1867 Nr. 1	Schw.	—	3,600	0,08285	—	—	0,1083	0,227	0,329	0,288	37,9	0,695	0,0237	0,065	15,9	0,394	55,3	42,2	
Measurements with differenct floats „ 2	Schw.	—	4,062	0,09927	—	—	0,1155	0,237	0,340	0,315	37,8	0,700	0,0242	0,074	17,1	0,407	54,9	41,3	
„ 3	Schw.	—	4,191	0,10677	—	—	0,1182	0,241	0,344	0,327	37,2	0,722	0,0245	0,079	17,4	0,405	53,0	40,8	
„ 4	Schw.	—	4,737	0,08285	—	—	0,1773	0,316	0,421	0,288	39,0	0,660	0,0270	0,091	15,0	0,520	52,0	37,0	
„ 5	Schw.	—	5,574	0,09927	—	—	0,1932	0,334	0,440	0,315	40,2	0,618	0,0273	0,105	16,7	0,559	53,0	36,6	
„ 6	Schw.	—	5,844	0,10677	—	—	0,1971	0,338	0,444	0,327	40,2	0,618	0,0274	0,111	17,3	0,565	52,7	36,5	W. R. Kutter: "The New Formulas for Water Movement" Vienna, 1871
Shell of Gerbebach at Thunersee, Kutter, 1867 Nr. 1	Schw.	—	2,583	0,1117	—	—	0,0591	0,1517	0,243	0,334	31,8	0,988	0,0219	0,0507	17,1	0,244	51,0	45,7	
„ 2	Schw.	—	2,715	0,1375	—	—	0,0591	0,1517	0,243	0,371	30,1	1,100	0,0225	0,0562	17,9	0,231	48,3	44,4	
„ 3	Schw.	—	2,799	0,1679	—	—	0,0591	0,1517	0,243	0,409	28,1	1,270	0,0236	0,0620	18,5	0,216	45,2	42,3	

TABLE 8

MEASUREMENT Location & Date	Type	Q m^3/sec	v_m m/sec	J	T_a m	B_o m	R m	$R^{2/3}$ $m^{2/3}$	$R^{1/2}$ $m^{1/2}$	$J^{1/2}$	c	$\frac{1000}{c^2}$	Gang.-Kutter n	$v = k \cdot R^{2/3} \cdot J^{1/2}$ $R^{2/3} \cdot J^{1/2}$	v'	v''	k	$\frac{1}{n}$		REFERENCES
ADITS																				
Sitter Adit (E. W. Kubel)																				
24. VII. 1906	Fl.	0,547	0,879	0,000555	0,41	1,89	0,270	0,418	0,519	0,02355	71,81	0,194	0,0115	0,0099	3,11	1,175	88,8	87,0	Smoothed Concrete	Dr. Epper: Die Entwicklung der Hydrometrie in der Schweiz. Tafel 36.
23. VII. 1906	Fl.	1,604	1,203	0,000555	0,78	1,98	0,436	0,575	0,660	0,02355	77,33	0,167	0,0116	0,0136	2,09	1,615	88,5	86,2		
23. VII. 1906	Fl.	2,457	1,346	0,000555	1,03	1,97	0,513	0,642	0,716	0,02355	79,77	0,157	0,0115	0,0151	2,09	1,805	89,0	87,0		
24. VII. 1906	Fl.	3,480	1,449	0,000555	1,34	1,80	0,573	0,690	0,757	0,02355	81,25	0,151	0,0115	0,0163	2,10	1,945	89,0	87,0		
24. VII. 1906	Fl.	4,135	1,498	0,000555	1,55	1,51	0,586	0,701	0,765	0,02355	83,07	0,145	0,0113	0,0165	2,13	2,010	90,9	88,5		
Bottom discharge adit of the mine Muhleberg																				
Nr. 1	Fl.	52,63	2,02	0,000457	—	—	1,600	1,37	1,265	0,0214	74,8	0,178	0,0141	0,0293	1,46	2,96	68,5	70,9	Smoothed cement plaster on concrete	„Schweizer. Wasserwirtschaft" 25. Juli 1922: A. J. Keller: „Die Versuche am Grundablassstollen Mühleberg und deren Verarbeitung".
„ 2	Fl.	58,31	2,23	0,000664	—	—	1,517	1,32	1,230	0,0258	70,4	0,202	0,0149	0,0341	1,70	2,73	66	67,1		
„ 3	Fl.	78,55	2,95	0,001040	—	—	1,450	1,28	1,205	0,0322	75,6	0,175	0,0138	0,0412	2,30	2,90	72	72,5		
„ 4	Fl.	178,53	9,05	0,008050	—	—	1,590	1,37	1,260	0,0895	80,1	0,156	0,0131	0,1230	6,60	3,19	73,5	76,3		
„ 5	Fl.	283,08	12,90	0,0149	—	—	1,690	1,42	1,300	0,1220	81,1	0,152	0,0130	0,1730	9,65	3,33	74,5	76,9		
„ 6	Fl.	335,93	13,60	0,0250	—	—	1,695	1,42	1,300	0,1580	66,2	0,229	0,0161	0,2240	10,10	2,72	61	62,1		
Navizance Adit of the electric power plant Chippis (Wallis)	—	11,55	3,65	0,0034	—	—	0,584	0,696	0,764	0,0583	81,6	0,150	0,0115	0,0405	5,25	1,98	89	87,0	Adit bricked up & plastered	„Schweizer. Bauzeitung" 1911, Bd. 58, S. 100.
Simme (E. W. Spiez)	Fl.	—	1,31	0,00046	—	—	0,590	0,704	0,768	0,0214	79,6	0,158	0,0117	0,0151	1,86	1,93	86,5	85,5	Adit reinforced with concrete & plastered	„Schweizer. Bauzeitung" 1906, Bd. 52, S. 206 u. Mitteilung der B. K. W.
Adit of the Kallnach mine	Fl.	—	2,72	0,00065	—	—	1,370	1,234	1,170	0,0255	91,5	0,119	0,0115	0,0315	2,21	3,36	86,1	87,0	Smoothly plastered concrete	„Schweizer. Wasserwirtschaft" 10. Okt. 1917 u. Mitteilung der B. K. W.
Adit of the electric power plant at: **Martigny-Bourg**	—	10,0	2,010	0,0025	—	—	0,710	0,796	0,845	0,050	47,7	0,440	0,0192	0,0398	2,52	1,27	50,2	52,1	Adit not bricked up	
Ackersand	—	4,0	1,33	0,0025	—	—	0,453	0,591	0,674	0,050	39,5	0,640	0,0203	0,0296	2,25	0,84	45,0	49,2	Bottom reinforced with concrete; otherwise not bricked up	
Gampel II	—	3,0	1,11	0,0030	—	—	0,428	0,568	0,655	0,055	31,0	1,040	0,0245	0,0312	1,95	0,637	35,6	40,8	Adit not bricked up but with cement plastering	
Biaschina	—	15,0	2,30	0,0015	—	—	0,890	0,925	0,944	0,039	63,0	0,252	0,0156	0,0361	2,48	1,86	63,8	64,1	"	

TABLE 9

MEASUREMENT	Nr.	v_m m/sec	J	R m	$R^{2/3}$ $m^{2/3}$	$J^{1/2}$	c	n. G.-Kutter v_m	$R^{2/3} \cdot J^{1/2}$	k
Test Channel of Darcy u. Bazin, 1865										
								n = 0,0100		
Series 24 Pure cement, semicircular D = 1,25 m	1	0,921	0,001424	0,1116	0,251	0,03775	73,0	0,909	0,0095	97
	2	1,135	0,001424	0,1533	0,286	0,03775	76,8	1,135	0,0108	105
	3	1,267	0,001424	0,1844	0,324	0,03775	78,2	1,289	0,0123	103
	4	1,401	0,001424	0,2080	0,351	0,03775	81,4	1,397	0,0133	100,5
	5	1,483	0,001424	0,2286	0,374	0,03775	82,2	1,488	0,0141	100
	6	1,562	0,001424	0,2465	0,394	0,03775	83,3	1,565	0,0149	105
	7	1,612	0,001424	0,2642	0,412	0,03775	83,1	1,639	0,0156	103
	8	1,681	0,001424	0,2790	0,428	0,03775	84,3	1,698	0,0162	104
	9	1,754	0,001424	0,2893	0,437	0,03775	86,4	1,740	0,0165	106,5
	10	1,803	0,001424	0,3025	0,451	0,03775	86,9	1,792	0,0170	106
	11	1,847	0,001424	0,3137	0,462	0,03775	87,4	1,835	0,0175	105,5
	12	1,862	0,001424	0,3153	0,463	0,03775	87,9	1,841	0,0175	1056
								n = 0,0111		
Series 25 Cement mixed with 1/3 very fine river sand, semicircular D = 1,25 m	1	0,875	0,001380	0,1154	0,237	0,03715	69,3	0,875	0,0088	99,5
	2	1,047	0,001380	0,1612	0,296	,003715	70,2	1,085	0,0110	95,3
	3	1,179	0,001380	0,1937	0,335	0,03715	72,1	1,220	0,0124	95
	4	1,311	0,001380	0,2153	0,360	0,03715	76,0	1,303	0,0134	98
	5	1,375	0,001380	0,2399	0,386	0,03715	75,6	1,394	0,0143	96
	6	1,463	0,001380	0,2558	0,403	0,03715	77,9	1,452	0,0150	97,7
	7	1,506	0,001380	0,2743	0,423	0,03715	77,4	1,514	0,0157	96
	8	1,584	0,001380	0,2869	0,436	0,03715	79,6	1,558	0,0162	98
	9	1,640	0,001380	0,2997	0,448	0,03715	80,6	1,599	0,0167	98
	10	1,670	0,001380	0,3067	0,455	0,03715	81,2	1,619	0,0169	99
	11	1,691	0,001380	0,3114	0,459	0,03715	81,6	1,633	0,0171	99
	12	1,726	0,001380	0,3165	0,465	0,03715	82,6	1,651	0,0173	99,7
								n = 0,0130		
Series 39 Trimmed ashlars very regular, Cross-section rectangular D = 1,20 m	1	1,746	0,00810	0,1238	0,248	0,090	55,1	1,710	0,0223	78,2
	2	2,293	0,00810	0,1742	0,312	0,090	61,1	2,182	0,0281	81,9
	3	2,495	0,00810	0,2074	0,351	0,090	60,9	2,468	0,0315	79,2
	4	2,666	0,00810	0,2336	0,380	0,090	61,3	2,680	0,0342	78,0
$B_o = 1,20$ m										

MEASUREMENT	Nr.	v_m m/sec	J	R m	$R^{2/3}$ $m^{2/3}$	$J^{1/2}$	c	G.-Kutter v_m bei	$R^{2/3} \cdot J^{1/2}$	k
								n = 0,0120		
Series 7 Broad channel with rectangular cross-section, 1.99 m wide	1	0,826	0,00489	0,0573	0,181	0,070	49,3	0,824	0,0127	65
	2	1,127	0,00489	0,0830	0,190	0,070	55,9	1,090	0,0133	85
	3	1,325	0,00489	0,1042	0,221	0,070	58,7	1,291	0,0154	86
	4	1,479	0,00489	0,1224	0,247	0,070	60,5	1,450	0,0173	85,5
	5	1,612	0,00489	0,1382	0,267	0,070	62,0	1,583	0,0187	86
	6	1,711	0,00489	0,1535	0,287	0,070	62,5	1,704	0,0201	85,4
	7	1,808	0,00489	0,1668	0,303	0,070	63,3	1,808	0,0212	85,4
	8	1,898	0,00489	0,1789	0,317	0,070	64,2	1,898	0,0222	85,4
	9	1,967	0,00489	0,1913	0,332	0,070	64,3	1,991	0,0232	85
	10	2,045	0,00489	0,2018	0,344	0,070	65,1	2,045	0,0241	85
	11	2,102	0,00489	0,2129	0,357	0,070	65,1	2,142	0,0250	84
	12	2,179	0,00489	0,2215	0,366	0,070	66,2	2,202	0,0257	85
								n = 0,0115		
Series 8 as Series 7	1	1,074	0,00816	0,0447	0,126	0,0903	56,2	0,938	0,0114	94,5
	2	1,348	0,00816	0,0703	0,170	0,0903	56,3	1,315	0,0154	88
	3	1,594	0,00816	0,0882	0,198	0,0903	59,4	1,556	0,0179	89
	4	1,776	0,00816	0,1041	0,221	0,0903	60,9	1,758	0,0199	89
	5	1,902	0,00816	0,1197	0,243	0,0903	60,8	1,944	0,0220	86,6
	6	2,053	0,00816	0,1313	0,258	0,0903	62,7	2,056	0,0233	88
	7	2,186	0,00816	0,1420	0,272	0,0903	64,2	2,196	0,0246	89,3
	8	2,268	0,00816	0,1543	0,288	0,0903	63,9	2,328	0,0260	87
	9	2,357	0,00816	0,1649	0,301	0,0903	64,2	2,440	0,0272	86,5
	10	2,447	0,00816	0,1744	0,312	0,0903	64,8	2,535	0,0282	87
	11	2,518	0,00816	0,1842	0,324	0,0903	64,9	2,633	0,0293	86
	12	2,612	0,00816	0,1919	0,333	0,0903	66,0	2,707	0,0302	86,4
								n = 0,0120		
Series 26 Board channel with semi-circular shape	1	0,795	0,00152	0,1189	0,242	0,0390	59,4	0,787	0,0094	84,5
	2	0,984	0,00152	0,1636	0,299	0,0390	62,9	0,989	0,0117	84
	3	1,132	0,00152	0,1926	0,334	0,0390	66,5	1,109	0,0131	86,5
	4	1,230	0,00152	0,2187	0,364	0,0390	67,9	1,212	0,0142	86,5
	5	1,297	0,00152	0,2425	0,389	0,0390	68,0	1,301	0,0152	85,5
	6	1,374	0,00152	0,2610	0,408	0,0390	69,5	1,367	0,0159	86,5
	7	1,413	0,00152	0,2806	0,429	0,0390	68,8	1,437	0,0167	84,7
	8	1,486	0,00152	0,2937	0,442	0,0390	70,7	1,483	0,0172	86,5
	9	1,524	0,00152	0,3093	0,458	0,0390	70,7	1,534	0,0179	85
	10	1,579	0,00152	0,3213	0,469	0,0390	72,0	1,573	0,0183	86,3
	11	1,612	0,00152	0,3341	0,482	0,0390	72,0	1,618	0,0188	86
	12	1,660	0,00152	0,3442	0,492	0,0390	73,1	1,650	0,0192	86,5
	13	1,689	0,00152	0,3511	0,498	0,0390	73,5	1,672	0,0194	87

TABLE 10

PIPE LINE	Location of pipe or researcher	Q m^3/sec	v_m m/sec	D m	$R = \frac{D}{4}$ m	$R^{2/3}$ $m^{2/3}$	$R^{1/3}$ $m^{1/3}$	J	$J^{1/2}$	c	$\frac{1000}{c^2}$	λ	k	Relation between formulas	REFERENCES
IRON PRESSURE LINES															
Tarred cast iron pipe with valve joint	St. Gallen, Water Supply measurements of Ostertag	0,84	0,885	0,350	0,0875	0,197		0,00258	0,0508	59,0	0,30		89		Weyrauch, Hydraul. Rechnen, 3. Aufl. Seite 107. Schweiz. Bauzeitung 1910, Bd. 55, Seite 25.
		0,84	0,667	0,400	0,100	0,215		0,00133	0,0365	58,0	0,30		85		
New asphalted cast iron pipe, many angles and elbows	In New Jersey			0,58	0,145		0,526			64,0	0,244	0,0184	88,5	$hw = \lambda \frac{L}{D} \cdot \frac{v_m^2}{2g}$ $v_m = k \cdot R^{2/3} \cdot J^{1/2}$	Weyrauch, Seite 108. Journal f. Gasbeleuchtung und Wasserversorgung 1896.
New asphalted cast iron pipe, slight curves	In Boston			1,22	0,305		0,674			76,7	0,170	0,0130	93,5	$k = \sqrt{\frac{8g}{\lambda \cdot R^{1/3}}}$	Dieselben Quellen.
New cast iron or tarred pipes	from C.H. Tutton	$v_m = 34{,}8 \cdot D^{0,66} \cdot J^{0,51} \sim 87{,}5\ R^{2/3} \cdot J^{1/2}$								$87{,}5\ R^{1/6}$			87,5		
	From Vidal & Kauffmann		5,16	0,47	0,1175	0,240	0,489	0,0469		69,5	0,207		100		Annales des ponts et chaussées, 1907.
Riveted sheet iron pipe	Newark & New Jersey	1,533	1,35	1,20	0,30	0,445	0,671			55,2	0,328	0,026	67,5		Weyrauch, Seite 108. Journal f. Gasbeleuchtung und Wasserversorgung 1896, Seite 269.
	in America (measurement)		0,91	1,80	0,45	0,588	0,767			59,8	0,280	0,022	68,5		Weyrauch, Seite 109. Génie civil T. 36 1899/1900. Seite 151.
Riveted, cast iron without encrustation	H. Smith in New Bloomfield		2,44	3,00	0,75	0,827	0,910	0,00109	0,033	64,0	0,245	0,019	67		Weyrauch, Seite 109. Rheinhards Kalender.
Pipes riveted from cast pipe		$v_m = 30{,}8 \cdot D^{0,66} \cdot J^{0,51} \sim 78\ R^{2/3} \cdot J^{1/2}$								$78 \cdot R^{1/6}$	$\frac{1000\ J}{V}$		78		Forchheimer, Seite 44/45. Journal of the Association of Engineering Societies 13 1889, Seite 191.
cast pipe	Machine Lab. of the E.T.H. Zurich	0,0232	1,315	0,15	0,0375	0,0112		0,0189	0,1375		14,38		85,4		
		0,0280	1,585	0,15	0,0375	0,0112		0,0284	0,1685		17,92		84,0		
		0,0300	1,700	0,15	0,0375	0,0112		0,0324	0,1800		19,06		84,3		
		0,0355	2,010	0,15	0,0375	0,0112		0,0453	0,2128		22,54		84,3		
		0,0415	2,350	0,15	0,0375	0,0112		0,0622	0,2494		26,46		84,2		
		0,0495	2,810	0,15	0,0375	0,0112		0,0831	0,2882		29,56		87,0		
		0,0550	3,110	0,15	0,0375	0,0112		0,1061	0,3260		34,18		85,2		
		0,0625	3,540	0,15	0,0375	0,0112		0,1331	0,3645		37,62		86,7		
		0,0680	3,860	0,15	0,0375	0,0112		0,1568	0,3962		40,60		87,9		
		0,0740	4,190	0,15	0,0375	0,0112		0,1838	0,4280		43,86		87,5		

TABLE 11

PIPE	RESEARCHER	Q m^3/sec	v_m m/sec	D m	$R=\frac{D}{4}$ m	$R^{2/3}$ $m^{2/3}$	$R^{1/2}$ $m^{1/2}$	J	$J^{1/2}$	c	λ	k		REFERENCES
Used cast iron pipe, well cleaned	Fitz-Gerald	0,893	0,765	1,22	0,305	0,453	0,552	0,000323	0,0180	77,2	0,0132	94,0		Biel, Lit. Nr. 1, Seite 55, Nr. 66.
		0,887	0,76	1,22	0,305	0,453	0,552	0,000327	0,0181	76,2	0,0136	92,6		
		1,203	1,03	1,22	0,305	0,453	0,552	0,000577	0,0240	77,7	0,01305	94,6		
		1,313	1,125	1,22	0,305	0,453	0,552	0,000686	0,0262	78,0	0,01297	94,9		
		1,330	1,14	1,22	0,305	0,453	0,552	0,000718	0,0268	77,0	0,01333	93,5		
		1,775	1,52	1,22	0,305	0,453	0,552	0,00125	0,03535	78,0	0,01297	94,9		
		2,185	1,87	1,22	0,305	0,453	0,552	0,00184	0,0429	80,2	0,01267	96,0		
Wood pipe, carefully planed & jointed	Marx-Wing-Hoskins	1,754	0,66	1,84	0,46	0,597	0,678	0,000208	0,0144	67,4	0,01723	76,8		Biel, Lit. Nr. 1, Seite 55, Nr. 69.
		1,728	0,65	1,84	0,46	0,597	0,678	0,000214	0,0146	65,6	0,01826	74,6		
		2,365	0,89	1,84	0,46	0,597	0,678	0,000378	0,0194	67,4	0,0173	76,7		
		2,420	0,91	1,84	0,46	0,597	0,678	0,000401	0,0200	67,1	0,01743	76,3		
		2,685	1,01	1,84	0,46	0,597	0,678	0,000495	0,02225	66,9	0,01754	76,1		
		2,845	1,07	1,84	0,46	0,597	0,678	0,000557	0,0236	66,9	0,01754	76,1		
		3,590	1,35	1,84	0,46	0,597	0,678	0,000890	0,0298	66,8	0,01762	75,9		
		3,800	1,43	1,84	0,46	0,597	0,678	0,000960	0,0310	68,1	0,01700	77,3		
		3,935	1,48	1,84	0,46	0,597	0,678	0,001035	0,03216	67,9	0,01712	77,1		
		4,230	1,59	1,84	0,46	0,597	0,678	0,00121	0,0348	67,4	0,01736	76,5		
		4,280	1,61	1,84	0,46	0,597	0,678	0,00124	0,0352	67,7	0,01718	76,9		
		4,290	1,615	1,84	0,46	0,597	0,678	0,00126	0,0355	67,0	0,01751	76,2		
New cast iron pipe, tarred	Iben	0,0293	0,41	0,305	0,076	0,1795	0,276	0,00060	0,0245	60,8	0,0213	93,2		T. Christen, Lit. Nr. 3, Seite 166, Nr. 419—426.
		0,0390	0,53	0,305	0,076	0,1795	0,276	0,00101	0,0318	60,5	0,0215	92,8		
		0,0483	0,66	0,305	0,076	0,1795	0,276	0,00149	0,0386	62,2	0,02045	95,2		
		0,0549	0,75	0,305	0,076	0,1795	0,276	0,00189	0,0435	62,6	0,02015	95,9		
		0,0675	0,92	0,305	0,076	0,1795	0,276	0,00284	0,0533	62,8	0,0201	96,0		
		0,0803	1,10	0,305	0,076	0,1795	0,276	0,00394	0,0628	63,6	0,0195	97,6		
		0,1076	1,47	0,305	0,076	0,1795	0,276	0,00700	0,0836	63,6	0,0193	98,0		
		0,1350	1,85	0,305	0,076	0,1795	0,276	0,01122	0,1060	63,3	0,0196	97,2		
New cast iron pipe, heavily encrusted	Iben	0,0344	0,47	0,305	0,076	0,1795	0,276	0,00500	0,0707	24,1	0,1354	37,0		T. Christen, Lit. Nr. 3, Seite 167, Nr. 441—447.
		0,0431	0,59	0,305	0,076	0,1795	0,276	0,00750	0,0866	24,8	0,1285	38,0		
		0,0526	0,72	0,305	0,076	0,1795	0,276	0,01105	0,1050	24,8	0,1270	38,2		
		0,0636	0,87	0,305	0,076	0,1795	0,276	0,01643	0,1280	24,6	0,1286	37,9		
		0,0782	1,07	0,305	0,076	0,1795	0,276	0,02311	0,1518	25,6	0,1195	39,4		
		0,0789	1,08	0,305	0,076	0,1795	0,276	0,02386	0,1545	25,4	0,1220	39,0		
		0,0972	1,33	0,305	0,076	0,1795	0,276	0,03803	0,1950	24,8	0,1285	38,0		

TABLE 12

Power Plant - Laufenburg

Stagnation Computation for
$Q = 980\ m^3/sec$

Profile (km.)	Distance L (m.)	F m^2	F_m m^2	U m	U_m m	R m	R_m m	v_m m/sec	k	C $=k\sqrt[6]{R}$	A_1 m	βA_2 m	Δh m	Stagnation Height m. above sea level Computed	Observed[1]
16,952		2382		223		10,69		0,411						302,00	302,00
	180		2014		187		10,79		14,9	22,14	0,008	− 0,006	0,002		
16,772		1646		151		10,89		0,595						302,002	
	170		1452		151		9,60		14,9	21,71	0,017	− 0,008	0,009		
16,602		1258		151		8,32		0,779						302,011	
	160		1221		135		9,09		14,9	21,51	0,025	− 0,003	0,022		
16,442		1184		120		9,86		0,827						302,033	
	69		1145		126		9,08		14,9	21,51	0,012	− 0,003	0,009		
16,373		1105		133		8,30		0,886						302,042	
	84		1088		131		8,27		14,9	21,19	0,018	− 0,002	0,016		
16,289		1072		130		8,25		0,914						302,058	
	41		1071		123		8,69		14,9	21,32	0,009	0,000	0,009		
16,248		1070		117		9,14		0,916						302,067	
	91		1206		124		9,58		14,9	21,70	0,014	+ 0,016	0,030		
16,157		1343		132		10,02		0,729						302,097	
	146		1215		127		9,42		14,9	21,70	0,021	− 0,010	0,011		
16,011		1086		123		8,82		0,904						302,108	
	164		1065		135		7,98		14,9	21,06	0,040	− 0,002	0,038		
15,847		1044		146		7,15		0,939						302,146	
	70		1057		133		8,03		14,9	21,09	0,017	+ 0,002	0,019		
15,777		1070		120		8,91		0,915						302,165	
	38		1128		134		8,46		14,9	21,25	0,0075	+ 0,008	0,016		
15,739		1187		148		8,01		0,826						302,181	302,11
15,739		1174		148		7,93		0,834						302,110	302,11
	159		1087		138		7,86		35	49,32	0,067	− 0,009	0,058		
15,580		1000		128		7,80		0,980						302,168	(302,21)
	880		1065		158		6,91		35	48,29	0,048	+ 0,011	0,059		
14,700		1131		188		6,02		0,865						302,227	(302,28)
	670		1012		170		5,93		35	47,08	0,048	− 0,015	0,033		
14,030		894		153		5,84		1,096						302,260	(302,33)
	180		905		152		5,95		35	47,05	0,016	+ 0,003	0,019		
13,850		916		151		6,06		1,070						302,279	302,35
	1080		821		141		5,78		35	46,86	0,121	− 0,023	0,098		
12,770		727		132		5,51		1,348						302,377	(302,46)
	1110		687		139		4,97		35	45,69	0,219	− 0,016	0,203		
11,660		647		146		4,43		1,514						302,580	302,57
	1610		606		134		4,53		35	45,00	0,459	− 0,024	0,435		
10,050		565		122		4,63		1,735						303,015	303,00
	992		525		118		4,42		35	44,80	0,389	− 0,037	0,352		
9,058		484		115		4,21		2,025						303,367	(303,24)
	688		513		130		3,96		35	43,99	0,328	+ 0,043	0,371		
8,370		542		146		3,71		1,809						303,738	(303,65)
	290		611		166		3,67		35	43,42	0,107	+ 0,061	0,168		
8,080		680		187		3,63		1,440						303,906	(304,00)

The numbers in parentheses are not direct water level observations, but taken from the length-profile plot.

[1] Survey of the water level from 20 April 1917 by the Engineering Bureau, H.Z. Gruner, in Basle.

TABLE 13

Power Plant — Laufenburg

Stagnation Computation for $Q = 1570\ m^3/sec$

Profile (km.)	Distance L (m.)	F m^2	F_m m^2	U m	U_m m	R m	R_m m	v_m m/sec	k	c $=k\sqrt[6]{R}$	A_1 m	βA_2 m	Δh m	Stagnation Height m. above sea level Computed	Observed[1]
16,952		2343		223		10,51		0,670						301,800	301,80
	180		1982		187		10,62		14,9	22,09	0,022	− 0,016	0,006		
16,772		1622		151		10,73		0,966						301,806	(301,80)
	170		1433		151		9,48		14,9	21,68	0,046	− 0,015	0,031		
16,602		1244		151		8,24		1,262						801,837	(301,82)
	160		1210		135		9,02		14,9	21,50	0,065	− 0,009	0,056		
16,442		1176		120		9,80		1,336						301,893	(301,88)
	69		1136		126		9,02		14,9	21,50	0,032	− 0,009	0,023		
16,373		1097		133		8,24		1,434						301,916	(301,92)
	84		1081		131		8,25		14,9	21,18	0,048	− 0,003	0,045		
16,289		1066		129		8,26		1,471						301,961	(301,98)
	41		1064		122		9,17		14,9	21,54	0,022	0,000	0,022		
16,248		1063		116		10,09		1,475						301,983	(301,99)
	91		1199		124		10,10		14,9	21,89	0,034	+ 0,041	0,075		
16,157		1336		132		10,11		1,175						302,058	(302,03)
	146		1209		128		9,46		14,9	21,65	0,056	− 0,024	0,032		
16,011		1083		123		8,81		1,447						302,090	(302,09)
	164		1063		134		7,98		14,9	21,05	0,102	− 0,006	0,096		
15,847		1044		146		7,15		1,505						302,186	(302,13)
	70		1058		133		8,04		14,9	21,08	0,044	+ 0,006	0,050		
15,777		1072		120		8,94		1,464						302,236	(302,18)
	38		1133		134		8,50		14,9	21,28	0,019	+ 0,021	0,040		
15,739		1194		148		8,07		1,314						302,276	302,20
15,739		1187		148		8,01		1,324						302,200	302,20
	159		1093		138		7,88		35	49,35	0,017	− 0,024	0,000		
15,580		1000		129		7,75		1,570						302,200	(302,20)
	880		1074		159		6,91		35	48,29	0,118	+ 0,030	0,148		
14,700		1148		189		6,07		1,369						302,348	(130,32)
	670		1031		171		6,00		35	47,14	0,116	− 0,037	0,079		
14,030		914		154		5,93		1,718						302,427	(302,42)
	180		927		153		6,05		35	47,19	0,038	+ 0,008	0,046		
13,850		940		152		6,18		1,670						302,473	302,44
	1080		853		142		6,00		35	47,14	0,274	− 0,047	0,227		
12,770		767		132		5,82		2,043						302,700	(302,78)
	1110		740		141		5,29		35	46,15	0,450	− 0,022	0,428		
11,660		714		150		4,76		2,200						303,128	(303,21)
	1610		698		142		4,90		33	42,98	0,898	− 0,015	0,883		
10,050		683		135		5,05		2,300						304,011	(304,00)

The numbers in parentheses are not direct water level observations, but taken from the length-profile plot.

[1] Survey of the water level from 30 June 1914 by the Power Plant Laufenburg.

TABLE 14

Power Plant — Laufenburg

Stagnation Computation for
Q = 2280 m^3/sec

Profile (km.)	Distance L (m.)	F m^2	F_m m^2	U m	U_m m	R m	R_m m	v_m m/sec	k	C $= k\sqrt[6]{R}$	A_1 m	βA_2 m	Δh m	Stagnation Height m. above sea level Computed	Observed[1]
16,952		2343		223		10,51		0,971						301,800	(301,83)
	180		1982		187		10,62		14,9	22,09	0,046	−0,035	0,011		
16,772		1622		151		10,73		1,402						301,811	(301,92)
	170		1437		151		9,51		14,9	21,69	0,096	−0,046	0,050		
16,602		1252		151		8,30		1,819						301,861	(301,97)
	160		1218		135		9,08		14,9	21,51	0,135	−0,013	0,122		
16,442		1184		120		9,86		1,924						301,983	(302,03)
	69		1144		126		9,08		14,9	21,51	0,065	−0,019	0,046		
16,373		1104		133		8,30		2,063						302,029	(302,10)
	84		1090		131		8,28		14,9	21,19	0,099	−0,008	0,091		
16,289		1076		130		8,26		2,119						302,120	(302,19)
	41		1076		123		8,72		14,9	21,38	0,046	0,000	0,046		
16,248		1076		117		9,19		2,119						302,166	(302,20)
	91		1221		125		9,73		14,9	21,75	0,0685	+0,0865	0,155		
16,157		1366		133		10,27		1,670						302,321	(302,29)
	146		1238		129		9,61		14,9	21,72	0,110	−0,048	0,062		
16,011		1110		124		8,95		2,054						302,383	(302,42)
	164		1094		136		8,11		14,9	21,12	0,198	−0,008	0,190		
15,847		1078		148		7,28		2,115						302,573	(302,57)
	70		1101		135		8,25		14,9	21,18	0,082	+0,018	0,100		
15,777		1124		122		9,21		2,028						302,673	(302,71)
	38		1195		136		8,82		14,9	21,40	0,038	+0,044	0,082		
15,739		1265		150		8,43		1,802						302,755	302,80
15,739		1272		152		8,37		1,790						302,800	302,80
	159		1176		141		8,31		35	49,70	0,029	−0,038	0,000		
15,580		1081		131		8,26		2,106						302,800	(302,84)
	880		1178		161		7,45		35	48,88	0,189	+0,063	0,252		
14,700		1275		192		6,64		1,789						303,052	(303,03)
	670		1153		174		6,61		35	47,91	0,173	−0,056	0,117		
14,030		1032		157		6,58		2,205						303,169	(303,28)
	180		1040		156		6,67		32,5	44,56	0,065	+0,007	0,072		
13,850		1049		155		6,76		2,173						303,241	303,44
	1080		970		145		6,68		30,5	41,82	0,509	−0,062	0,447		
12,770		891		135		6,60		2,560						303,688	(303,79)
	1110		892		145		6,20		30,5	41,30	0,690	0,000	0,690		
11,660		892		154		5,19		2,559						304,378	(304,40)

The numbers in parentheses are not direct water level observations, but are taken from the length-profile plot.

---

[1] Survey of the water level from 28 July 1914 by the Power Plant Laufenburg

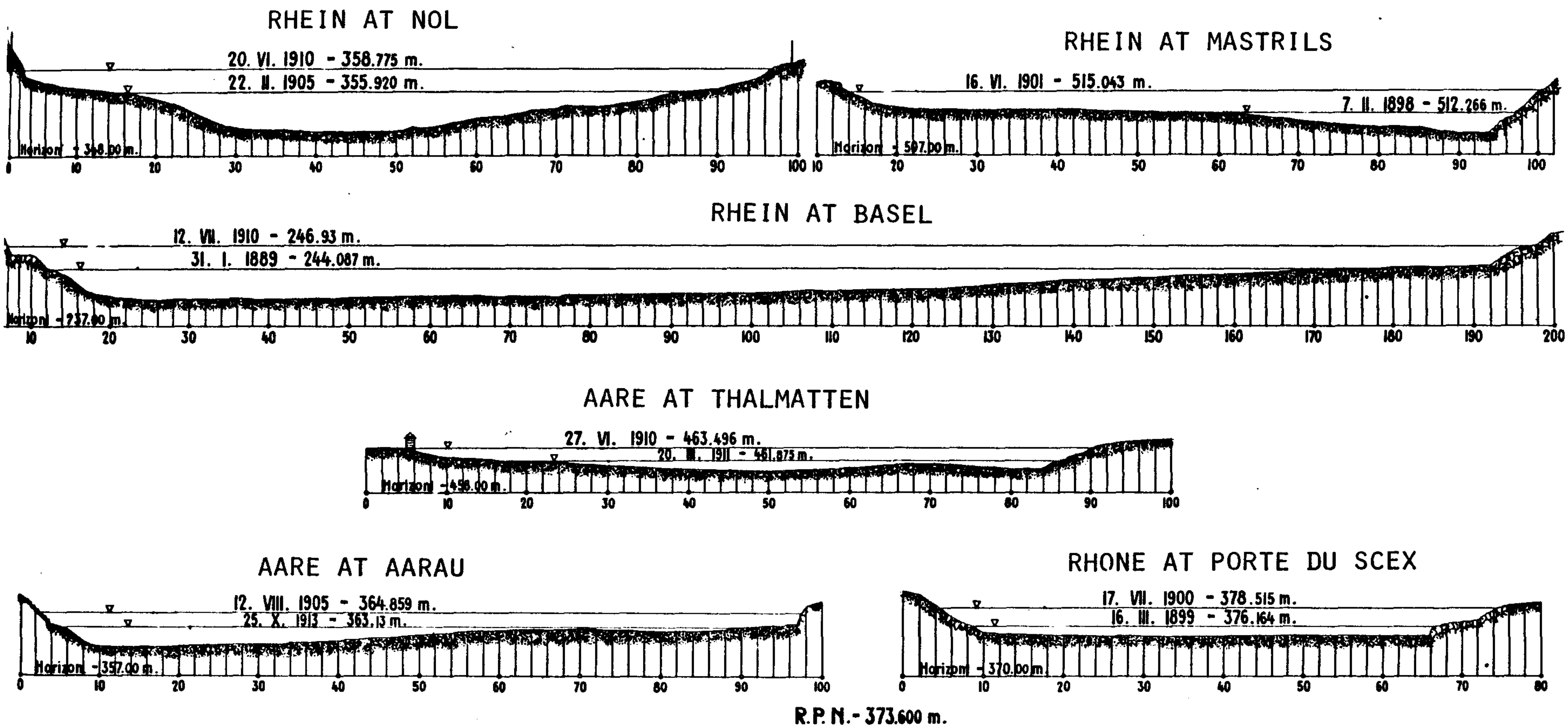

FIGURE 1 Cross-sections. Numbers on water surface give date followed by elevation of water surface.

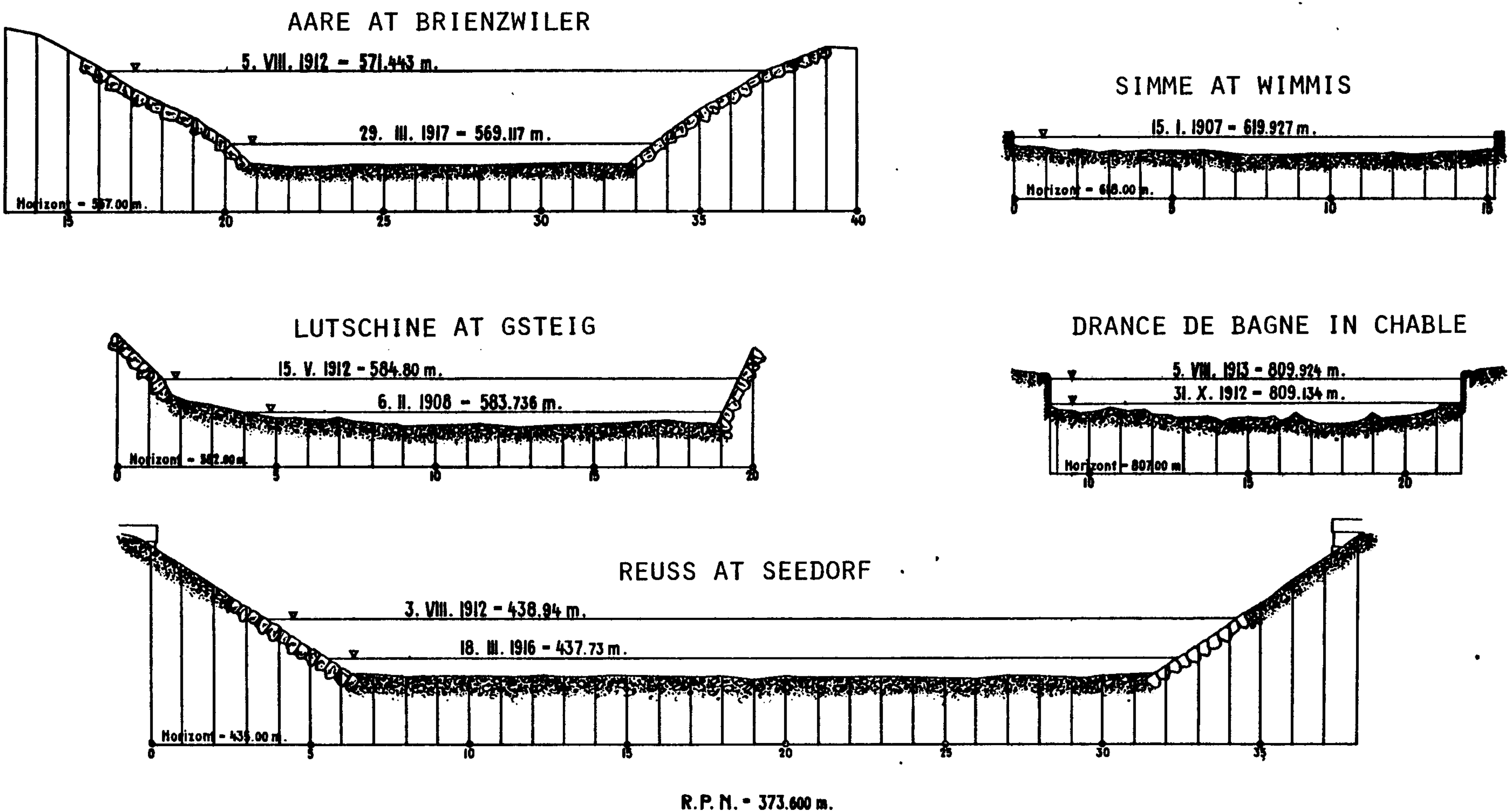

FIGURE 2 Cross-sections. Numbers on water surface give date followed by elevation of water surface.

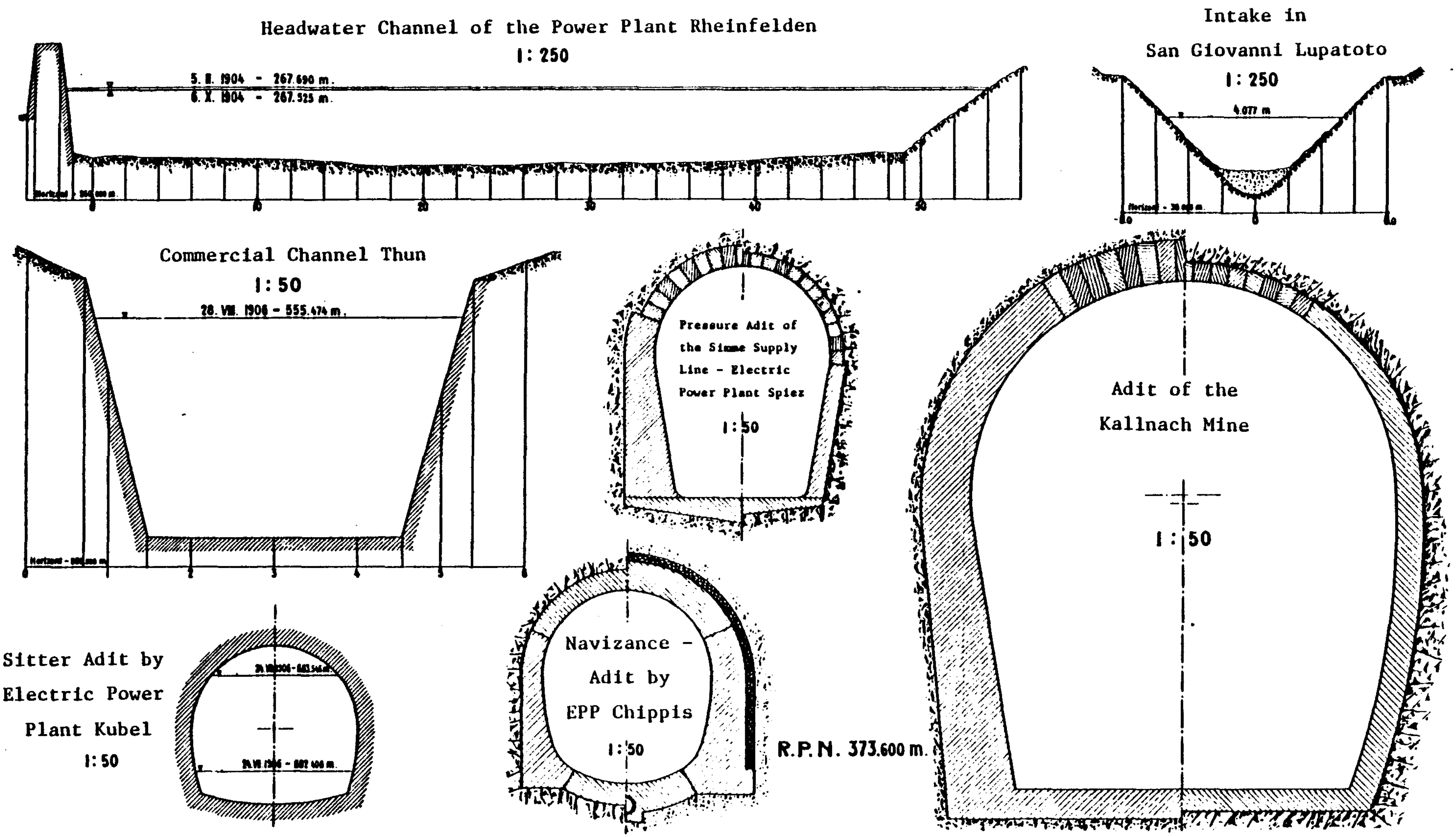

FIGURE 3 Cross-sections of intakes and adits.

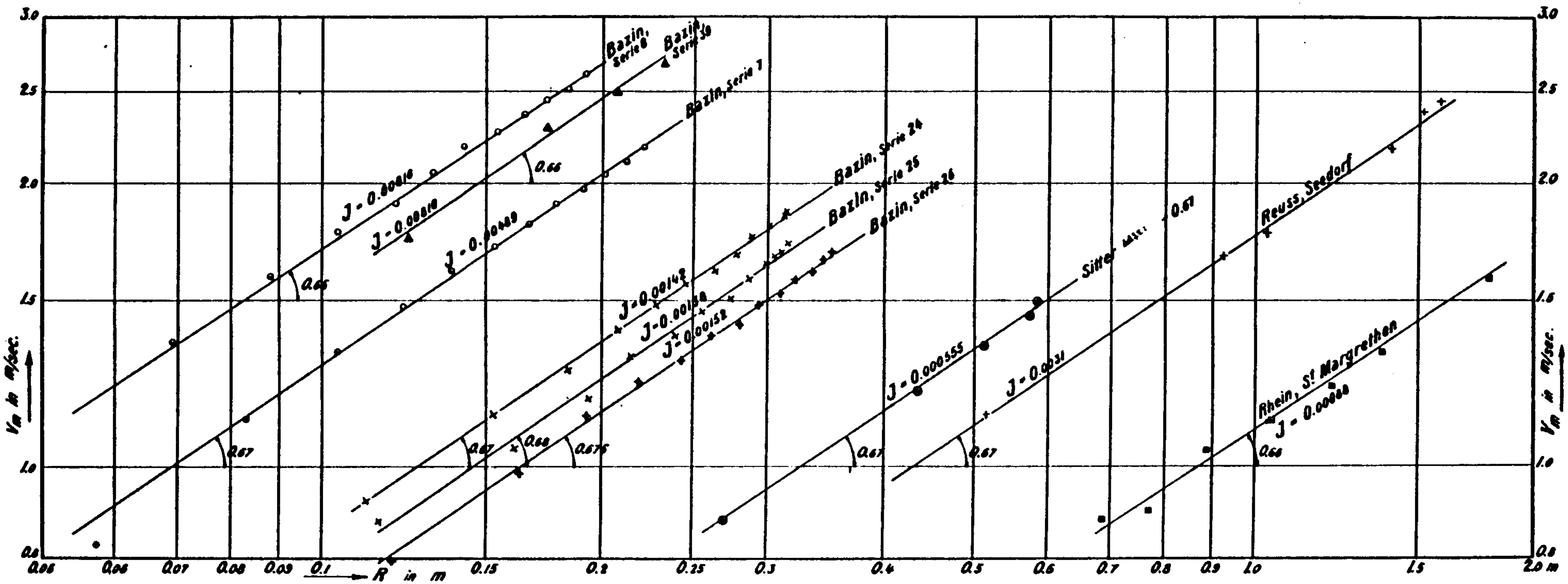

Series 7 & 8: Board channel with rectangular cross-section.
Series 39: Trimmed ashlar, very regular.
Series 26: Board channel with semicircular cross-section.
Series 24: Pure cement channel.
Series 25: Cement with 1/3 fine river sand.

Sitter Adit: Smoothed concrete
Reuss, Seedorf: Stone banks, bottom coarse gravel
Rhein, St. Margrethen: Medium gravel.

FIGURE 4 Determination of the Exponent "μ" in the formula $v_m = k\,R^{\mu}\,J^{\nu}$. Measurement series with constant J.

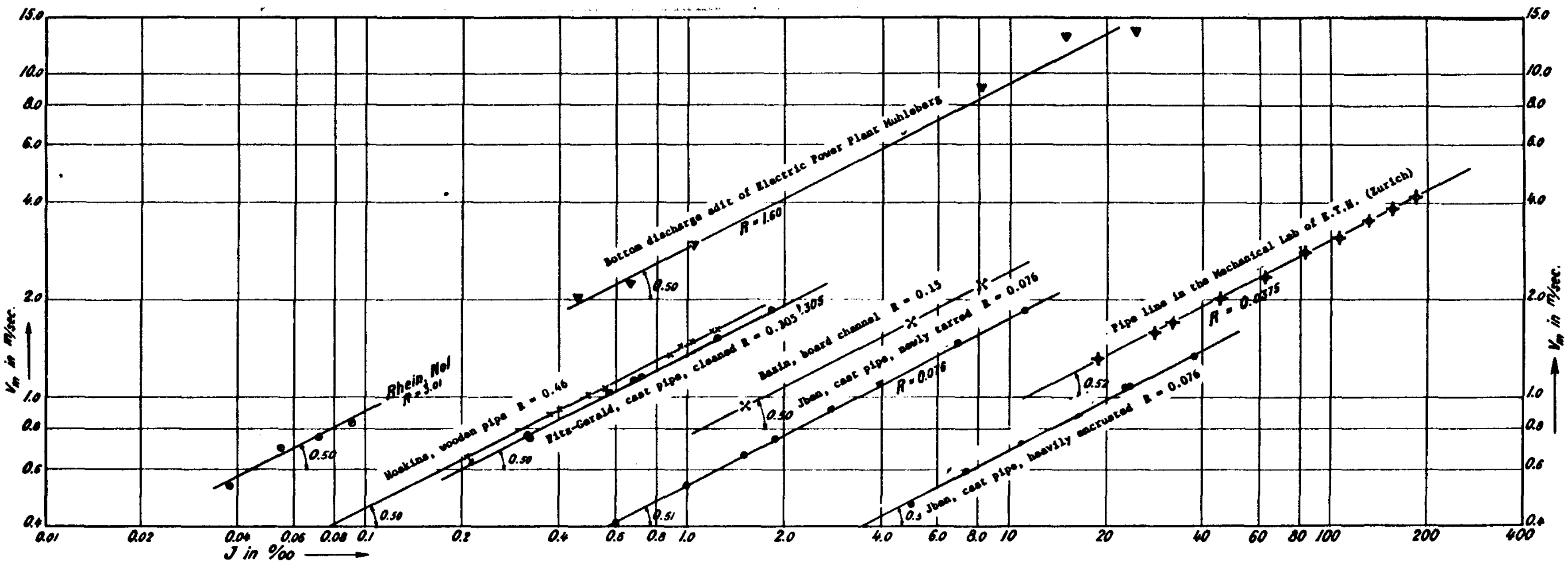

FIGURE 5 Determination of the exponent "ν" in the formula $v_m = k\, R^{\mu}\, J^{\nu}$. Measurement series with constant R.

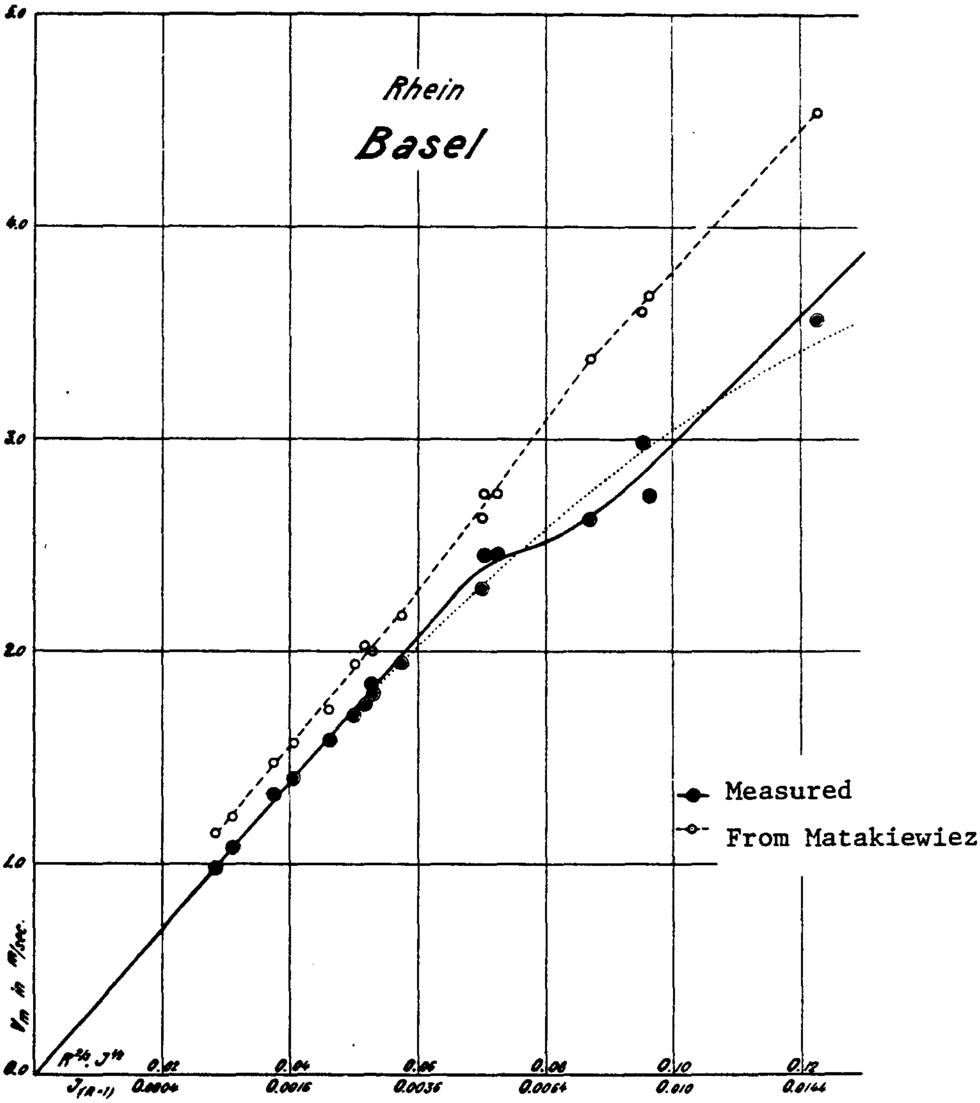

FIGURE 6 Mean velocity, v_m, as a function of $R^{2/3}J^{1/2}$ for streams.

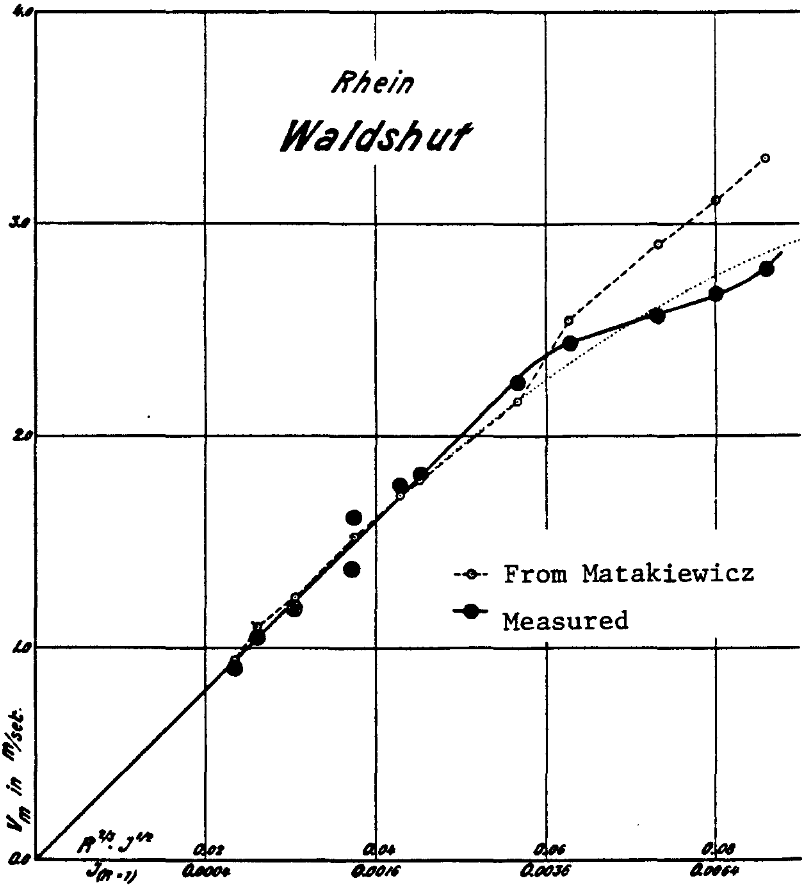

FIGURE 7 Mean velocity, v_m, as a function of $R^{2/3}\ J^{1/2}$ for streams.

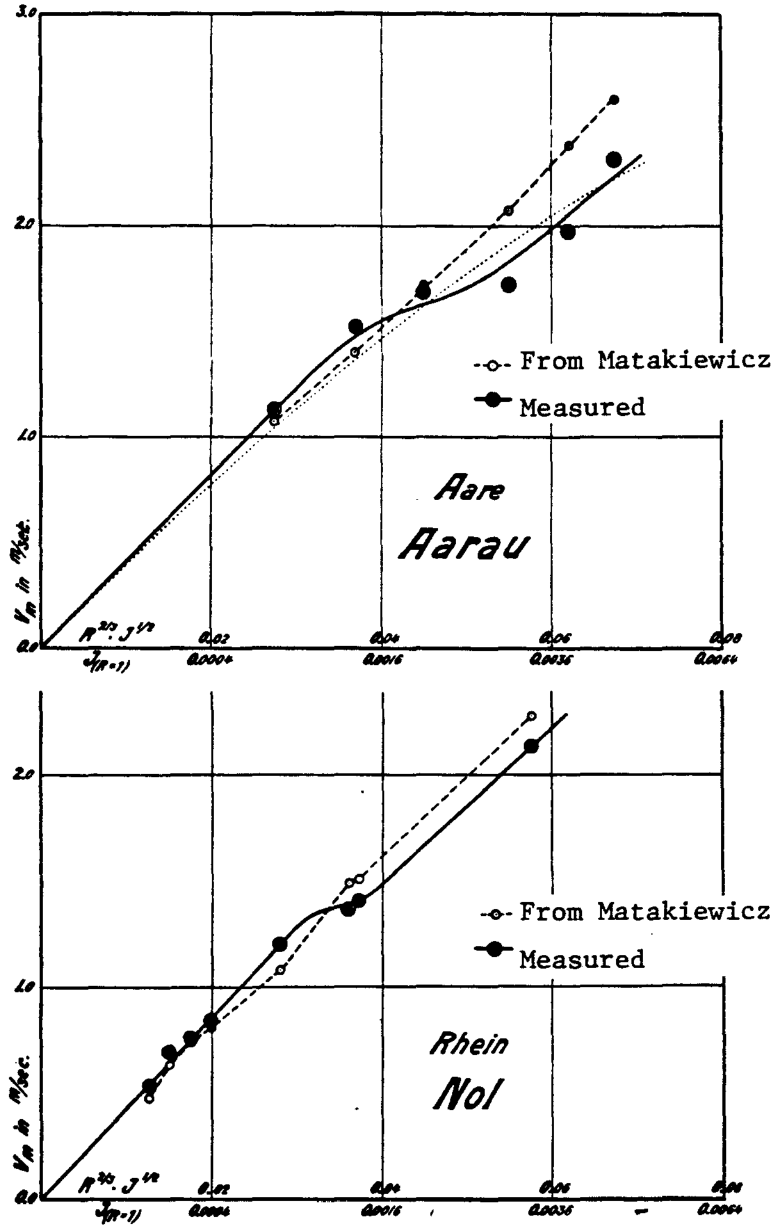

FIGURE 8 Mean velocity, v_m, as a function of $R^{2/3}\ J^{1/2}$ for streams.

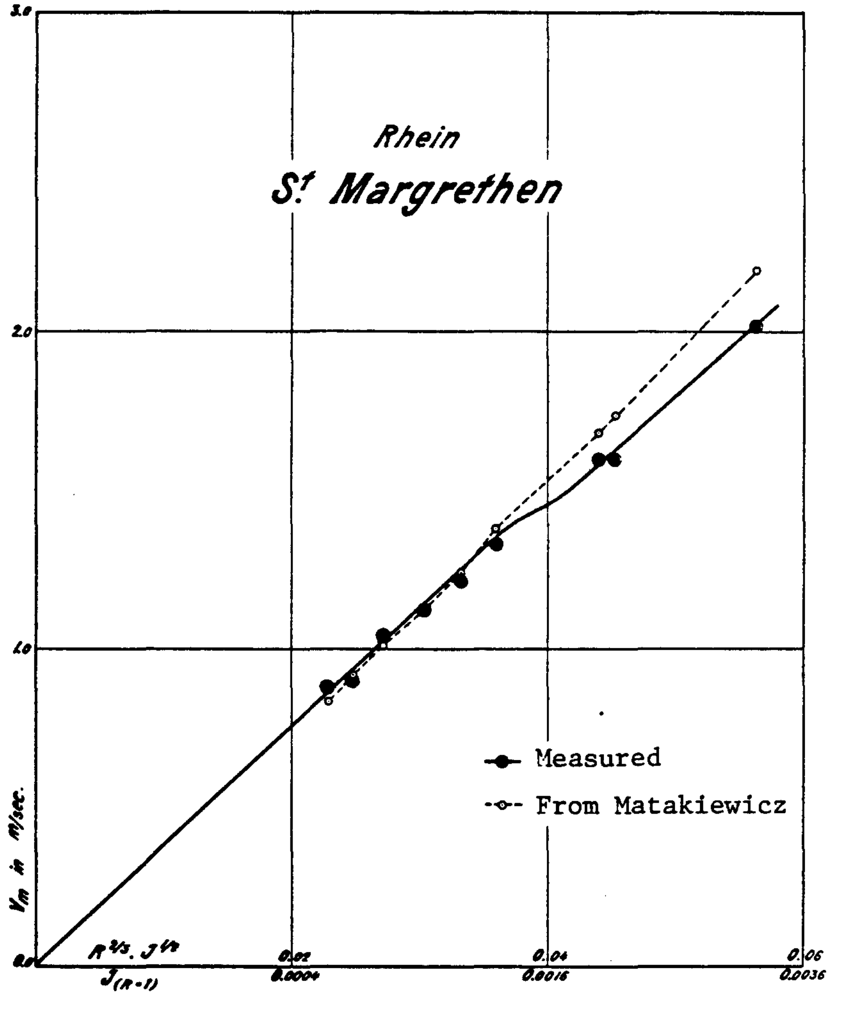

FIGURE 9 Mean velocity, v_m, as a function of $R^{2/3}\ J^{1/2}$ for streams.

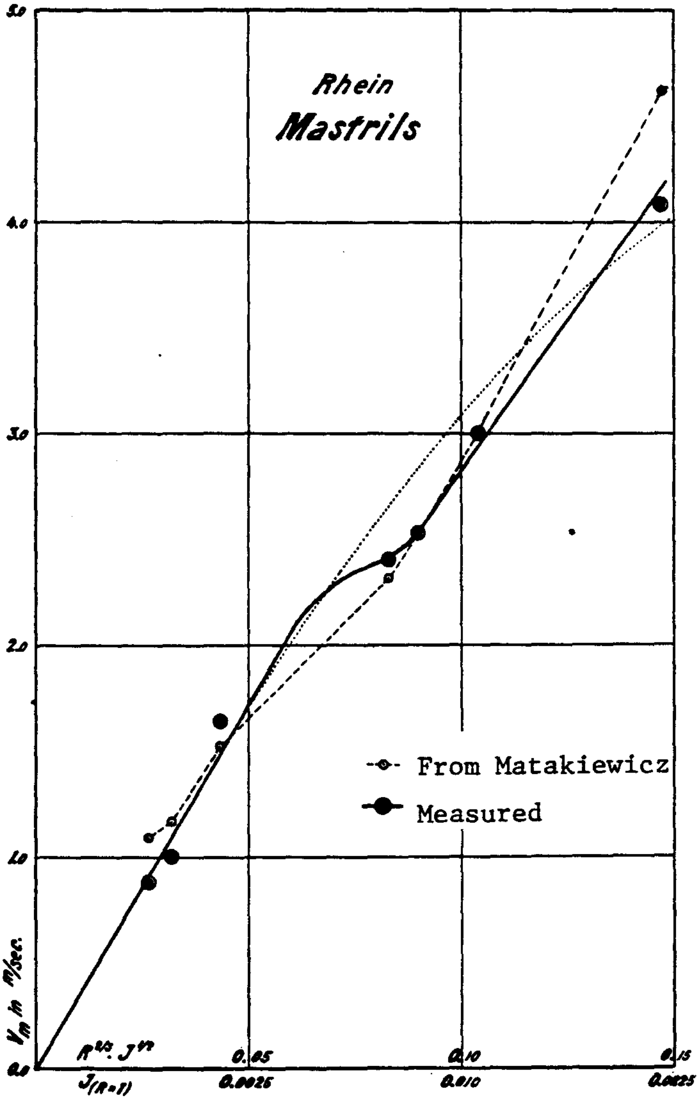

FIGURE 10 Mean velocity, v_m, as a function of $R^{2/3}\ J^{1/2}$ for streams.

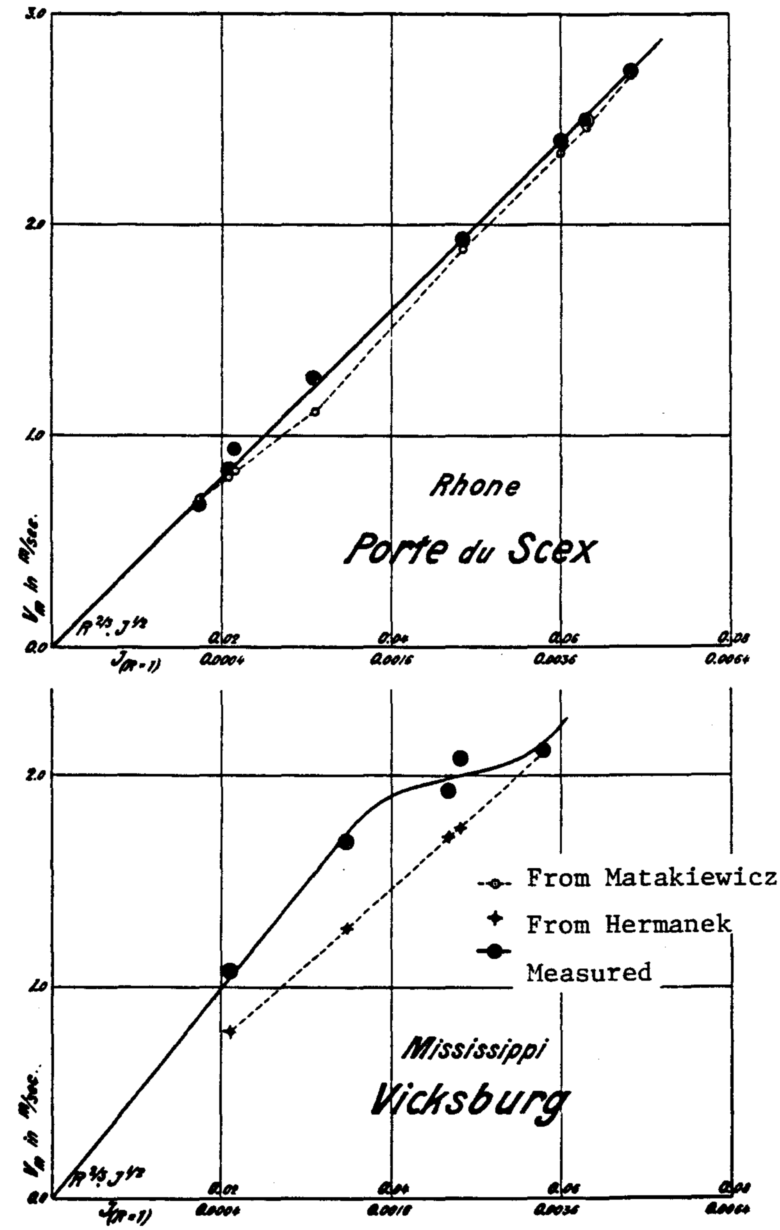

FIGURE 11 Mean velocity, v_m, as a function of $R^{2/3}\ J^{1/2}$ for streams.

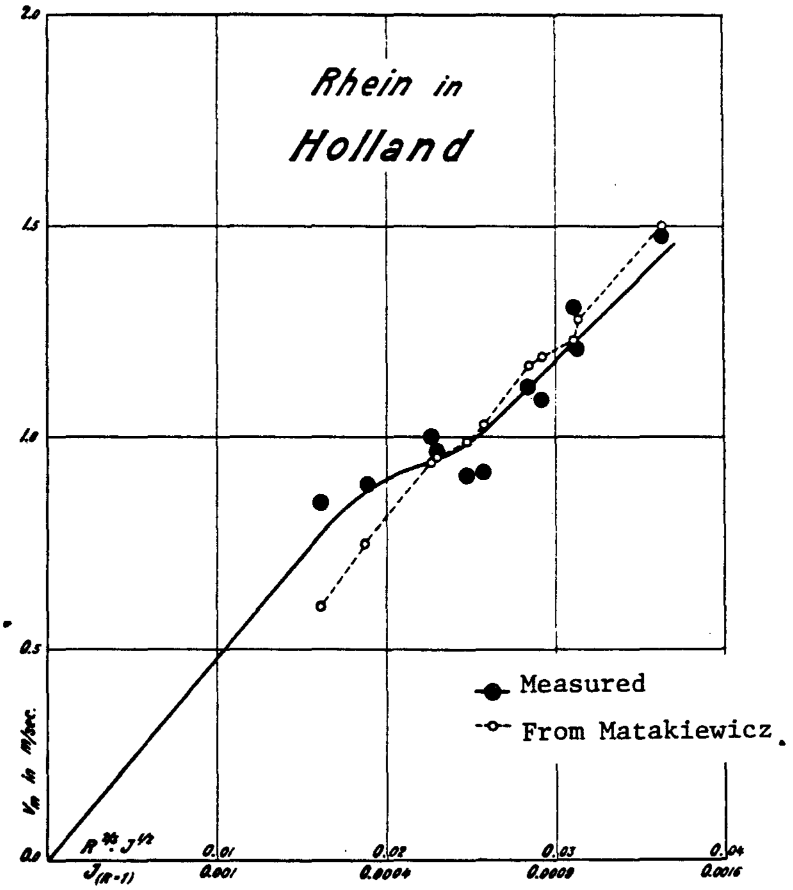

FIGURE 12 Mean velocity, v_m, as a function of $R^{2/3}\ J^{1/2}$ for streams.

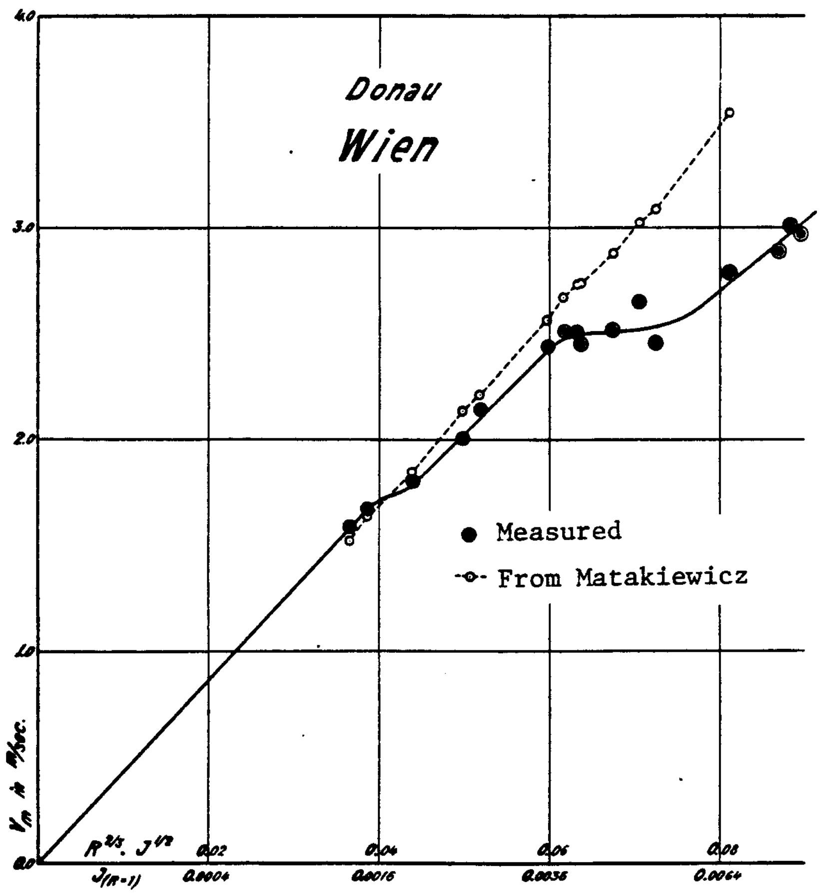

FIGURE 13 Mean velocity, v_m, as a function of $R^{2/3}$ $J^{1/2}$ for streams.

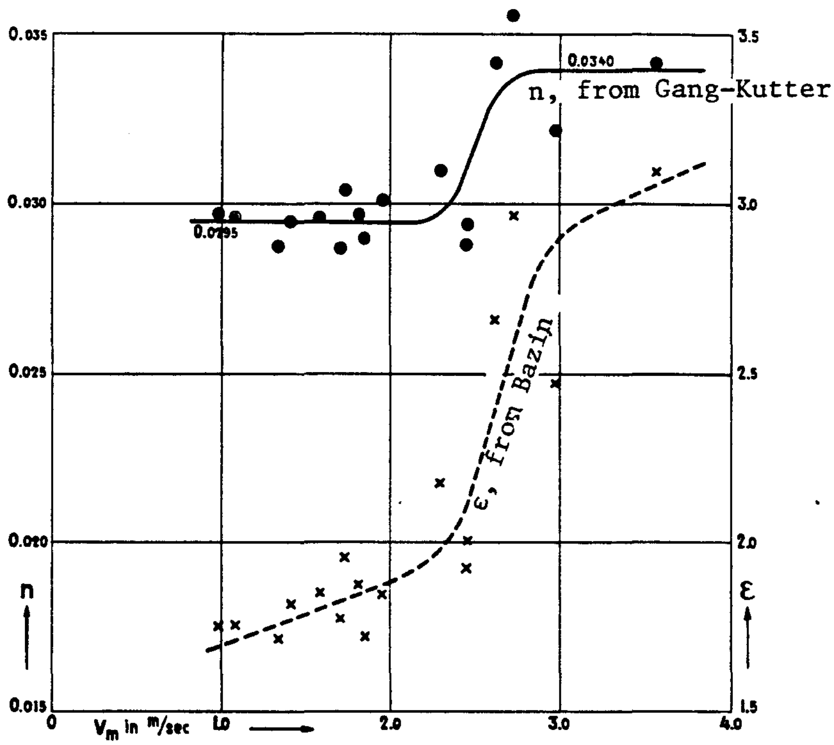

FIGURE 14 Kutter's roughness coefficient, n, and Bazin's coefficient, ε, for the Rhine at Basle, as functions of mean velocity, v_m.

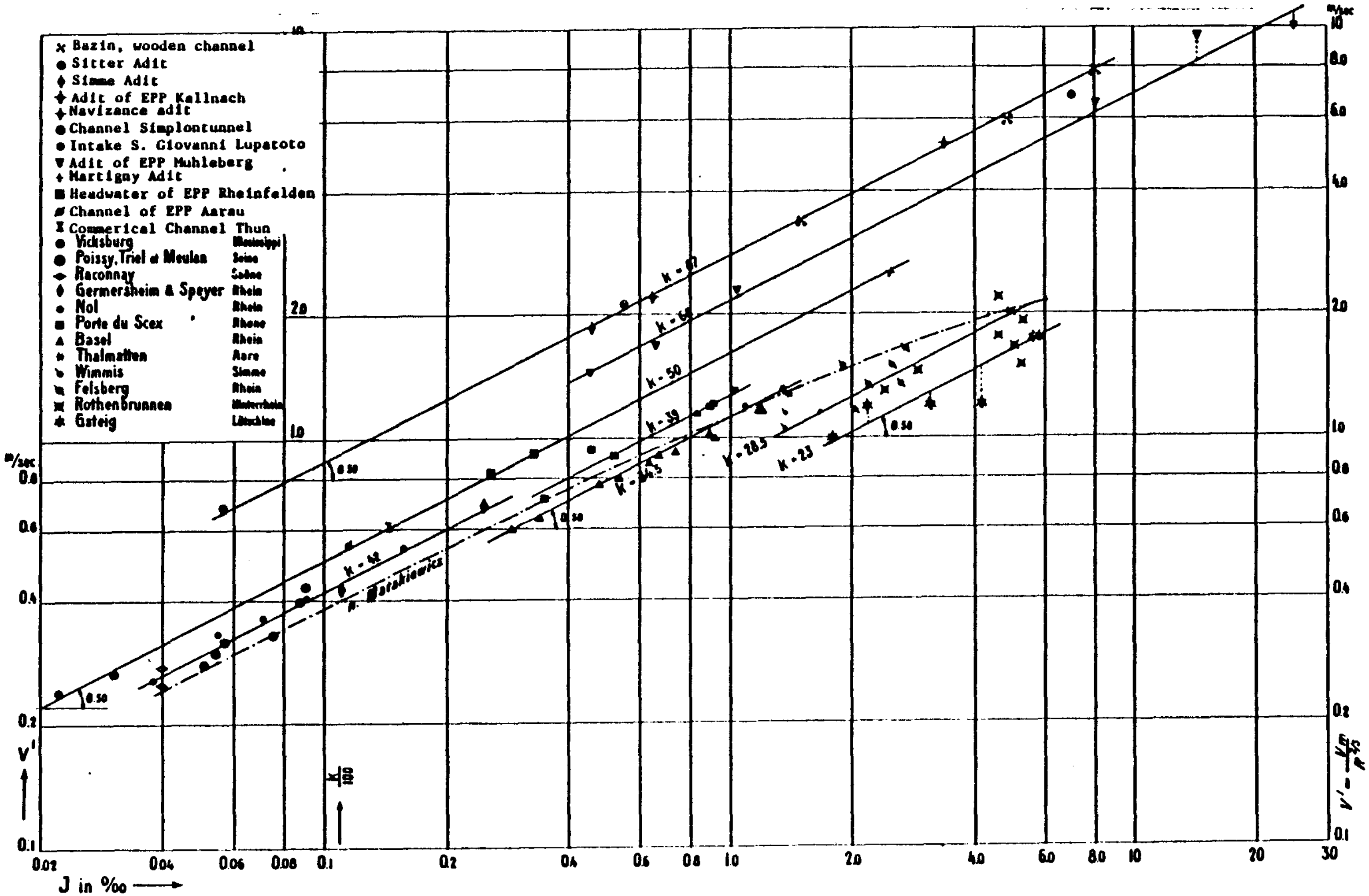

FIGURE 15 Determination of the coefficient k in the formula $v_m = k\ R^{2/3}\ J^{1/2}$. (Reduced velocities, v', for the hydraulic radius, R = 1, $v' = v_m/R^{2/3}$ as a function of the effective slope.)

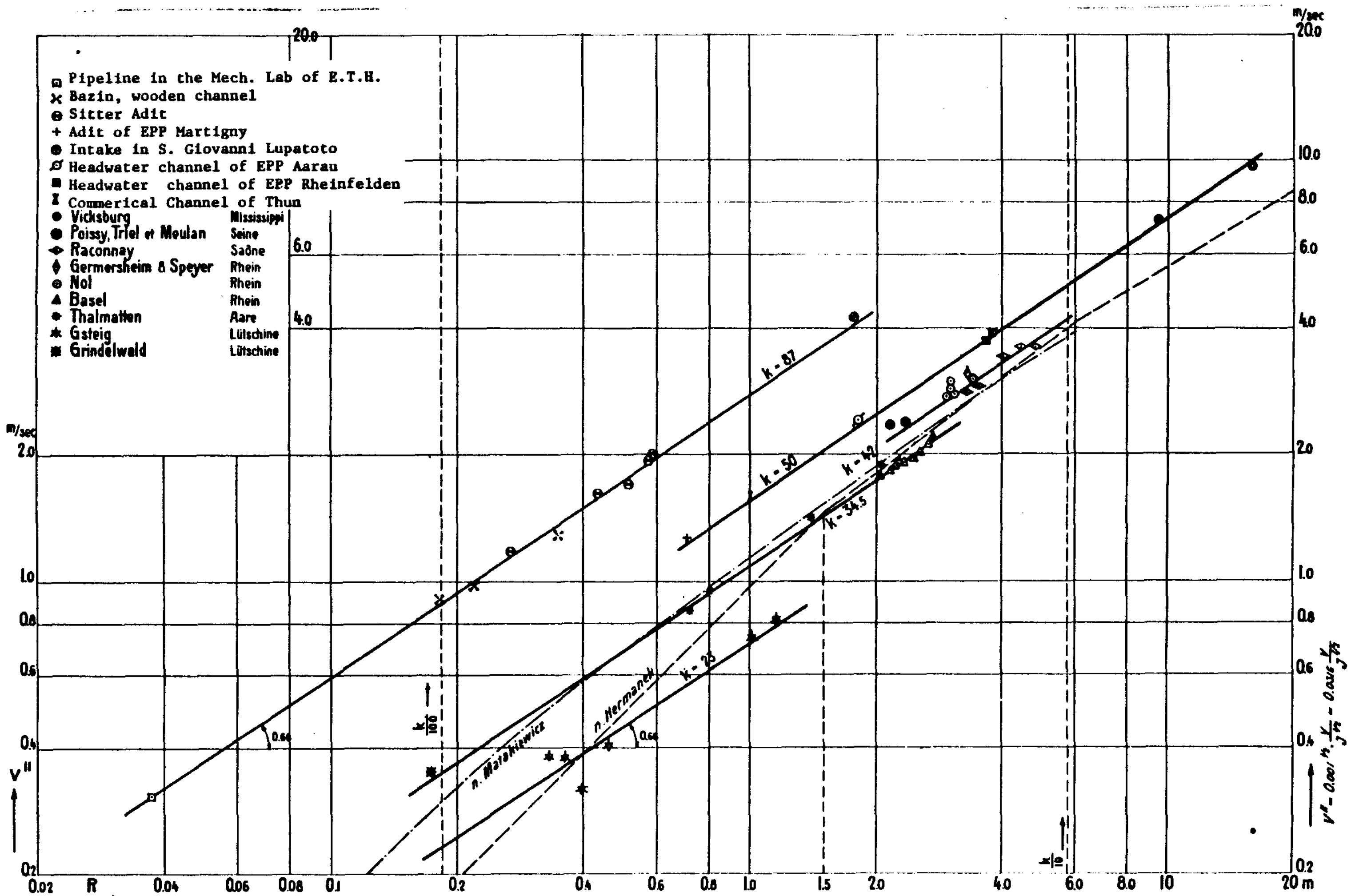

FIGURE 16 Determination of the coefficient, k, in the formula $v_m = k\ R^{2/3}\ J^{1/2}$. (Reduced velocities, v'', for slopes, J = 0.001 $v'' = 0.001^{1/2}(v_m/J^{1/2})$, as a function of the effective hydraulic radius.

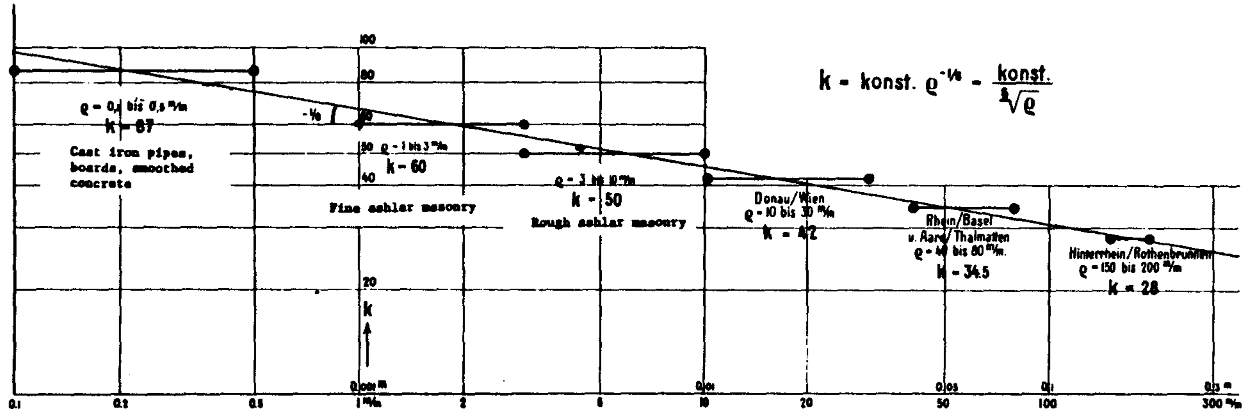

Wall Roughness, ρ (Size of irregularities on gravel particle-size in mm)

FIGURE 17 Dependence of the k-value on the absolute wall roughness.

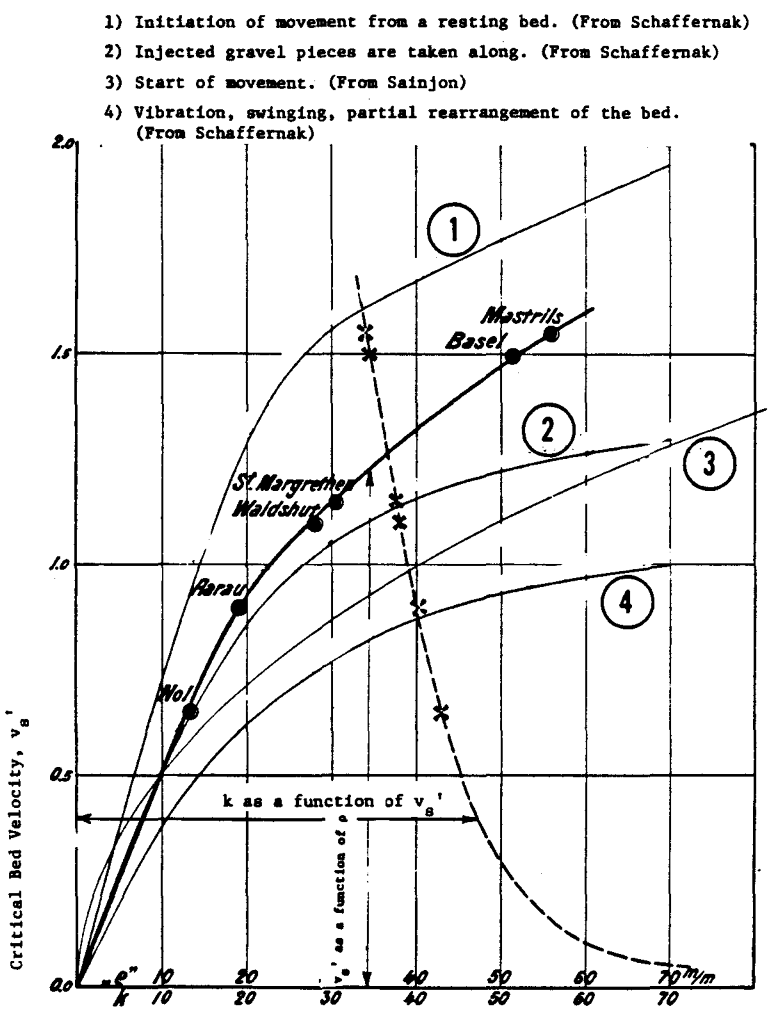

FIGURE 18 Relations between the coefficient k, the grain size, ρ, of the gravel and the critical bed velocity, v_s'; and the comparative plot of the limiting velocities according to the experiments of Professor Dr. F. Schaffernak.

Comparison with the formulas of

Bazin $C = \frac{87}{1 + \varepsilon/\sqrt{R}}$

Ganguillet - Kutter, $C = \frac{23 + \frac{1}{n} + \frac{0.00155}{J}}{1 + \left(23 + \frac{0.00155}{J}\right)\frac{n}{\sqrt{R}}}$

and Kutter (short formula) $C = \frac{100\sqrt{R}}{m + \sqrt{R}}$

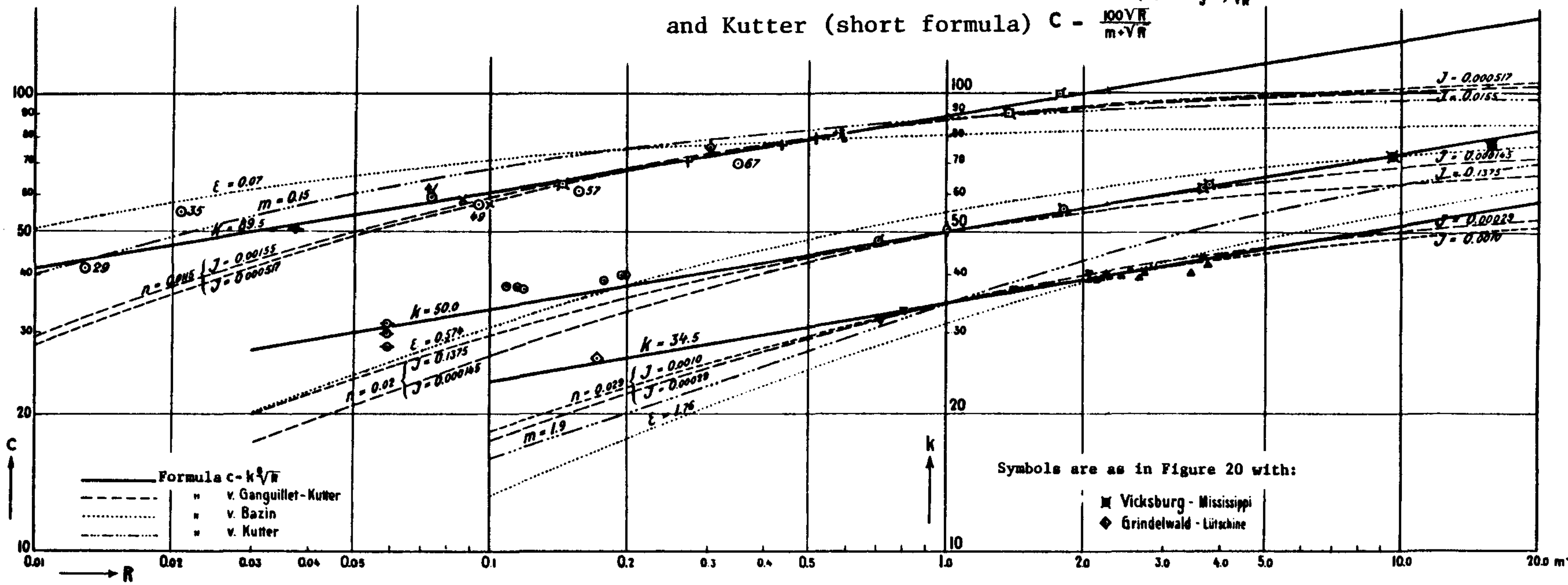

FIGURE 19 Dependence of the C-values on the hydraulic radius according to $C = k\ R^{1/6}$

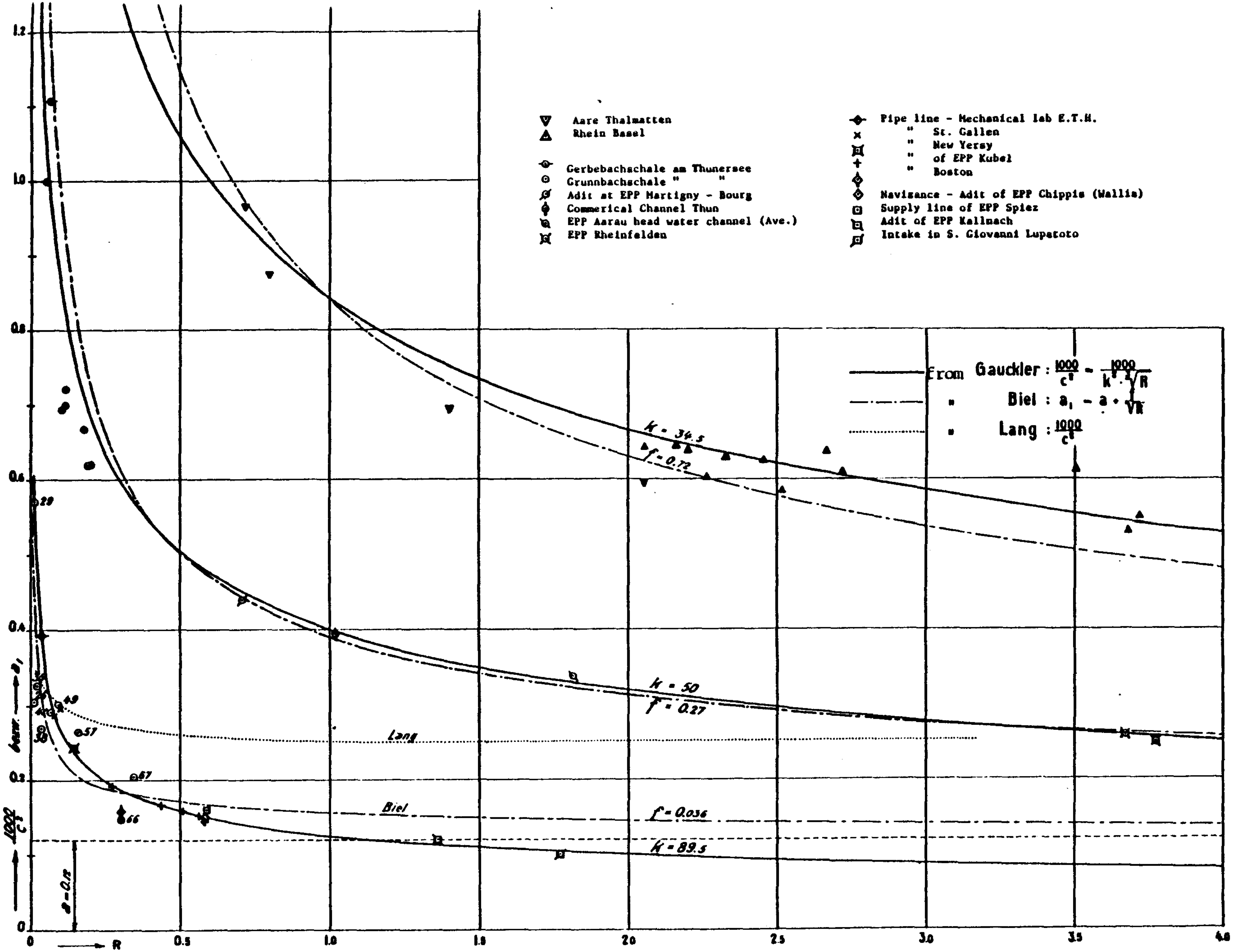

FIGURE 20 Comparison of Gaukler Formulas with the one of Biel and Lang

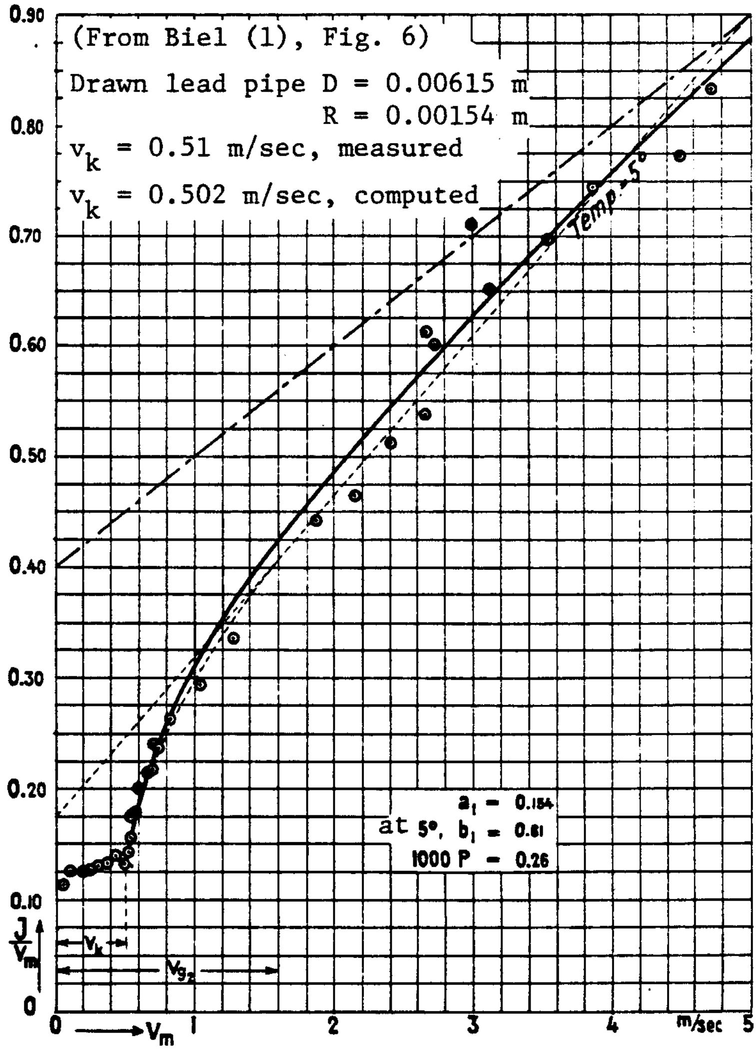

FIGURE 21 Experiment on head losses by Reynolds.

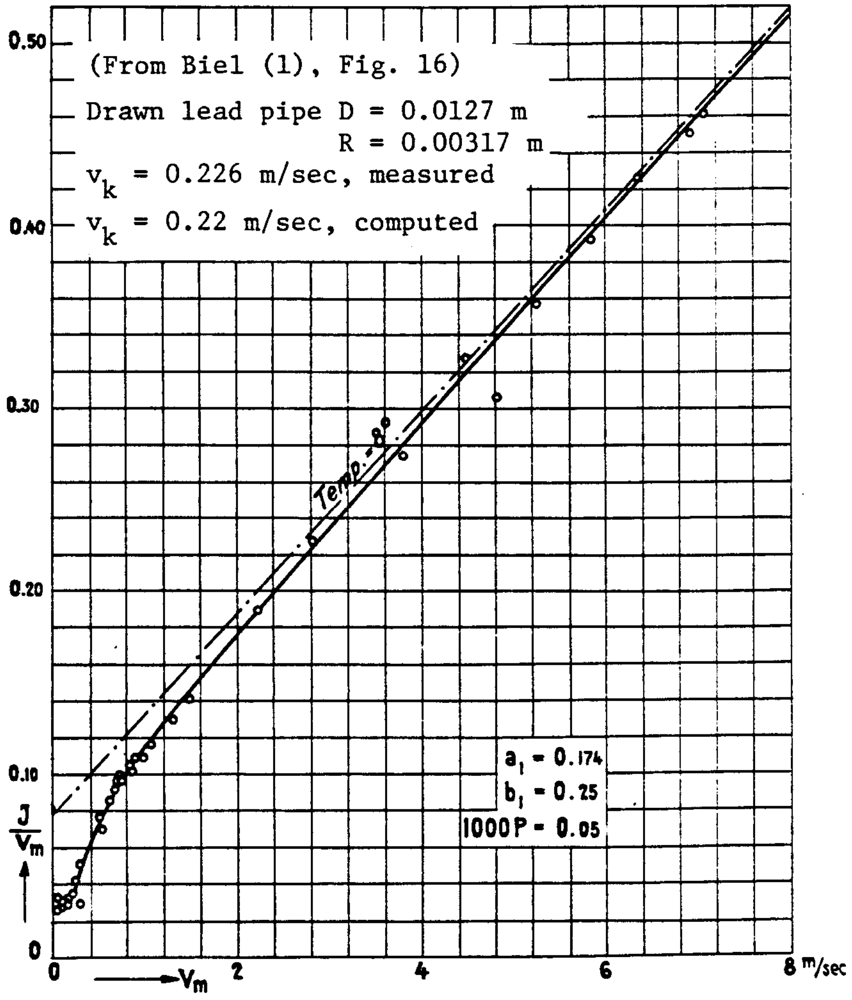

FIGURE 22 Experiment on head losses by Reynolds.

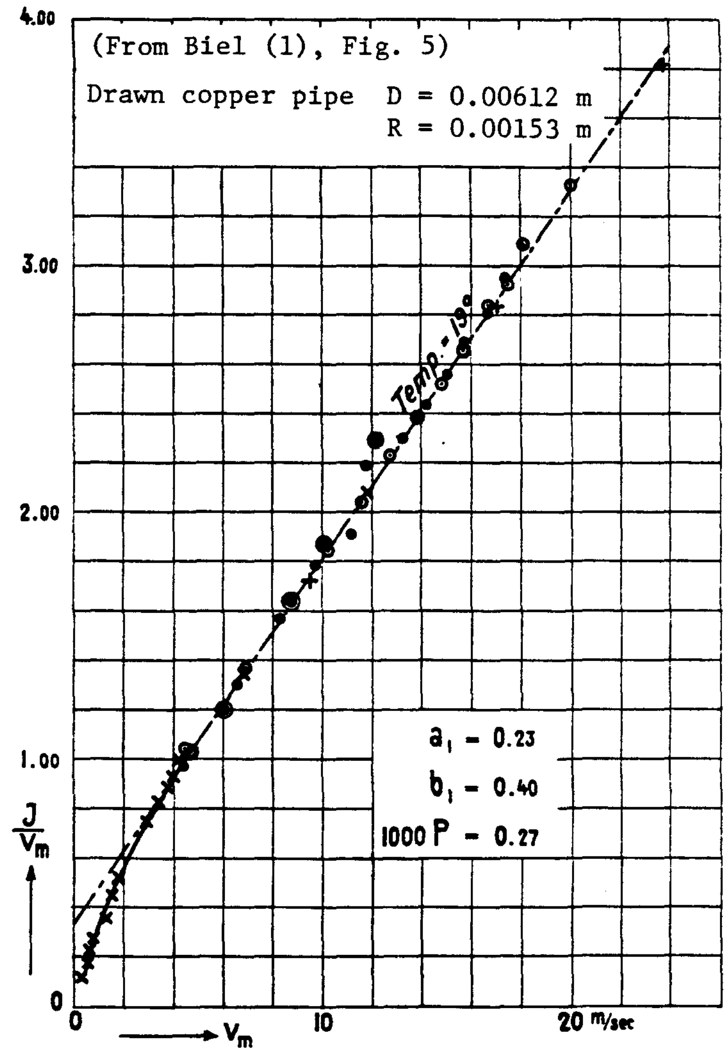

FIGURE 23 Experiment on head losses by Lang.

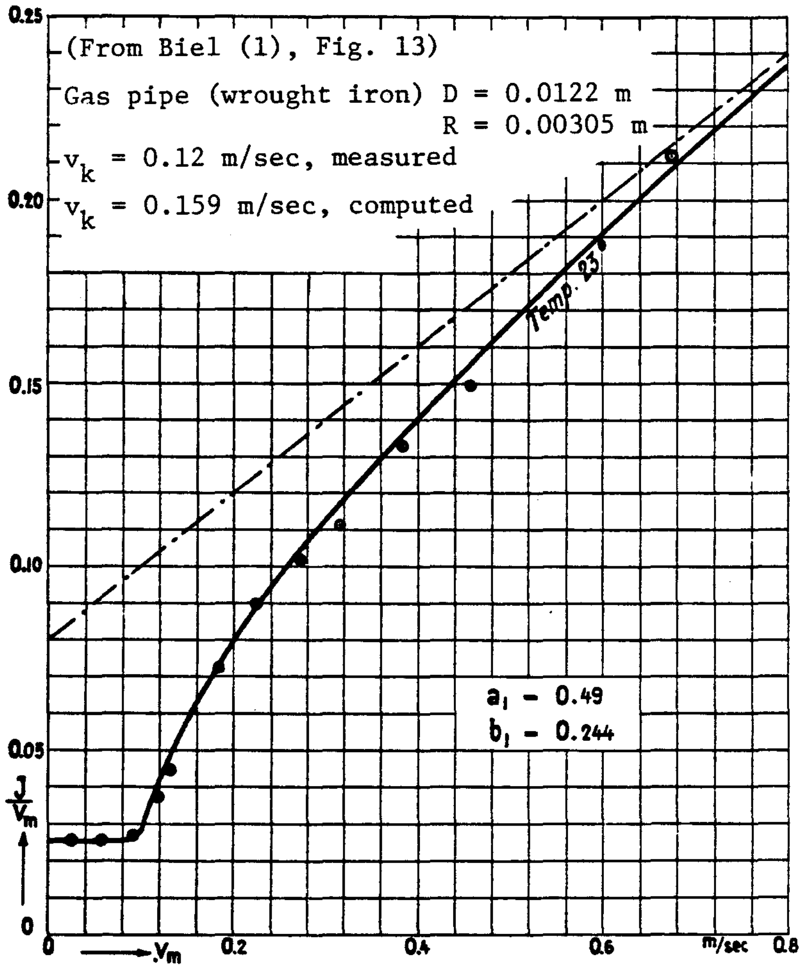

FIGURE 24 Experiment on head losses by Darcy.

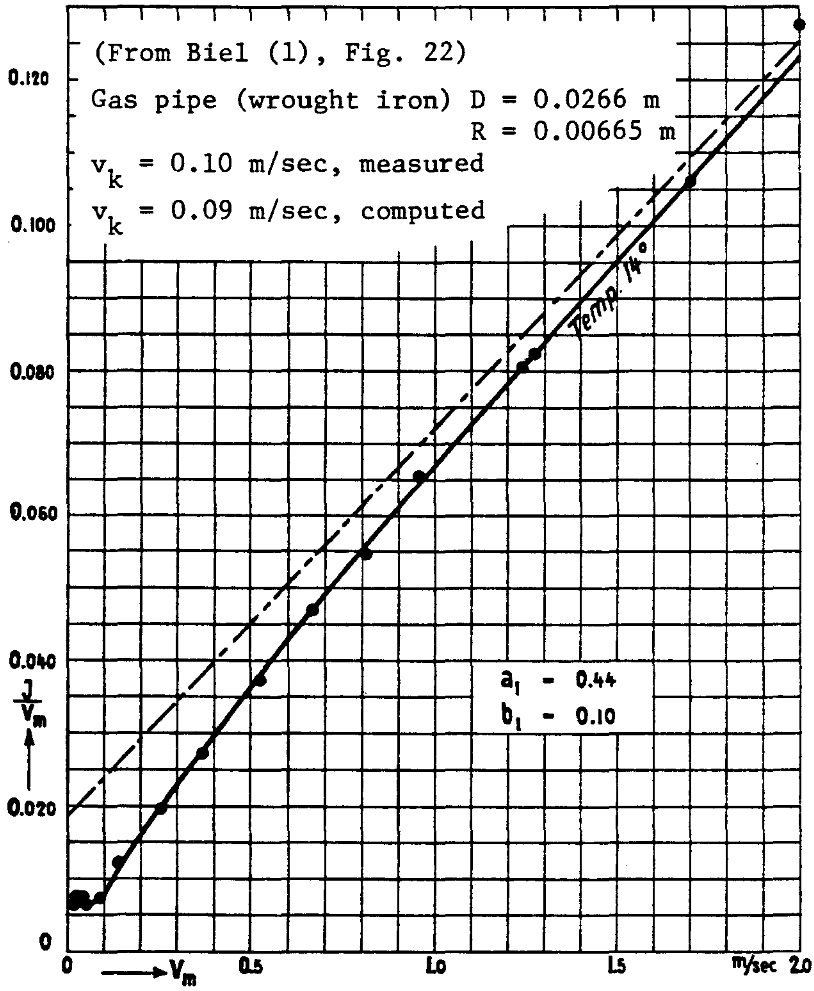

FIGURE 25 Experiment on head losses by Darcy.

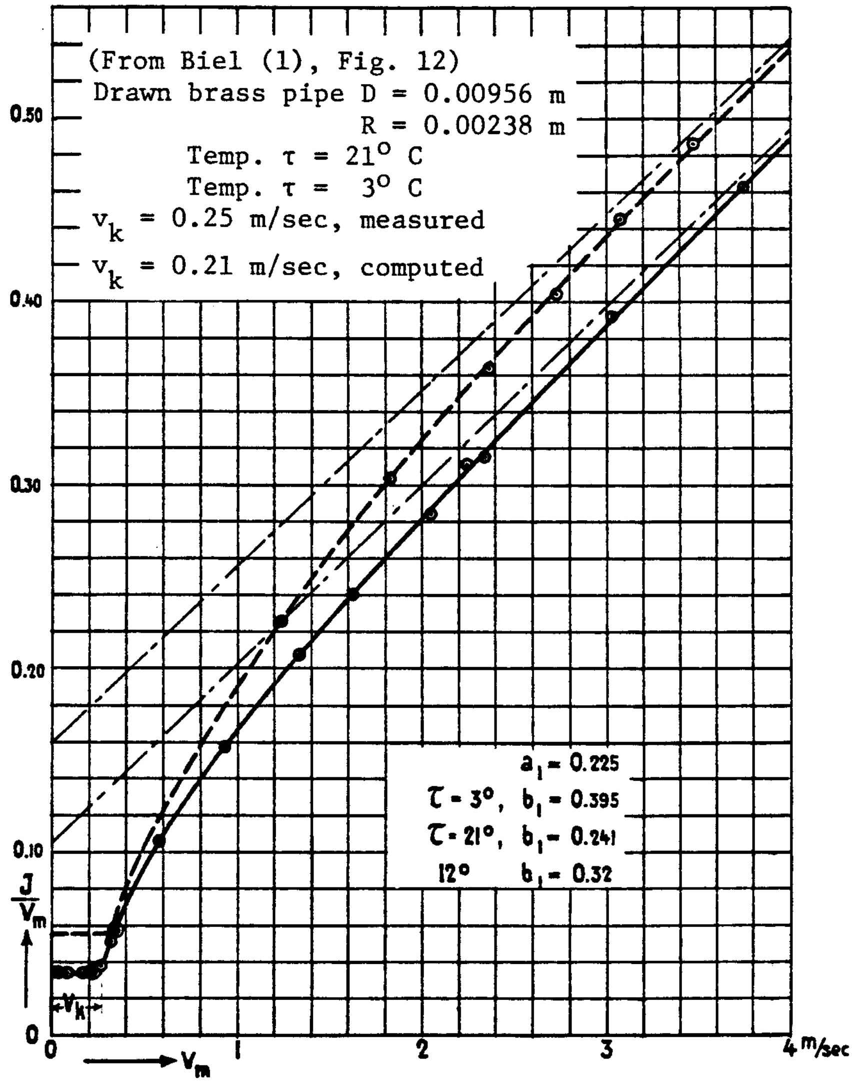

FIGURE 26 Experiment on head losses by Saph and Schoder.

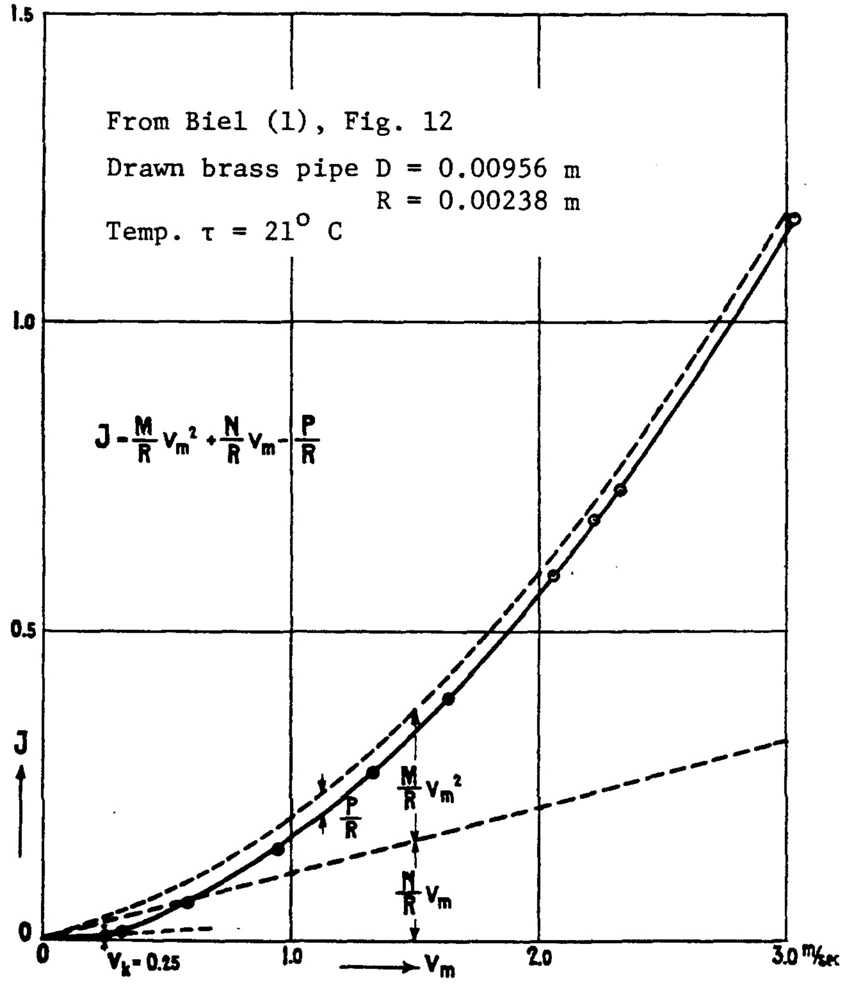

FIGURE 26a Experiment on head losses by Saph and Schoder.

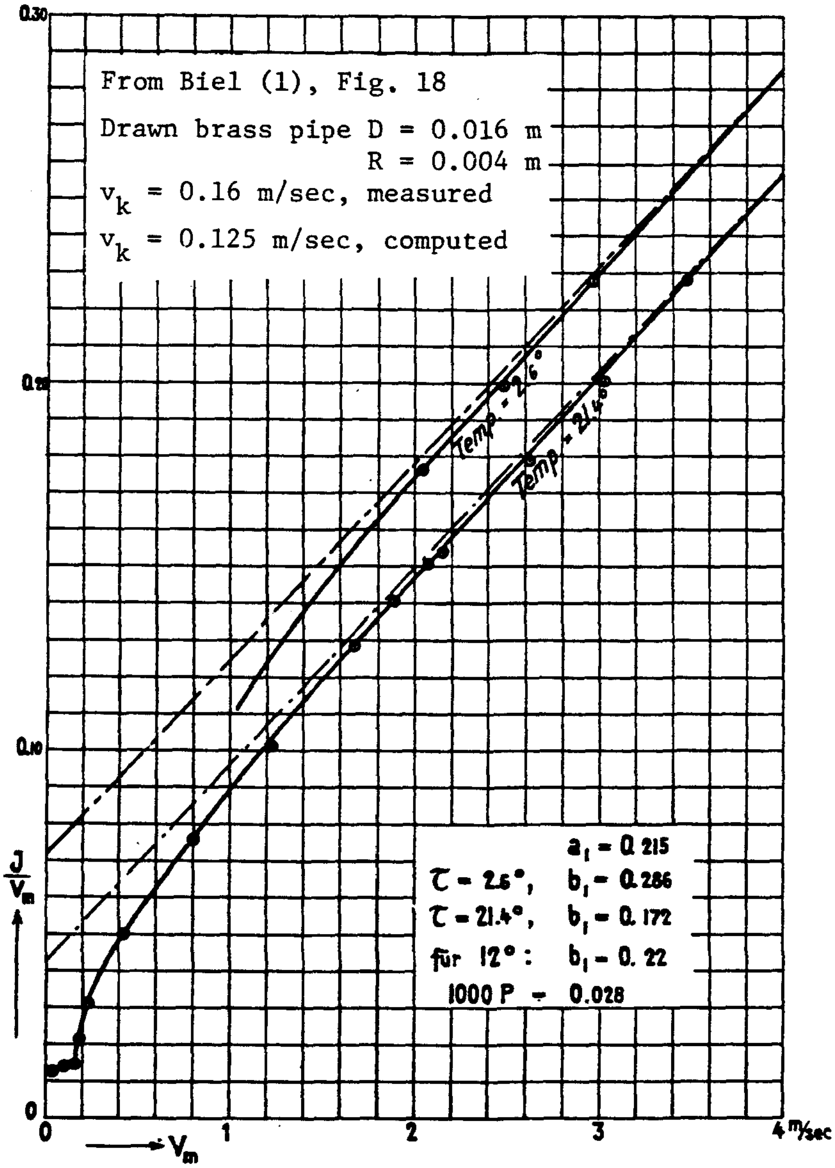

FIGURE 27 Experiment on head losses by Saph and Schoder.

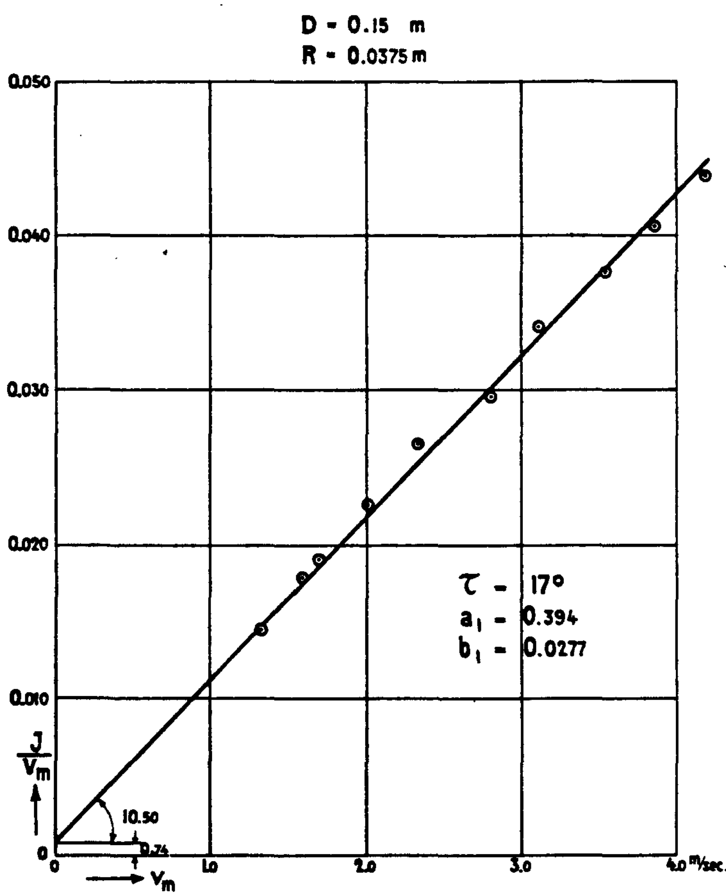

FIGURE 28 Cast iron pressure line in the mechanical laboratory of the E.T.H. (Zurich). Determination of Biel's coefficient, a_1 and b_1, after experiments of the author.

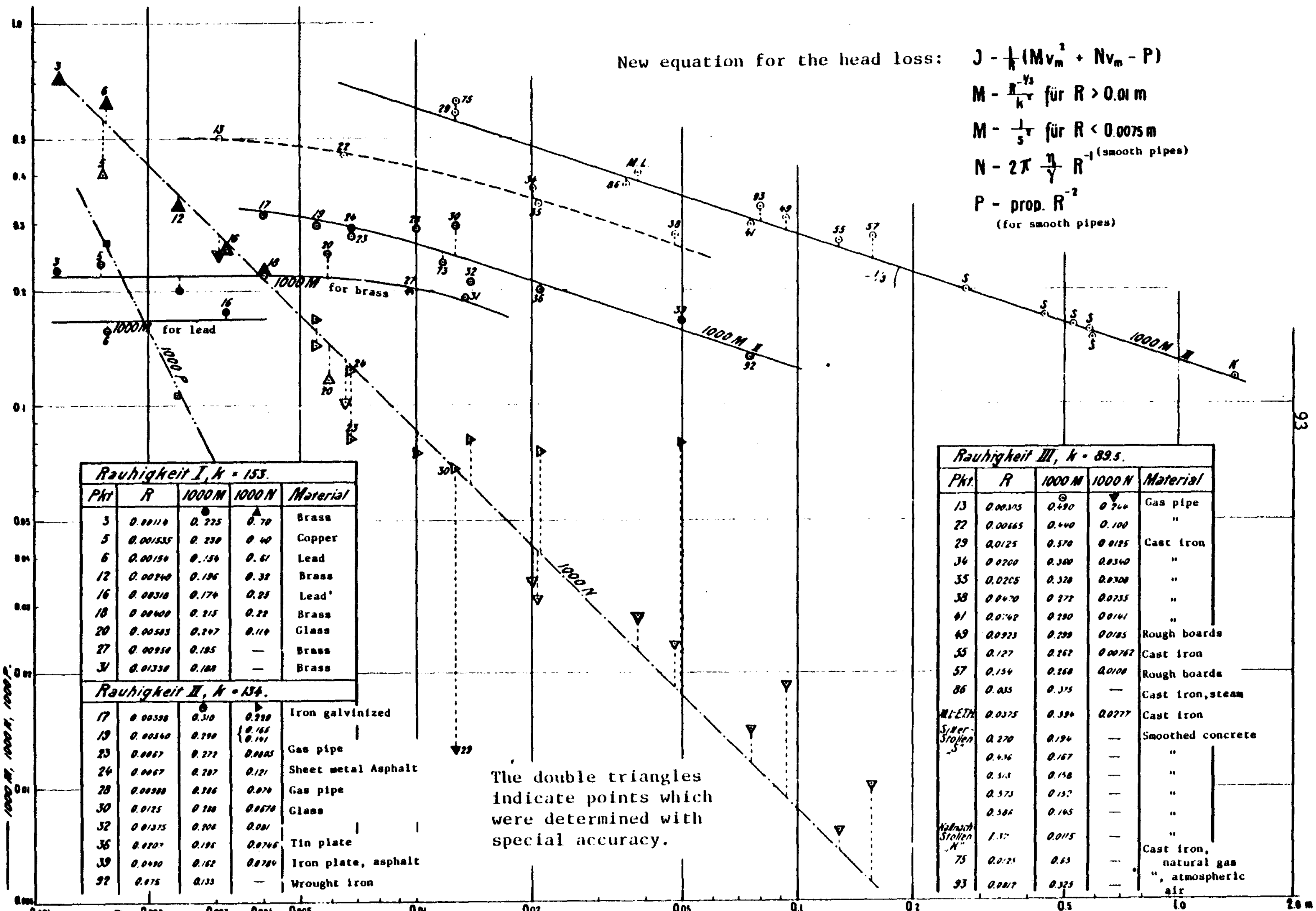

Rauhigkeit I, k = 153.				
Pkt	R	1000 M	1000 N	Material
3	0.00110	0.225	0.70	Brass
5	0.001535	0.230	0.40	Copper
6	0.00150	0.154	0.61	Lead
12	0.00240	0.196	0.38	Brass
16	0.00318	0.174	0.25	Lead'
18	0.00400	0.215	0.22	Brass
20	0.00505	0.207	0.110	Glass
27	0.00950	0.195	—	Brass
31	0.01330	0.188	—	Brass

Rauhigkeit II, k = 134.				
Pkt	R	1000 M	1000 N	Material
17	0.00338	0.310	0.220	Iron galvinized
19	0.00540	0.290	0.165 / 0.141	
23	0.0067	0.272	0.0805	Gas pipe
24	0.0067	0.287	0.121	Sheet metal Asphalt
28	0.00980	0.286	0.070	Gas pipe
30	0.0125	0.288	0.0670	Glass
32	0.01375	0.206	0.081	
36	0.0207	0.196	0.0746	Tin plate
39	0.0490	0.162	0.0784	Iron plate, asphalt
92	0.075	0.133	—	Wrought iron

Rauhigkeit III, k = 89.5.				
Pkt.	R	1000 M	1000 N	Material
13	0.00305	0.490	0.244	Gas pipe
22	0.00665	0.440	0.100	"
29	0.0125	0.570	0.0125	Cast iron
34	0.0200	0.360	0.0340	"
35	0.0205	0.328	0.0308	"
38	0.0470	0.272	0.0235	"
41	0.0742	0.290	0.0141	"
49	0.0925	0.299	0.0185	Rough boards
55	0.127	0.262	0.00762	Cast iron
57	0.154	0.260	0.0100	Rough boards
86	0.035	0.375	—	Cast iron, steam
ML-ETH	0.0375	0.394	0.0277	Cast iron
Siber-Stollen "S"	0.270	0.194	—	Smoothed concrete
	0.436	0.167	—	"
	0.513	0.158	—	"
	0.573	0.152	—	"
	0.586	0.165	—	"
Kallnach-Stollen "K"	1.37	0.0115	—	"
75	0.0125	0.63	—	Cast iron, natural gas
93	0.0817	0.325	—	", atmospheric air

FIGURE 29 Dependence of the coefficients M, N and P on the hydraulic radius in pipes and adits.

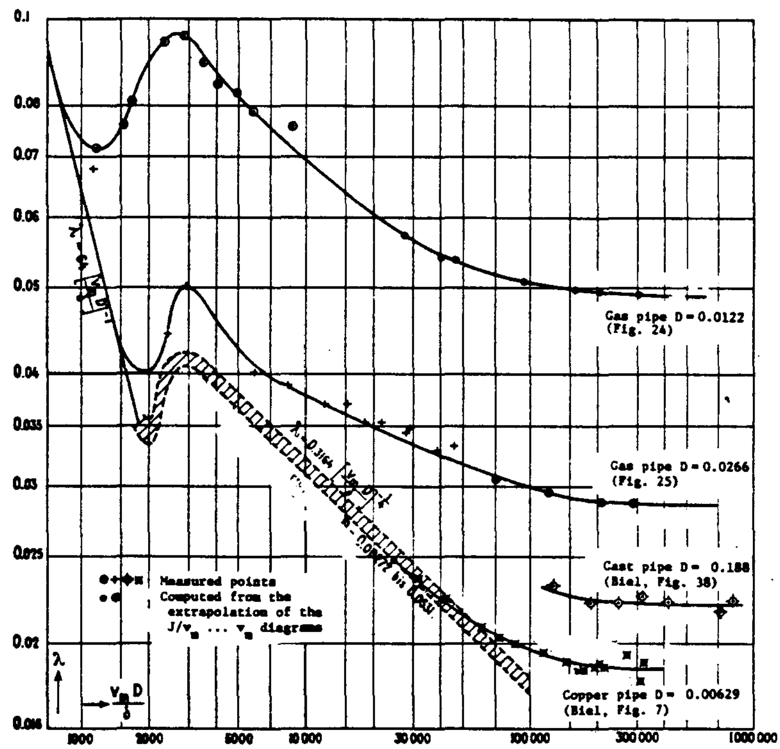

FIGURE 30 Drag coefficient, λ, as a function of the Reynolds number, $v_m \cdot D / \delta$. (*IU*) represents range for brass pipes from D = 0.00272 to 0.0531 from the experiments of Saph and Schoder.

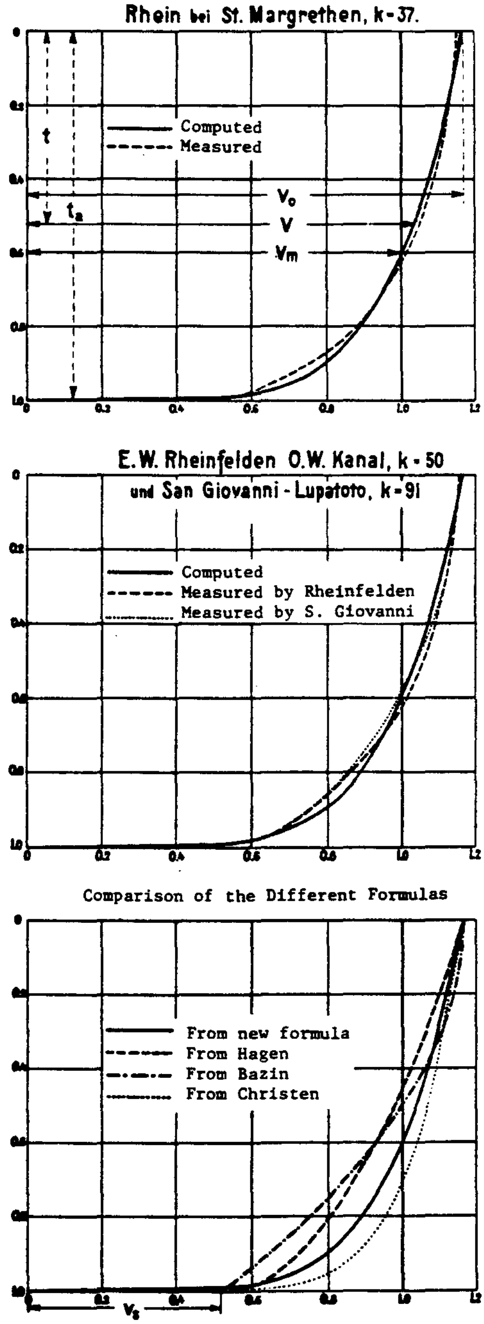

FIGURE 31 Velocity distributions in a vertical.

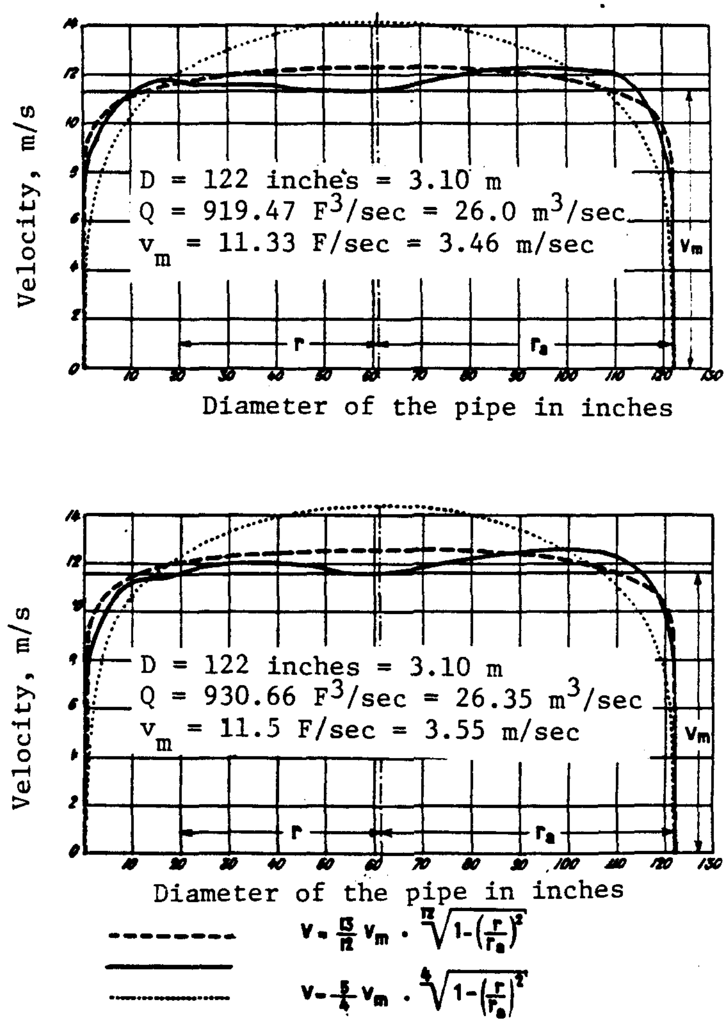

FIGURE 32 Velocity distribution in a pipe line, of the power plant at Niagara Falls (9, p. 159).

- - - - - - - Computed from $v = v_o\ [\ 1 - (r/r_a)^2\ ]^{1/12}$

——————— Measured

Curves of Equal Velocity

Distribution of the Velocities on the A - B Axis

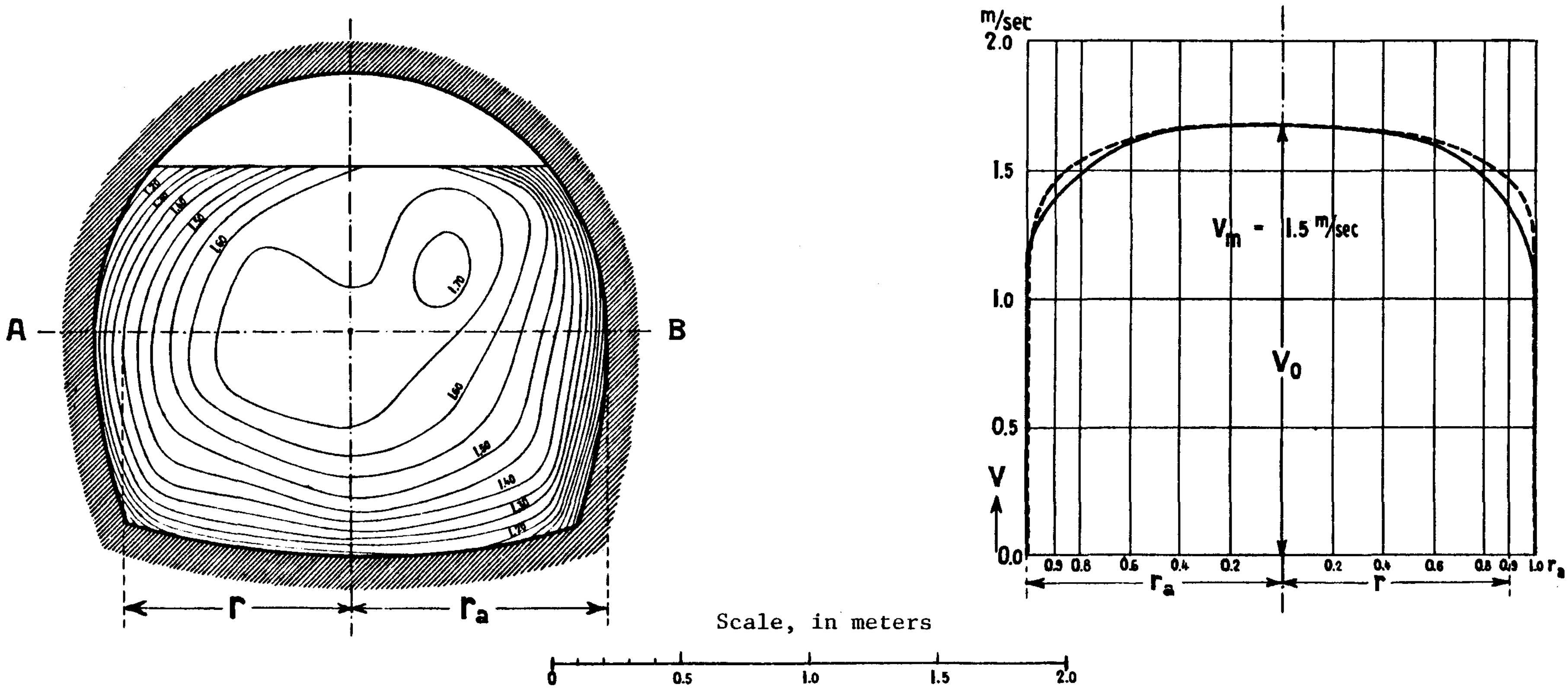

FIGURE 33 Velocity Distribution in the Sitter Adit.

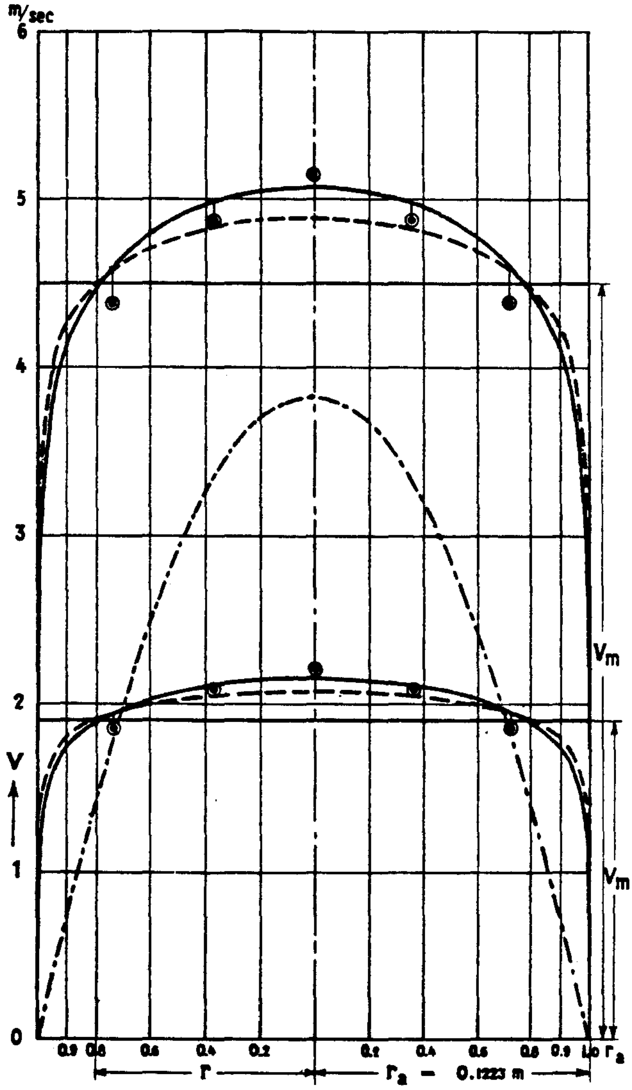

$V = \frac{12}{11} V_m \sqrt[12]{1-(\frac{r}{r_a})^2}$ computed (pure turbulence)

$V = 2 V_m [1-(\frac{r}{r_a})^2]$ computed (pure friction)

$V = \frac{9}{8} V_m \sqrt[8]{1-(\frac{r}{r_a})^2}$ measured

FIGURE 34 Velocity Distribution in a cast iron pipe from measurements of Darcy (3, p.84)

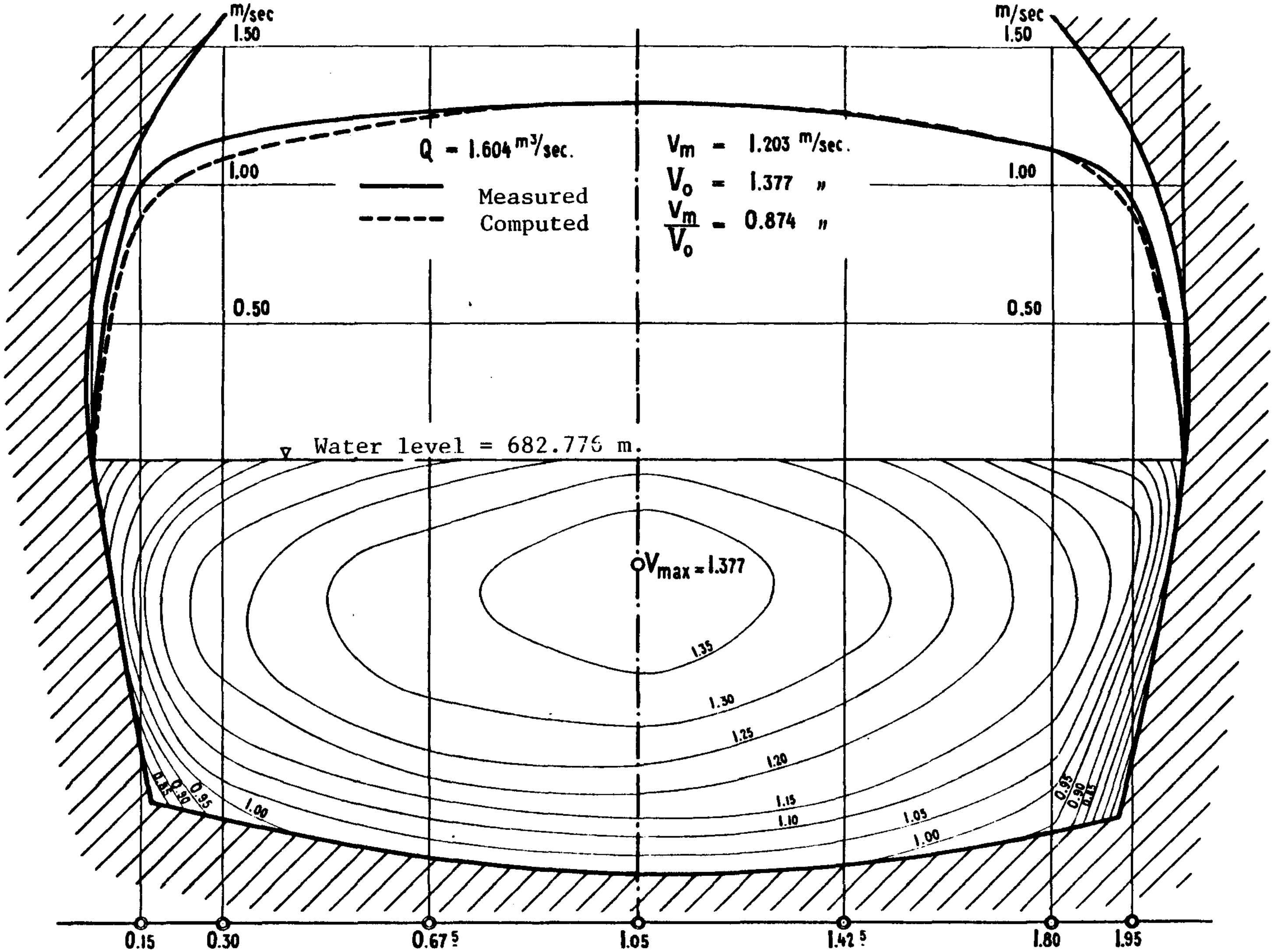

FIGURE 35 Sitter Adit. Curves of the mean velocities from measurement IV of July 23, 1906.

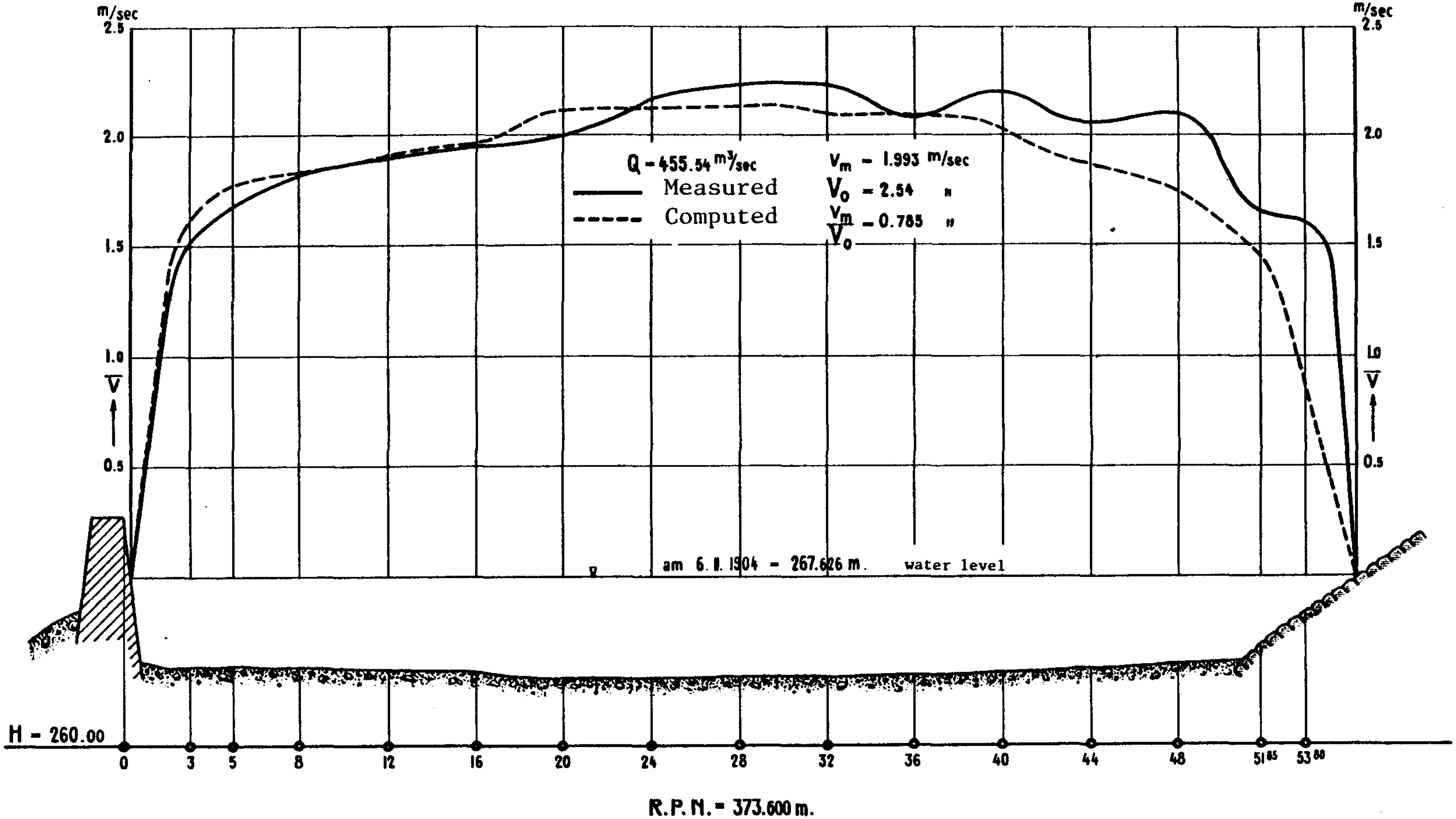

FIGURE 36 Head water channel of the power plant Rheinfelden, curves of the mean velocities.

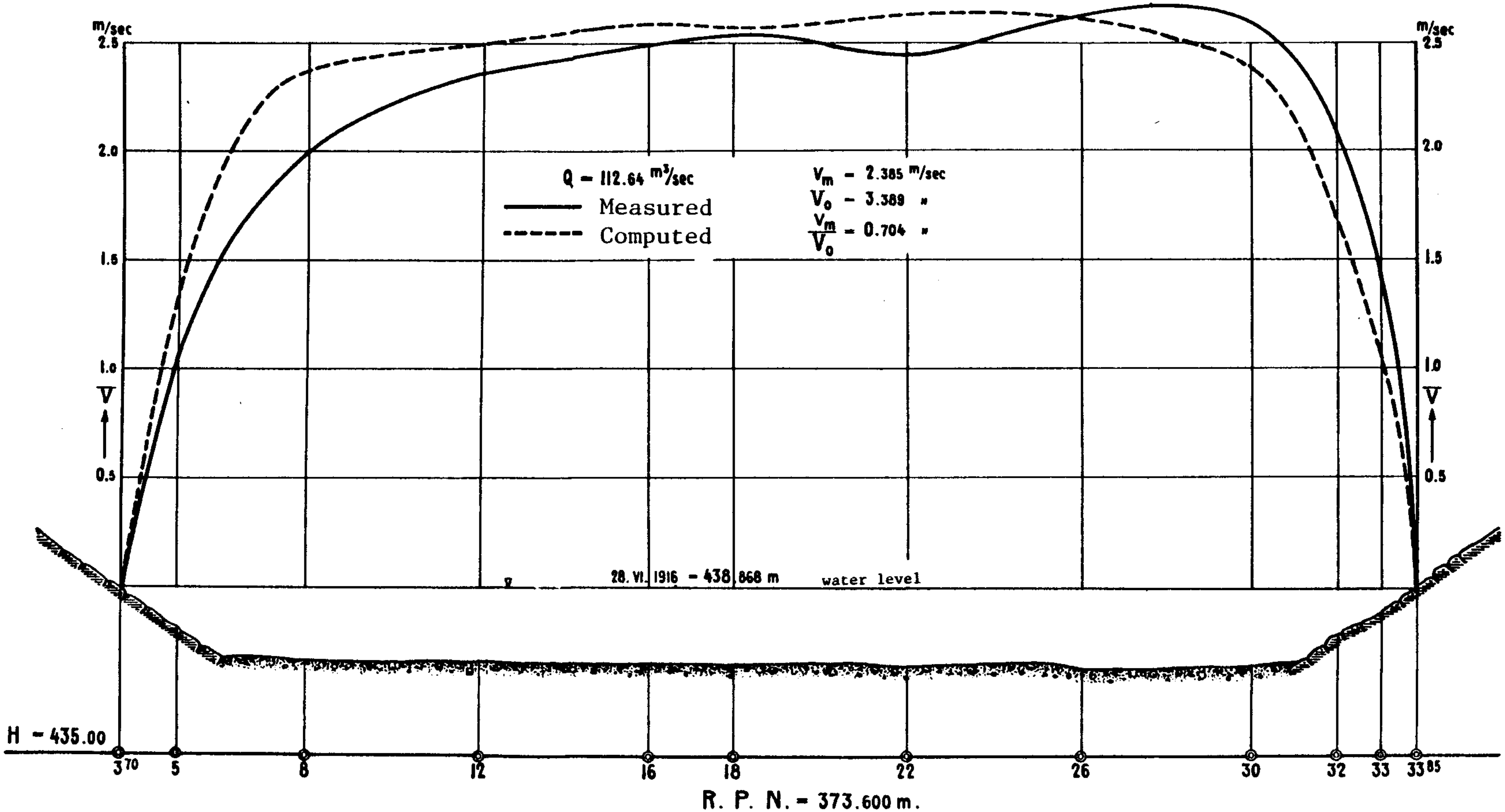

FIGURE 37 Reuss at Seedorf, curves of the mean velocities.

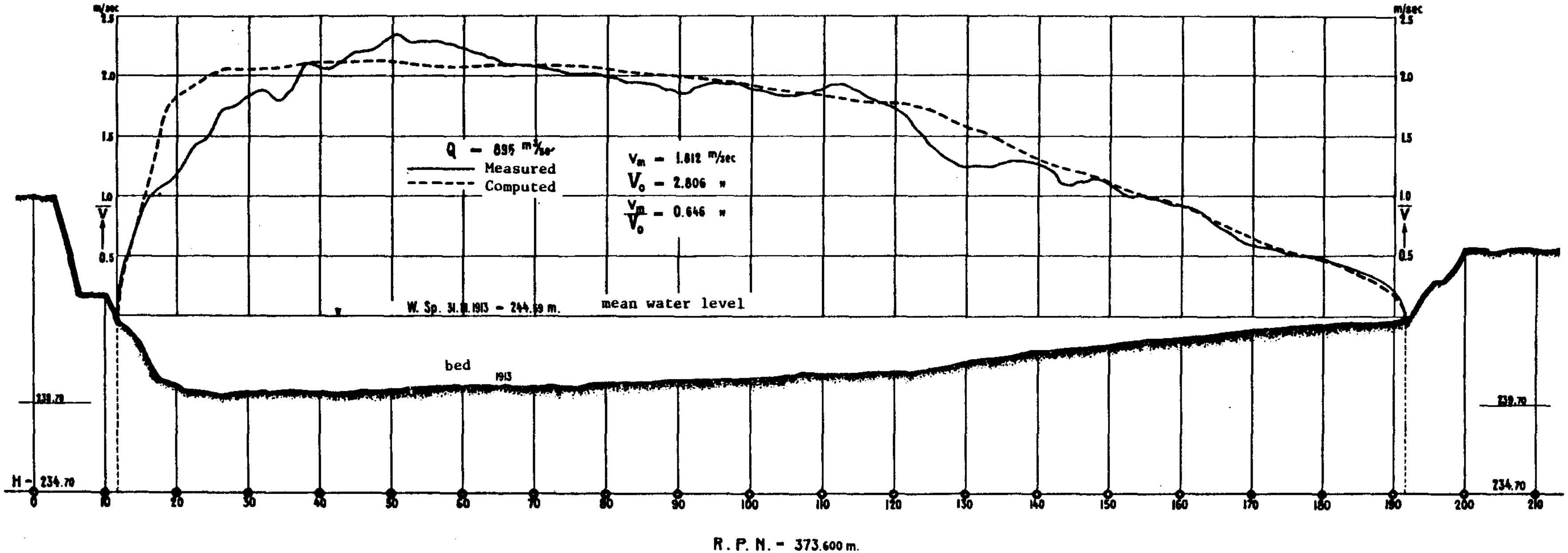

FIGURE 38 Rhine at Basle, curves of the mean velocities in the water measurement profile - Klingental Ferry.

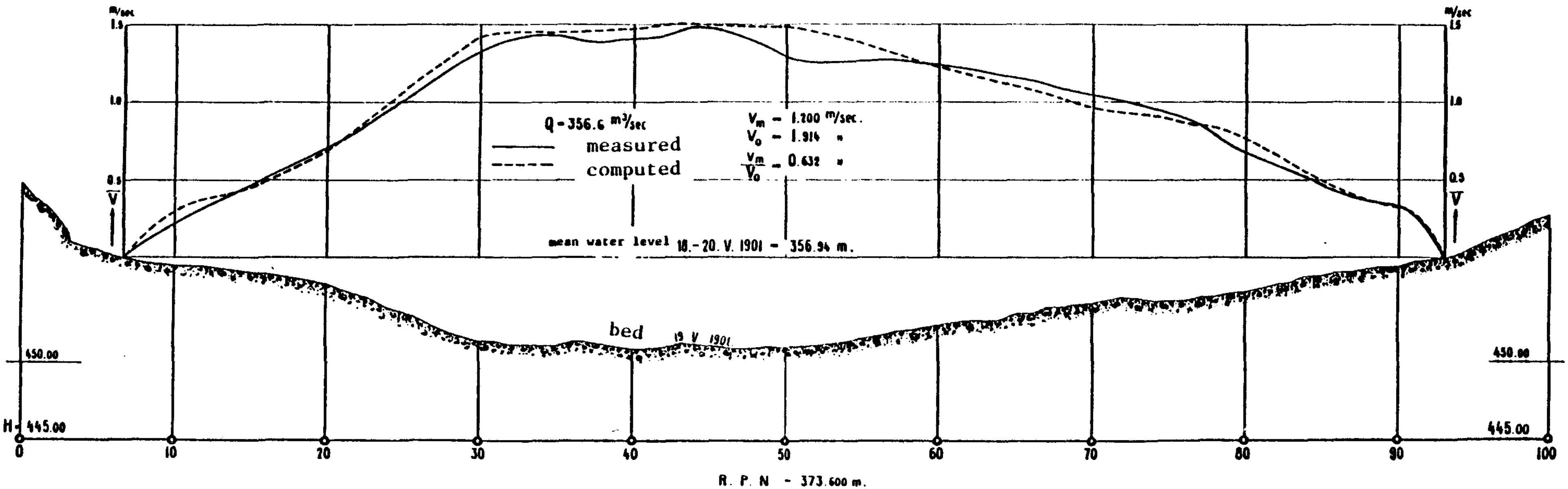

FIGURE 39 Rhine at Nol, curves of the mean velocities

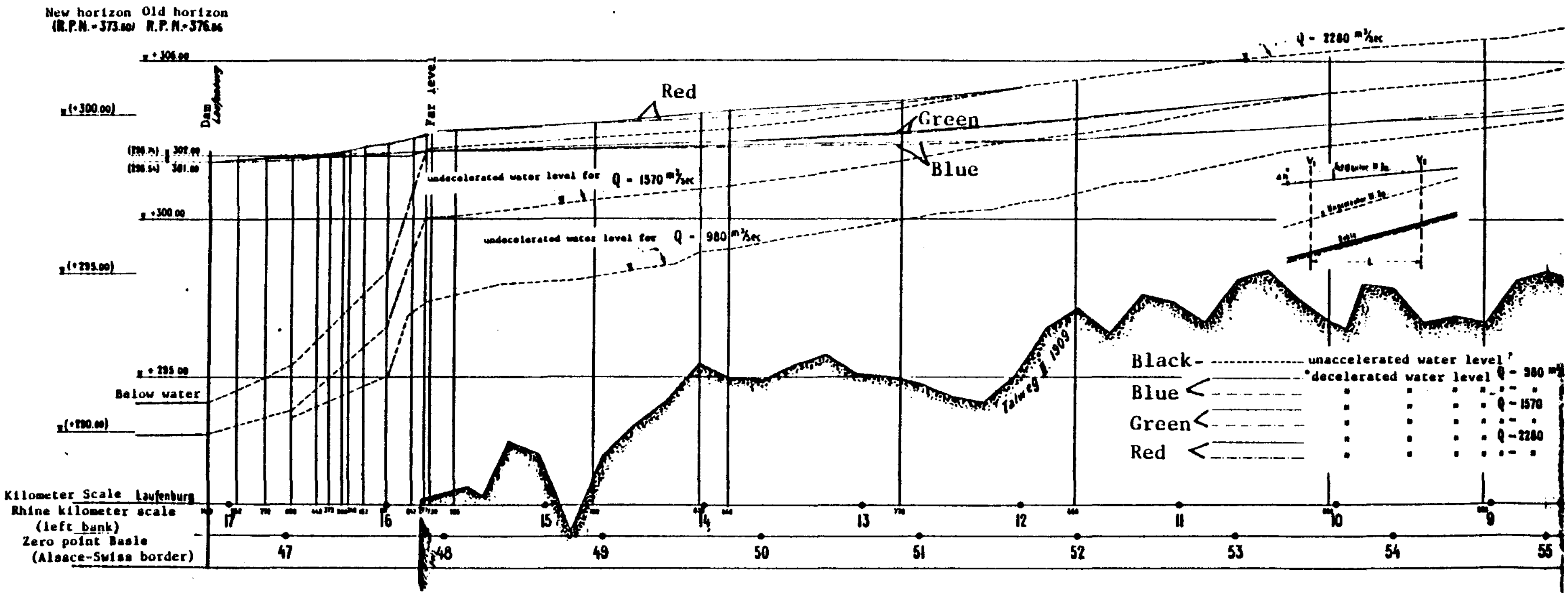

FIGURE 40 Longitudinal profile of the Rhine at Laufenberg
Plot of the observed and computed stagnation
(back water) lines.